Zootaxa 5422 (1): 001–066
https://www.mapress.com/zt/

Monograph

ISSN 1175-5326 (print edition)
ZOOTAXA
ISSN 1175-5334 (online edition)

https://doi.org/10.11646/zootaxa.5422.1.1
http://zoobank.org/urn:lsid:zoobank.org:pub:AE955C5E-803E-44CB-A3B2-9C2616D9F185

ZOOTAXA

5422

Taxonomy and stratigraphic distribution of *Lotagnostus* (Agnostida: Agnostidae) and associated trilobites and conodonts in the Upper Cambrian (Furongian) of Laurentia

JOHN F. TAYLOR[1], JAMES D. LOCH[2] & JOHN E. REPETSKI[3]
[1]*Department of Geography, Geology, Environment and Planning, Indiana University of Pennsylvania, Indiana, Pennsylvania 15705.*
jftaylor@iup.edu; https://orcid.org/0000-0003-0162-0087
[2]*Department of Physical Sciences, University of Central Missouri, Warrensburg, Missouri, 64093*
loch@ucmo.edu; https://orcid.org/0000-0003-4468-3512
[3]*U. S. Geological Survey, MS 926A, National Center, Reston, Virginia 20192.*
jrepetski@usgs.gov; https://orcid.org/0000-0002-2298-7120

Magnolia Press
Auckland, New Zealand

Accepted by J. Adrain: 9 Feb. 2024; published: 11 Mar. 2024

JOHN F. TAYLOR, JAMES D. LOCH & JOHN E. REPETSKI

Taxonomy and stratigraphic distribution of *Lotagnostus* (Agnostida: Agnostidae) and associated trilobites and conodonts in the Upper Cambrian (Furongian) of Laurentia

(*Zootaxa* 5422)

66 pp.; 30 cm.

11 Mar. 2024

ISBN 978-1-77973-004-6 (paperback)

ISBN 978-1-77973-005-3 (Online edition)

FIRST PUBLISHED IN 2024 BY

Magnolia Press

P.O. Box 41-383

Auckland 1041

New Zealand

e-mail: magnolia@mapress.com

https://www.mapress.com/zt

ISSN 1175-5326 (Print edition)

ISSN 1175-5334 (Online edition)

Table of Contents

Abstract

Two *Lotagnostus*-dominated faunas from the Windfall Formation at Ninemile Canyon in the Antelope Range of Nevada, USA, are described: an older *Lotagnostus nolani* Fauna and younger *L. rushtoni* Fauna. The former is dominated by two morphs of *Lotagnostus,* one strongly scrobiculate and the other smooth to weakly scrobiculate. Both morphs fall within the broad concept advocated for *L. americanus* by Peng *et al*. (2015). The numerous (>1400 sclerites) specimens of *Lotaganostus* in collections of the *L. nolani* Fauna confirm that the two morphs do not intergrade and remain distinct throughout ontogeny. Both display multiple traits that distinguish them from the type material of *L. americanus,* justifying treatment as separate species. Similarly unique, diagnostic features were identified to restore the Asian species *L. punctatus* and *L. asiaticus* to full species status, whereas deficiencies in the type material for *L. americanus* warrant restriction of the name to the holotype. New species described from the Windfall include five agnostoids (*Lotagnostus nolani, L. clarki, L. morrisoni, L. rushtoni,* and *Neoagnostus parki*) and one trilobite (*Bienvillia eurekensis*). *Plicatolina nyensis* Taylor is reassigned to *Mendoparabolina* on the form of its pygidium.

Conodonts from the Catlin Member of the Windfall Formation and overlying informal *Caryocaris* shale member of the Goodwin Formation at Ninemile Canyon provide a late Sunwaptan (*Eoconodontus* Zone) age for the *Lotagnostus rushtoni* Fauna and assign the entire *Caryocaris* shale to the early Ordovician *Rossodus manitouensis* Zone. Combined with published data on trilobite faunas, the conodont faunas confirm strong diachroneity for the top of the Catlin, and a lack of overlap in age between the *Caryocaris* shale and Bullwhacker Member of the Windfall in ranges to the north and east.

Co-occurrence of *Lotagnostus nolani* and *Mendoparabolina nyensis* establishes age equivalence of the *L. nolani* Fauna with the *Hedinaspis*-*Charchaqia* (*HC*) Fauna at the base of the Hales Limestone in the Hot Creek Range, and earlier correlations of the latter with the *L. punctatus* Zone in Asia are supported. However, isolation of the *HC* Fauna in starved-basin deposits above a major sequence boundary at the base of the Hales, and ecologic restriction of *Lotagnostus* to lower slope and basinal environments that prevented association with endemic shallow marine taxa, renders correlation into the biostratigraphy of Laurentian upper slope and platform imprecise on the order of 10s, if not 100s of meters.

Key words: Agnostidae, Trilobita, conodonts, *Lotagnostus,* Cambrian

Introduction

When the agnostoid arthropod *Lotagnostus americanus* (Billings, 1860) emerged as a leading candidate for defining the base of the 10th and uppermost Cambrian stage, there was reason for optimism. It was hoped that it might serve that purpose as well as other agnostoids such as *Glyptagnostus reticulatus* and *Lejopyge laevigata* have done in defining the bases of subjacent Cambrian stages. The biostratigraphic utility of *Lotagnostus* species with short stratigraphic ranges has been demonstrated in various areas of Asia (Lu & Lin, 1980,1989; Peng, 1992; Apollonov *et al*., 1988). Further, the number of paleocontinents where *L. americanus* is thought to occur has risen steadily through the preceding decade with reports of that species (or others deemed to be junior synonyms, such as *L. trisectus*) from North America (Ludvigsen *et al*., 1989), Argentina (Shergold *et al.,* 1995), Australia (Bao & Jago, 2000), and Siberia (Pegel, 2000).

More recently, however, a significant and growing number of specialists have expressed misgivings over the number of pre-existing species synonymized with *Lotagnostus americanus,* in part because most are based on very limited and often poorly preserved material. Collectively, the numerous species synonymized by Peng *et al.* (2015) endow *L. americanus* with an exceptionally wide range of morphologic variation that encompasses differences that had served in earlier studies not only to separate species, but to distinguish subgenera (Shergold *et al.,* 1990; Shergold & Laurie, 1997). Yet the range of intraspecific variation within any of the synonymized species has not been objectively established with large, stratigraphically constrained collections from a single bed or thin interval. In fact, such documentation provided in recent studies of other species of *Lotagnostus* confirms only modest amounts of intergrading morphologic variation (Rushton, 2009, for Avalonian Britain; Tortello, 2014, 2018, for Argentina; Westrop *et al*., 2011, and Westrop and Landing, 2016, for Avalonian Canada). These observations reinforce concerns expressed by some (e.g., Westrop & Landing, 2016, p. 8) that the exceptionally broad range of variation claimed for *L. americanus* sensu Peng *et al.* (2015) was actually the product of a biostratigraphically motivated consolidation of multiple species to create a single taxon with nearly global distribution. Such consolidation does enhance the apparent utility of the broadly defined taxon by expanding its geographic range to include additional paleocontinents. If the defining taxon, however, actually comprises multiple species whose appearances on their respective continents

differ significantly in age, this defeats the purpose of a Global Boundary Stratotype Section and Point (GSSP), the ultimate goal of which is to provide an effectively age-equivalent horizon for precise intercontinental correlation. Such diachroneity of the stage boundary is particularly likely if the species involved is/are uncommon to rare or taphonomically compromised, which regrettably is the situation for *L. americanus* on multiple paleocontinents, even when the broad definition advocated by Peng *et al*. (2015) is applied.

Those questioning the suitability of *Lotagnostus americanus sensu* Peng *et al.* (2015) for defining the base of Cambrian Stage 10 have also expressed concern regarding the limited paleoenvironmental range of the genus. As noted by Landing *et al.* (2011, p. 627) there is a disconcertingly consistent association of *Lotagnostus* species with trilobite taxa that occupied dysoxic environments. The lack of co-occurrence with shallow marine taxa that results from restriction to such marginal, deep-water settings limits the precision of correlation possible into the thick and widespread successions of shallow marine deposits that formed on tropical paleocontinents such as Laurentia. In this paper, we utilize the information available on morphologic variation, faunal associations, and paleoenvironmental preferences from all Laurentian occurrences of *Lotagnostus* to assess the merits of these challenges to its suitability.

Distribution of *Lotagnostus* in Laurentia

The few occurrences of *Lotagnostus* in eastern North America (i.e., southern Laurentia) can be placed only imprecisely into the highly resolved Furongian biostratigraphy established for much of Laurentian North America (see Taylor *et al.,* 2012 for summary). Those in eastern Canada are in clasts of toe-of-slope limestone conglomerates of the Lévis Formation in Quebec (Rasetti, 1944) and the Cow Head Group of Newfoundland (Ludvigsen *et al*., 1989). As is typical of such amalgamated deposits, imprecision of correlation of these faunas with adjacent shallow marine successions is on the order of 10s meters at the very least. A lone occurrence in the central Appalachians (Rasetti, 1959) offers no additional constraints, as the two fragmentary cephala were recovered from a slab of limestone from a stone wall in Frederick, Maryland.

Occurrences within intact stratigraphic successions of deep-water deposits in western North America, which accumulated on the northern Laurentian margin, hold greater potential for refining the stratigraphic range and age of appearance of *Lotagnostus americanus* sensu Peng *et al.* (2015) on that paleocontinent. Archived, *Lotagnostus*-bearing faunas reported from the Hales Limestone (Taylor, 1976) and Windfall Formation (Nolan *et al.*, 1956) of Nevada were reprocessed to determine whether they contain other taxa characteristic of specific biozones or subzones that were established in shallow marine successions in Laurentian North America in recent decades. Excess matrix trimmed off archived specimens from both the Hales and the Windfall, along with our reconnaissance collections from the Windfall, was processed for conodonts, another faunal group of great biostratigraphic utility in uppermost Furongian and younger strata. Distributional data on the agnostoids, trilobites, and condonts were integrated to refine correlations within and beyond Laurentia.

Multiple sympatric species in the Windfall Formation: Our sampling in the Windfall Formation at Ninemile Canyon in the Antelope Range, Nevada (Figures 1, 2.1), produced thousands of well-preserved arthropod specimens from a bed of coquinoid limestone (Figure 2.4), providing the first opportunity for thorough documentation of the range of morphologic variation within a single, stratigraphically constrained collection of *Lotagnostus americanus* sensu Peng *et al.* (2015) from Laurentian strata. As in some occurrences in Asia, the Windfall collection contains two morphs, one strongly scrobiculate with well-developed trisection of the posteroaxis, and one smooth to weakly scrobiculate with little or no trisection. One of our objectives was to establish whether there was evidence of intergradation between the two morphs, which would support the interpretation of the features that distinguish them as intraspecific variation (Peng *et al.,* 2015). The alternative interpretation that they represent separate, sympatric species (Westrop *et al.,* 2011) requires the absence of transitional forms. The large collection from the Windfall revealed no such intergradation or transitional forms. The two morphs remain distinct throughout ontogeny (Plate 1) and are interpreted accordingly as separate species. Moreover, both display several characteristics that set them apart from the type material of *L. americanus* from the Lévis Formation in Quebec, and are named as new species herein. We selected one of these new species as the eponymous taxon for the particularly abundant fauna from the Windfall, the *L. nolani* Fauna.

The sampling at Ninemile Canyon also yielded a second Furongian fauna from higher in the Windfall Formation that also is dominated by *Lotagnostus,* but species that fall outside the morphologic range of *L. americanus* sensu

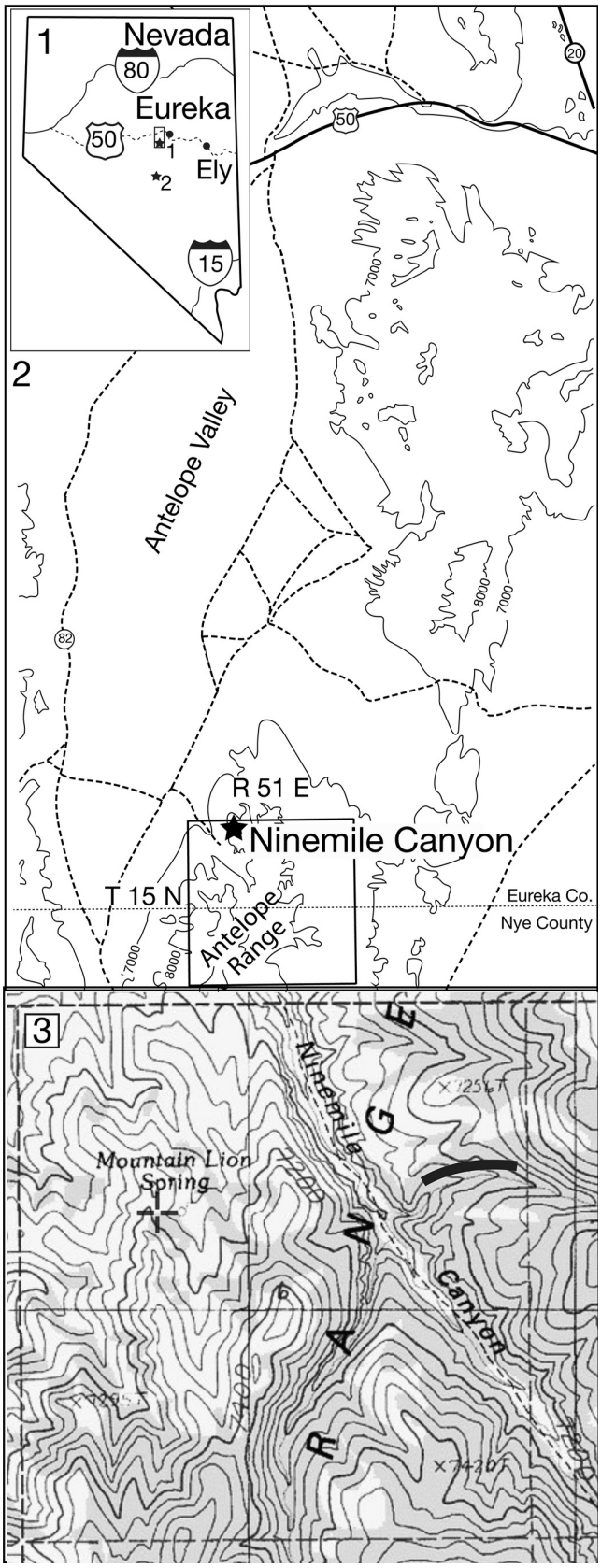

FIGURE 1. Index maps. (1) Outline map of Nevada, USA, indicating position of 1) Ninemile Canyon in the Antelope Range and 2) the Tybo and Hot Creek sections of Taylor (1976) in the Hot Creek Range. (2) Detail map of central Nevada with outline of T. 15 N., R. 51 E. and location of Ninemile Canyon. (3) Topographic detail of T. 15 N., R. 51 E. from the Ninemile Peak, Nevada 7.5' Quadrangle showing location of section (black band) measured through the Windfall Formation in the tributary on the northeast side of the Ninemile Canyon.

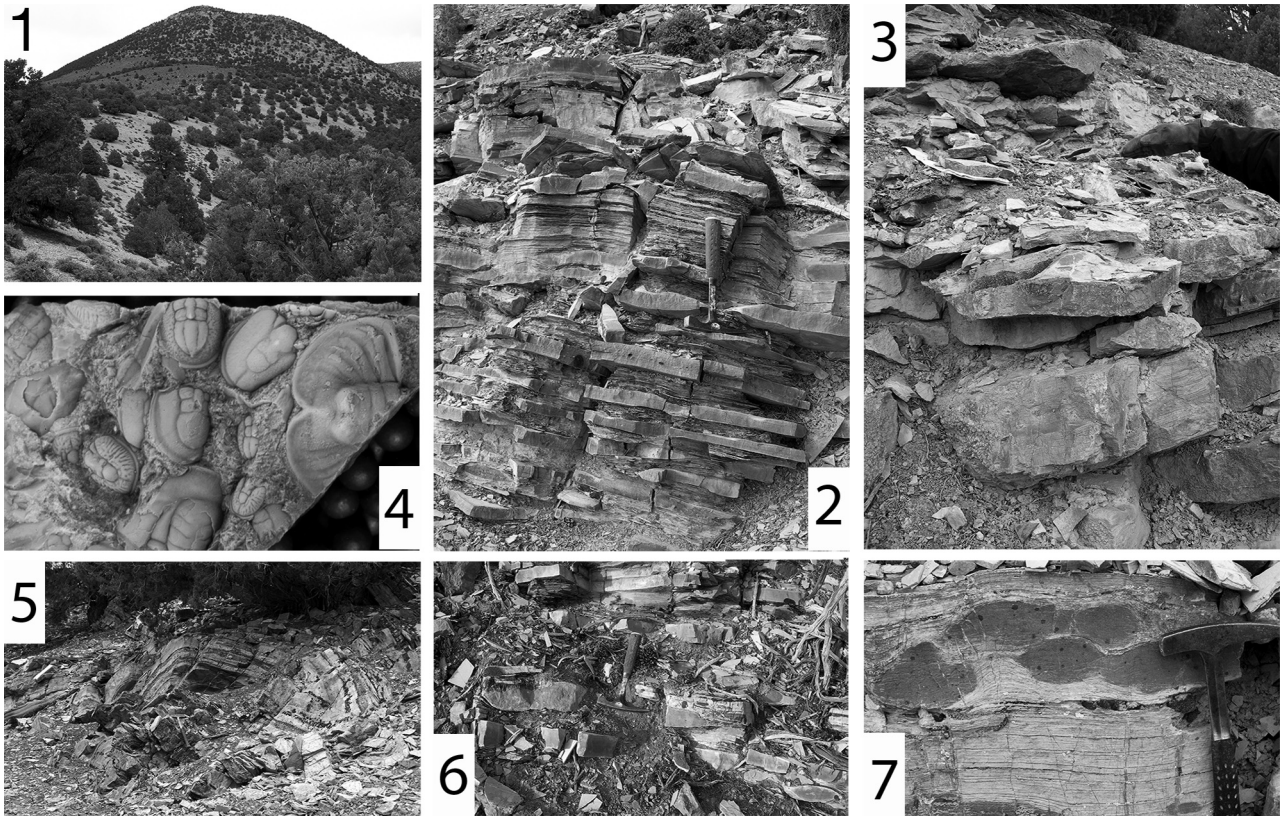

FIGURE 2. Field photographs of the Windfall Formation, Ninemile Canyon, Nevada. (1) View (facing east) of intermittent exposures of Windfall Formation sampled on north side of tributary of Ninemile Canyon. (2) Intercalated lime grainstone and calcareous shale. (3) Collection horizon for 5/22/08B at hand from middle Windfall. (4) Agnostoid-trilobite coquina from collection 5/22/08B; CM 41300. (5) Recumbent, soft-sediment folds in upper Windfall. (6) Grainstone lens in upper Windfall that yielded 5/22/08D at hammer head. (7) Grainstone boudins and laminated calcareous shales in middle Windfall.

Peng *et al*. (2015). This younger fauna, designated the *L. rushtoni* Fauna, also includes two new, distinct species of *Lotagnostus* that are described herein. The *L. rushtoni* Fauna proved valuable for comparison with the subjacent *L. nolani* Fauna, and conodonts extracted from the excess matrix generated during mechanical processing of the former provided a minimum age for the latter. Our re-assignment of the single specimen of *Lotagnostus* that Taylor & Cook (1976, text-fig. 29F) illustrated from the Hales Limestone from *L. trisectus* to *L. nolani* **n. sp.** confirms at least partial age-equivalence of the *L. nolani* Fauna to the *Hedinaspis-Charchaqia* Fauna (*HC*, hereafter) described by Taylor (1976) from the basal strata of the Hales. The presence in the *L. nolani* Fauna in the Windfall of the olenid trilobite *Plicatolina nyensis* (reassigned herein to *Mendoparabolina*), which Taylor (1976) described from *HC* Fauna, reinforces that temporal correlation. A more detailed treatment of the utility and limitations of species associated with *L. nolani* in the Hales for refining correlation with coeval strata in Asia and elsewhere is provided in later sections on age and correlation of the faunas.

Authorship

Repetski is responsible for the systematic treatment and biostratigraphic interpretation of the conodont faunas. Loch and Taylor are responsible for the systematic treatment of the agnostoid and trilobite taxa, and interpretation of the lithofacies and depositional settings of the Windfall and Hales strata. Joint authorship of new species should be attributed (names arranged alphabetically) to Loch and Taylor (*in* Taylor, Loch & Repetski).

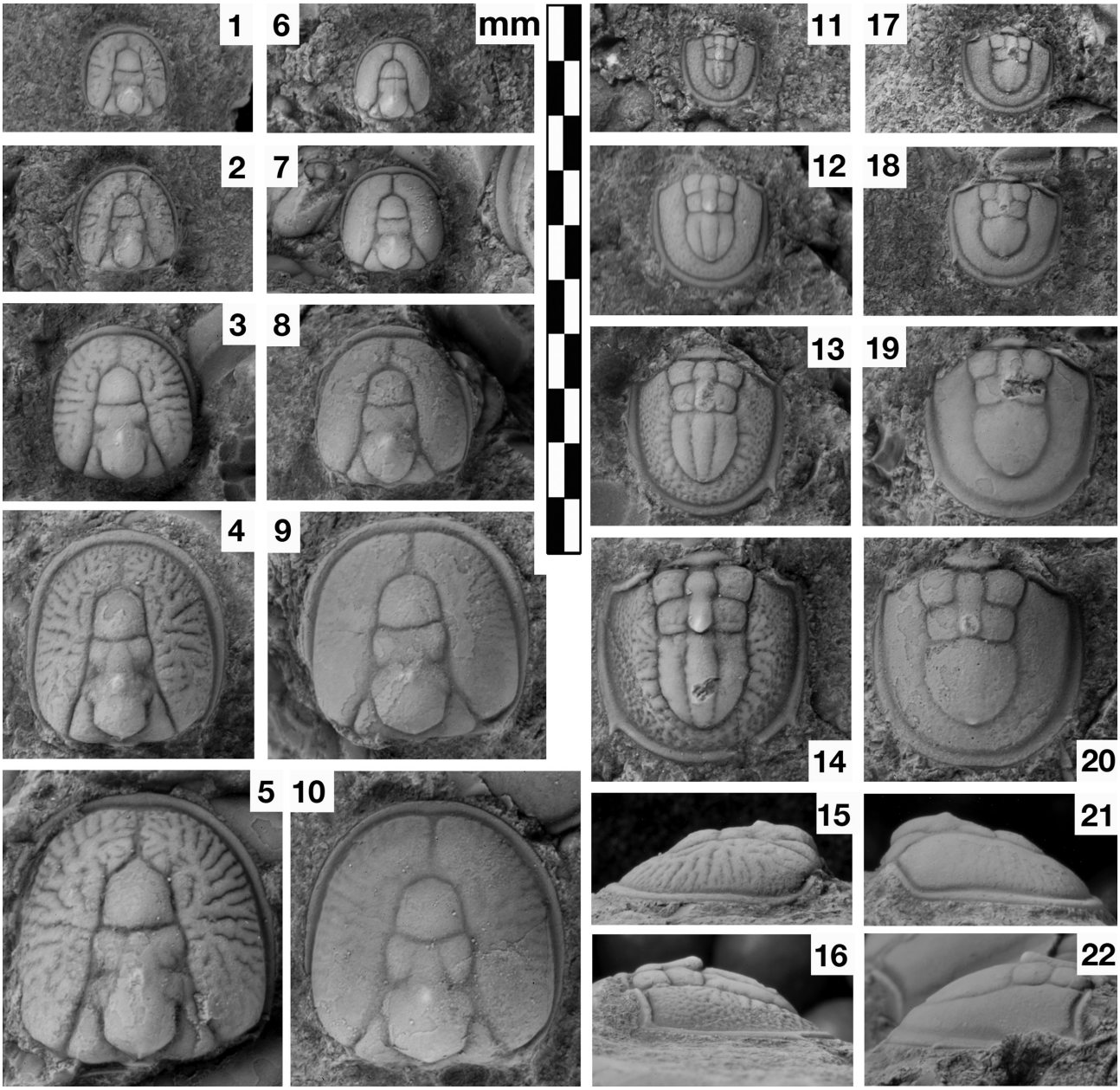

PLATE 1. Ontogenetic comparison of *Lotagnostus nolani* and *L. clarki* **n. sp.** All images at same scale and all from collection 5/22/08B. 1-5, 15. *L. nolani cephala.* 1. CM 41301. 2. CM 41302. 3. CM 41303. 4, 15. CM 41304. 5. CM 41305. 6-10, 21. *L. clarki* cephala. 6. CM 41310. 7. CM 41311. 8. CM 41312. 9, 21. CM 41313. 10. CM 41314. 11-14, 16. *L. nolani* pygidia. 11. CM 41306. 12. CM 41307. 13. CM 41308. 14,16. CM 41309. 17-20, 22. *L. clarki* pygidia. 17. CM 41315, 18. CM 41316. 19. CM 41317. 20. CM 41318. 22. CM 41319.

Windfall Formation

Lithostratigraphy of the Windfall Formation. Nolan *et al*. (1956) named the Windfall Formation after Windfall Canyon and the associated Windfall Mine in the Eureka District of Nevada and divided the formation into two members. The lower member, designated the Catlin Member, consists primarily of medium gray, thin- to thick-bedded limestone with dark shale interbeds (Figure 2.2, 2.3) and intervals rich in laminated chert. In its type area and in ranges to the north and east, the Catlin is overlain by a slope-forming unit of thinly bedded limestone named the Bullwhacker Member after another mine near Eureka. However, in the northern Antelope Range to the south, the Catlin is conformably overlain by an enigmatic dark shale package that occupies the same stratigraphic position as

the Bullwhacker Member to the north. Nolan *et al.* (1956) provisionally assigned the shale package to the Windfall and considered it to be a possible deeper water, lateral equivalent to the Bullwhacker. Merriam (1963), however, removed it from the Windfall and assigned it to the base of the overlying Goodwin Formation as his informal member A. Subsequent authors accepted the formational reassignment, but referred to the shale package as the *Caryocaris* Shale (Ethington, 1981) or *Caryocaris* Shale Member of the Goodwin Formation (Taylor & Repetski, 1985, fig. 3), naming the unit for a fossil arthropod that dominates its meager macrofauna. It is treated herein as an informal member of the Goodwin Formation, and referred to as the *Caryocaris* shale, pending formal description and selection of a more appropriate, geographic name. Later studies (Young, 1960; Palmer, 1971; Adrain & Westrop, 2004; Westrop & Adrain, 2007) further subdivided the Windfall Formation by setting apart the basal few meters of the formation, which differ both in lithology and fossil content from the rest of the Catlin, as a separate member, the Barton Canyon Member. Whether the Barton Canyon Member extends southward into the northern Antelope Range is unknown due to structural complications in the few areas where the Windfall is exposed for study.

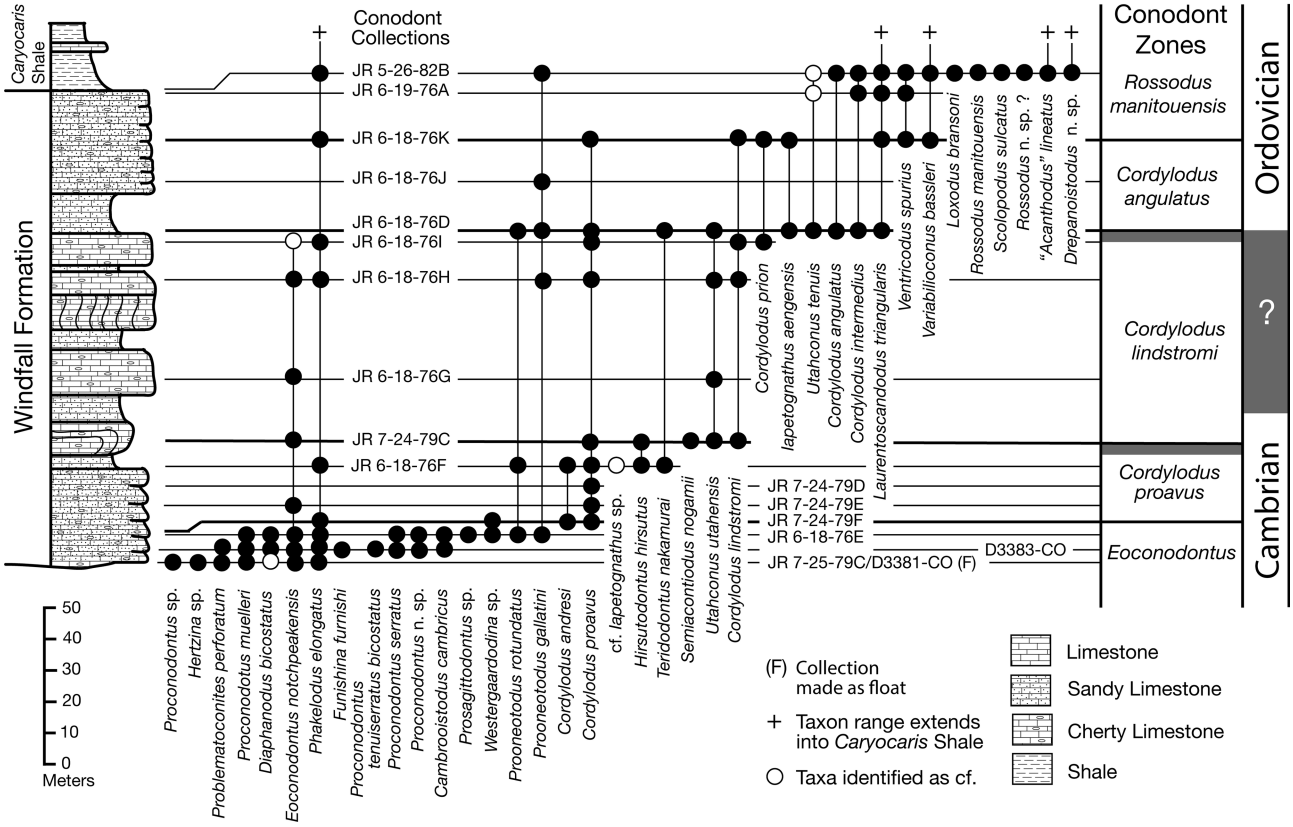

FIGURE 3. Stratigraphic distribution of conodont species from the Windfall Formation at Ninemile Canyon, Nevada. "JR" indicates collections of John Repetski.

Materials Studied. All material utilized from the Windfall Formation in the present study was collected from the Catlin Member where it is best exposed in the northern Antelope Range, near the mouth of Ninemile Canyon. Michael E. Taylor and J.E. Repetski, along with other U.S.G.S. personnel, conducted the first systematic sampling of the Ninemile Canyon section in 1976, 1979, and 1982. Repetski recovered conodonts from 15 collections made through the Windfall (Figure 3). Preliminary conodont data were presented in Taylor and Repetski (1985, fig. 4). Three macrofossil collections made by M.E. Taylor, two of the *Lotagnostus rushtoni* Fauna and one of the *L. nolani* Fauna, were borrowed and more completely processed for additional agnostoid and trilobite specimens. The excess matrix from each was processed for conodonts. Using M.E. Taylor's field notes, we were able to establish the precise position of one *L. rushtoni* collection (D3383-CO) relative to Repetski's conodont collections, adding an additional productive horizon to the final conodont range chart (Figure 3). His field notes indicate that second *L. rushtoni* collection (D3381-CO) was collected from float and the *L. nolani* collection (D3362-CO) from off the line of section. Consequently, the precise position of these latter collections within the member and relative to other collections is uncertain.

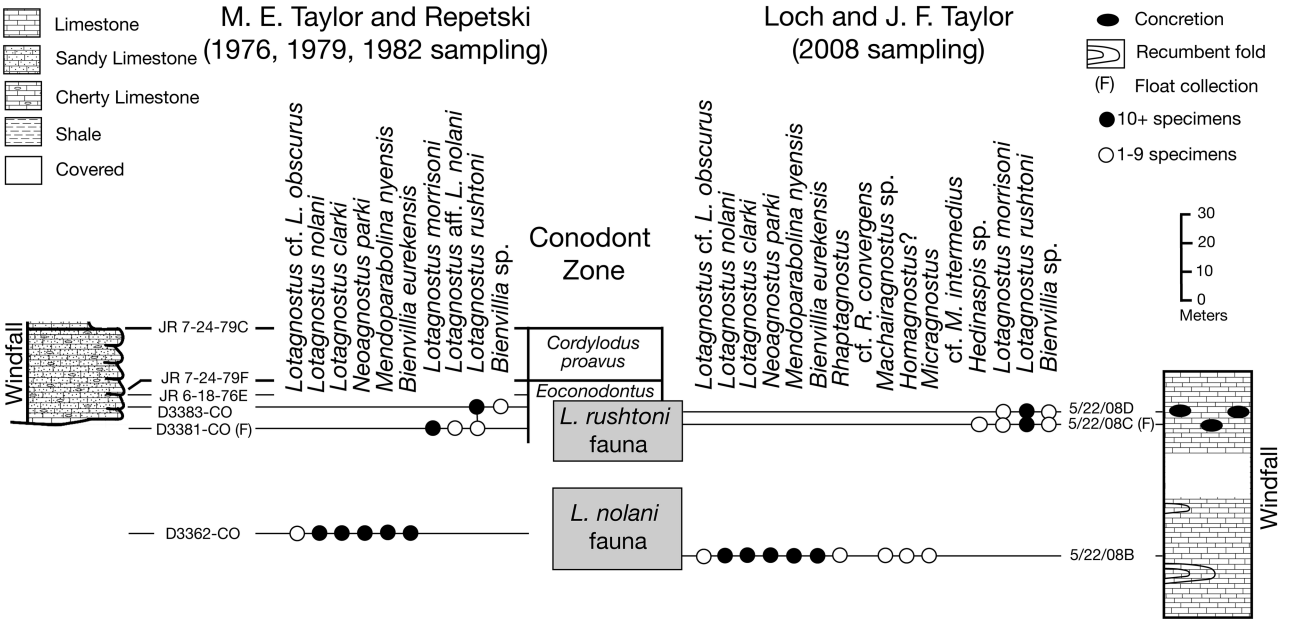

FIGURE 4. Agnostoid and trilobite species range chart, Windfall Formation, Ninemile Canyon, Nevada.

John F. Taylor and Loch conducted reconnaissance sampling through the Windfall Formation at Ninemile Canyon in 2008. Unfortunately, we were unable to relocate the base of the U.S.G.S. measured section or tie precisely into its footages. Consequently, the position of the macrofossil collections from our independent measured section (Figures 1, 4) within the conodont biostratigraphy is based on conodonts recovered from the excess matrix. Our lowest collection (5/22/08B) was made from a thin bed of medium gray, petroliferous packstone to grainstone (Figure 2.3) in which disarticulated agnostoids and olenid trilobites of the *L. nolani* Fauna occur in coquinoid abundance. Although the coquina consists entirely of disarticulated sclerites, there is little evidence of fragmentation, abrasion, or size sorting (Figure 5) to suggest long-distance transport or reworking of bioclasts. The higher collections (5/22/08C; 5/22/08D, Figure 2.6), which represent the *L. rushtoni* Fauna, were recovered from isolated lenses of dark gray bioclastic packstone to grainstone that occur within rhythmically interbedded finely laminated lime mudstone and calcareous shale (Figure 2.2). The exact stratigraphic separation between 5/22/08B and the higher 2 collections is uncertain due to non-continuous exposure and intervening syndepositional folds (Figure 2.5).

Lithofacies and depositional setting of the Windfall Formation in the Antelope Range. More recent studies of the Windfall provided detailed information on its constituent lithofacies and the succession of depositional environments represented by the Barton Canyon, Catlin, and Bullwhacker members (Brady & Rowell, 1976; Adrain & Westrop, 2004; Westrop & Adrain, 2007). Deposition of the basal member under shallow subtidal conditions was followed by significant deepening that initiated accumulation of the chert-rich, deep marine facies that characterize the Catlin Member. We interpret the prominent fine laminations of the lime mudstone rhythmically interbedded with dark shale (Figure 2.2, 2.7), and retained by the chert identified in early studies as a defining attribute of the Catlin Member, as an indication that these beds originated as dilute carbonate turbidites. The scattered bioclastic grainstone beds and lenses in the Catlin were formed by localized winnowing during occasional, higher energy events that concentrated skeletal fragments into coquinoid lags (Figure 2.4). The laterally tapering form of some grainstone lenses (e.g., Figure 2.2, 2.6) is consistent with deposition of a limited amount of coarser sediment as starved ripples on the depositional surface of the distal slope or basin floor. Intervals of syndepositionally folded beds (Figure 2.5) provide evidence of sediment instability on the sloping deep marine sediment surface.

A reconstruction of the northern Laurentian platform margin, depicting depositional settings interpreted for the Windfall and other formations in western North America that have yielded *Lotagnostus* is provided as Figure 6. The pie diagrams in the figure, showing the relative abundance of *Lotagnostus* in collections for which abundance data were available, illustrate how the genus is common only in facies deposited in the deep waters of the lower slope and basin. The only other known Laurentian occurrence of a *Lotagnostus*-dominated fauna is in the El Relincho Formation of the Precordillera of western Argentina, most recently described by Tortello (2014). A comparable deep-water origin for that fauna is confirmed by both the low-diversity olenid-agnostoid biofacies (Figure 7) and black lime mudstone-shale lithofacies (Keller, 1999, fig. 47).

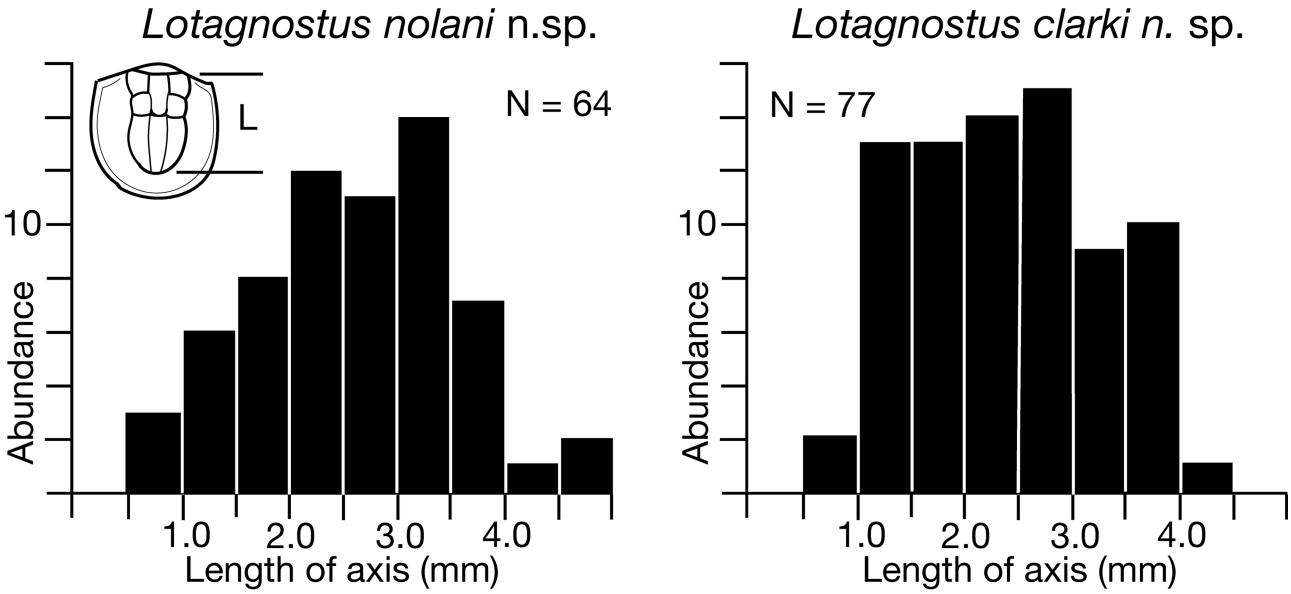

FIGURE 5. Size frequency distribution for lengths of pygidial axis for *Lotagnostus nolani* and *L. clarki* from Collection 5/22/5/22/08B, Windfall Formation, Ninemile Canyon, Nevada

The relative positions and water depths shown for the Windfall and Hales formations in Figure 6 are based on lithofacies of the Catlin Member in the Antelope Range from which the *Lotagnostus nolani* Fauna was recovered, and of the coeval strata at the base of the Hales Limestone in the Hot Creek Range that yield the *HC* Fauna. We follow earlier authors (e.g., Osleger & Read, 1993; Adrain & Westrop, 2004, text-fig. 2) in interpreting the Hales as having formed farther from the platform margin than the Windfall, and both the lithologies and state of preservation of the *HC* Fauna (discussed in more detail below) are consistent with deposition in a deeper, less energetic environment than that occupied by the *L. nolani* Fauna. Although their positions relative to the margin likely remained the same during deposition of the younger strata that yield the *L. rushtoni* Fauna, with the Hales forming farther from the platform margin, the lithologies and fauna of the Windfall represent less energetic and perhaps deeper conditions than those of the Hales. We attribute this reversal in the relative depth and energy of the depositional environments of the two units to the irregular and dynamic nature of gravity flow deposition along depositional strike seaward of the carbonate shelf. While relatively low-energy deposition of dilute turbidites continued in the Antelope Range, the segment of the carbonate margin farther south (modern coordinates) where the Hales was forming experienced an increase in downslope transport of coarse sediment from upper slope and/or shelfbreak environments to create the coeval limestone conglomerates of the Hales.

A more gently sloping, ramp profile likely characterized the margin farther north during deposition of the Bullwhacker Member in the Cherry Creek Range. As detailed by Adrain & Westrop (2004), the Bullwhacker Member comprises an upward-shoaling sequence with thinly bedded, non-burrowed lime mudstone at the base, grading upward into burrow-mottled lime mudstone in the middle of the member. The uppermost strata below the conformable contact with thick microbial reefs at the base of the Notch Peak Formation consist predominantly of various grain-supported carbonates that reflect higher-energy and shallower conditions, along with small microbial reefs. The succession is strikingly similar to coeval deposits of the Frederick Formation in Maryland that record comparable shoaling through the Sunwaptan. Thinly bedded lime mudstone of the Adamstown Member grade upward into burrowed upper-ramp carbonates with isolated microbial bioherms of the Lime Kiln Member, the conformable contact with the overlying Grove Formation being marked by the appearance of thick microbial reefs and sandy grainstone (Taylor *et al*., 2009; Brezinski *et al*., 2012). Another parallel between the Windfall and Frederick formations revealed by the data collected in the present study (and discussed in a later section) is significant diachroneity of some member/formation boundaries across short distances along the platform margin.

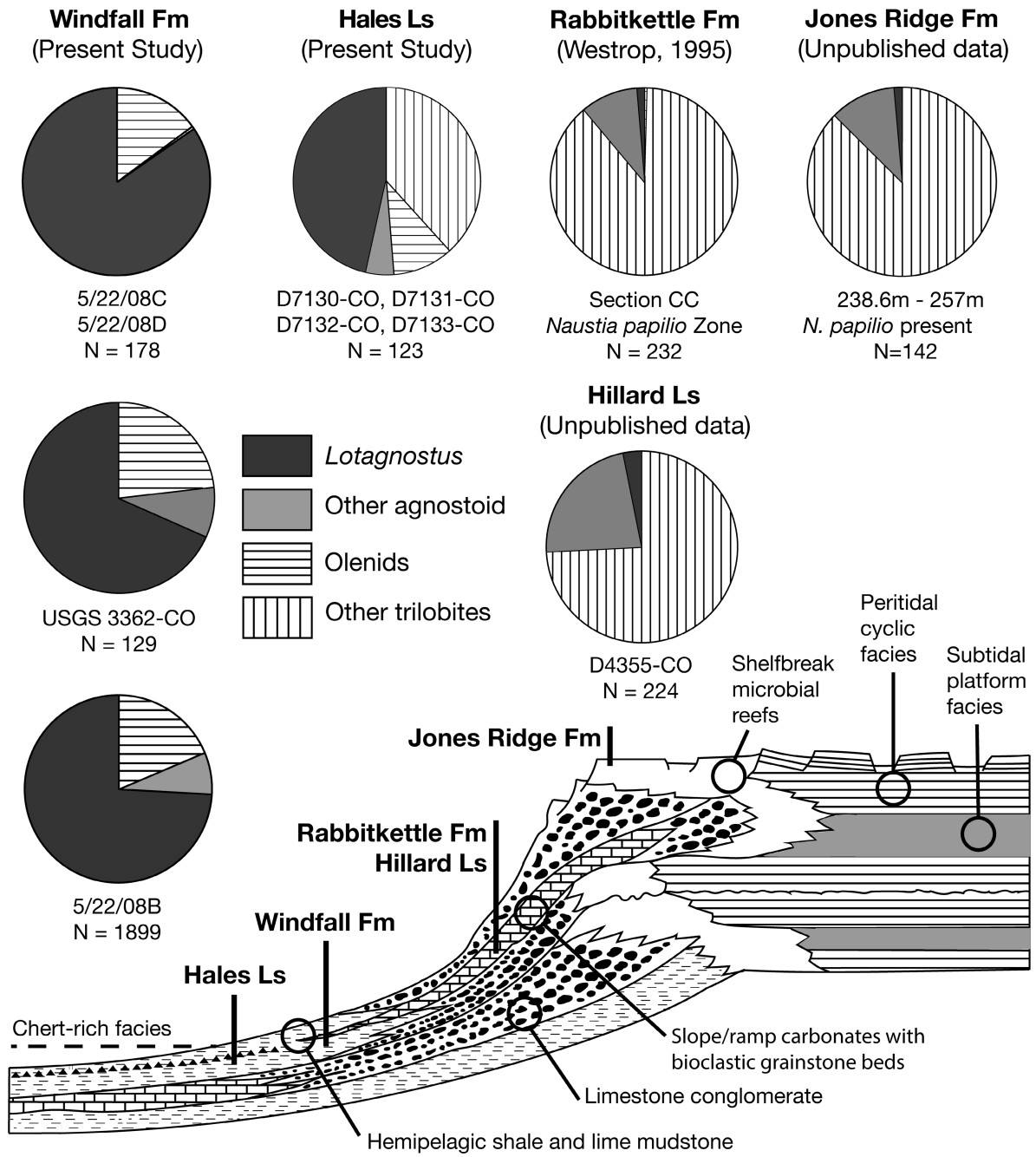

FIGURE 6. Reconstruction of northern Laurentian platform margin showing environmental settings interpreted for formations that have yielded *Lotagnostus,* and pie charts showing relative abundances of *Lotagnostus*, other agnostoids, olenids, and other trilobites. Position of Windfall Formation on the profile is based on the lithofacies documented in the Antelope Range. Rimmed platform profile and lithofacies patterned after reconstruction of Appalachian margin by James *et al.* (1989, fig. 12).

Conodont Faunas of the Windfall Formation. Repetski processed two kilograms of each conodont sample from the 1976, 1979, and 1982 field seasons using ca. 10% acetic acid. Insoluble residues were washed on 80- and either 140- or 170-mesh sieves and concentrated via tetrabromoethane heavy liquid. Some residues were further concentrated using a Frantz magnetic separator. Loch processed samples of varying mass from Hales Limestone collections D7129-CO, D7130-CO, and D7131-CO along with Windfall Formation collections 5/22/08B, 08C, and 08D, utilizing similar methods.

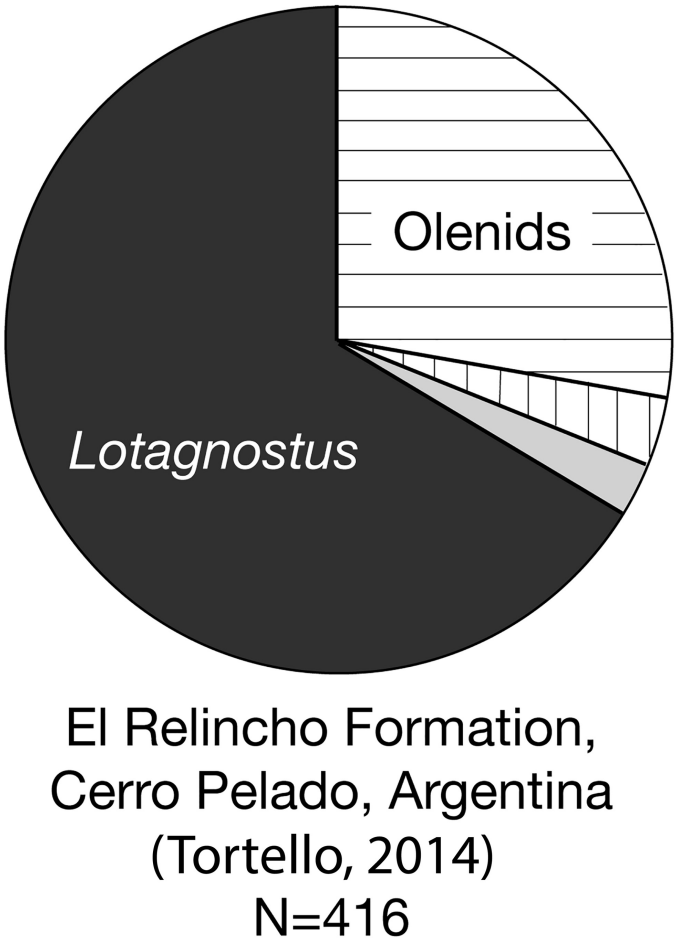

FIGURE 7. Relative abundance of *Lotagnostus* species, other agnostoids, olenid trilobites, and other trilobites in the El Relincho Formation, Cerro Pelado, of the Argentine Precordillera (Tortello, 2014). Relative abundance based upon total number of sclerites reported.

The conodont zonation utilized here is that of Miller *et al*. (2003, 2015), which was developed in shallow marine Laurentian successions but has been applied widely for international correlation (Taylor *et al*., 2012; Jahangir *et al*., 2016; Bagnoli *et al*., 2017; Dong & Zhang, 2017; Wang *et al*., 2021). The four lowest conodont collections from Ninemile Canyon (Figure 3) are assigned to the *Eoconodontus* Zone based upon the presence of *Eoconodontus notchpeakensis, Proconodontus serratus,* and *Cambrooistodus cambricus*. The latter two species are restricted to this zone. The absence of *Cambrooistodus minutus* precludes more precise assignment of any of these collections to either the *C. minutus* or underlying *E. notchpeakensis* subzone. The lowest occurrence of *Cordylodus proavus* and *Cordylodus andresi* in collection JR 7-24-79F marks the base of the *C. proavus* Subzone, which extends at least as high as collection JR 6-18-76F, the uppermost collection containing *C. andresi.* Limited conodont recovery does not permit resolution of the *Hirsutodontus hirsutus* and *Fryxellodontus inornatus* Subzones. The occurrence of *Cordylodus lindstromi* in the next higher collection marks the base of the *C. lindstromi* Zone, indicating that the subjacent *Cordylodus intermedius* Zone is either anomalously thin or absent from the section. Whether the attenuation or omission of this zone, which is 40 meters thick in the House Limestone in western Utah (Miller *et al*., 2003), is the product of depositional or deformational processes is uncertain.

None of the collections from the Windfall Formation contains *Iapetognathus fluctivagus* or another species restricted to the *Iapetognathus* Zone to allow recognition of that zone, whose base marks the Cambrian–Ordovician systemic boundary (Nicoll *et al*., 1999; Cooper *et al.,* 2001). The presence of cf. *Iapetognathus* in collection JR 6-18-76F was not considered conclusive enough to use it to assert the presence of the *Iapetognathus* Zone. Precise placement of the systemic boundary in sections where the conodont yield is low often is difficult, because *I.*

fluctivagus is a relatively uncommon species, and the *Iapetognathus* Zone typically is relatively thin. It spans only 5m of strata in the Auxiliary Boundary Stratigraphic Section at Lawson Cove in western Utah (Miller *et al.,* 2015). Consequently, the base of the Ordovician at Ninemile Canyon is very likely somewhat lower than where it is shown in Figure 3. However, it is certainly no higher than collection JR 6-18-76D, which contains *Cordylodus angulatus*, the eponymous species of the zone that overlies the *Iapetognathus* Zone. The lowest occurrence of *Ventricodus spurius* and *Variabilioconus bassleri* in collection JR 6-18-76K marks the base of the *Rossodus manitouensis* Zone.

The conodont faunas reported herein resolve the longstanding issue of age of the *Caryocaris* shale and its relationship to the Bullwhacker Member. Nolan *et al*. (1956) and Merriam (1963) were reluctant to assign an Ordovician age to the former, given the absence of graptolites. Ethington (1981) reported conodonts characteristic of the *Rossodus manitouensis* Zone (known at that time as Fauna C) from its uppermost strata, establishing an early Ordovician age for that part of the unit. The age of most of the shale package, however, remained undetermined. The recovery of taxa characteristic of the *R. manitouensis* Zone from the uppermost beds of the underlying Windfall in the present study establishes that the entire *Caryocaris* shale lies within that Lower Ordovician conodont zone. It is not, therefore, a lateral equivalent of the Bullwhacker Member.

Together with biostratigraphic data reported by Westrop & Adrain (2004) from the Bullwhacker Member and bounding units in the Cherry Creek Range, this new information from Ninemile Canyon reveals that deposition of the deep marine lithofacies that compose the Catlin Member continued in the northern Antelope Range throughout the deposition of the Bullwhacker Member, as well as a significant thickness of shallow marine strata at the base of the overlying Notch Peak Formation, to the northeast. As a result, the top of the Catlin Member is strongly diachronous, varying in age from middle Sunwaptan (*Illaenurus* Zone, or older) where it underlies the Bullwhacker in the Cherry Creek Range as opposed to upper Skullrockian (*R. manitouensis* Zone) where it is overlain by the *Caryocaris* shale less than 150km to the southwest in the Antelope Range. Similarly strong diachroneity has been demonstrated for upper Sunwaptan off-platform facies in the Frederick Valley of Maryland. In that area, the conformable boundary between upper ramp facies of the Frederick Formation and shelfbreak facies at the base of the overlying Grove Formation differs in age from middle Sunwaptan (lower *Saukia* Zone) to basal Skullrockian (*Tangshanaspis* Zone) over a distance of less than 20km, perhaps marking the location of an embayment in the Appalachian platform margin (Taylor *et al*., 1996).

Content, Age, and Correlation of the *Lotagnostus rushtoni* Fauna. This younger *Lotagnostus*-dominated fauna (Figure 4) in the Windfall Formation includes the following species, listed in decreasing order of abundance: *Lotagnostus rushtoni* **n. sp.**, *Lotagnostus morrisoni* **n. sp.**, *Bienvillia* spp., *Lotagnostus* aff. *L. nolani* and *Hedinaspis* sp. Conodont collections extracted from excess matrix of all *Lotagnostus rushtoni* Fauna samples contain *Eoconodontus notchpeakensis*, assigning them to the *Eoconodontus* Zone. Recovery of *Proconodontus serratus* from three of the four collections (3383-CO, 5/22/08C, and 5/22/O8D) places them in the middle to upper part of the *E. notchpeakensis* Subzone and/or the overlying *Cambrooistodus minutus* Subzone. This confirms age-equivalence with faunas somewhere within the upper part of the *Saukia* Zone in Laurentian platform successions where the *Eoconodontus* Zone spans the upper two thirds of *Saukiella junia* Subzone and the entire *Prosaukia serotina* Subzone (Miller *et al*., 2011, 2015).

The estimated ranges of the three *Lotagnostus* species in the *L. rushtoni* Fauna within the established conodont and trilobite zonations are shown in Figure 8. It is important to note that this figure is not a conventional range chart in which the vertical bar for each species is based on its documented highest and lowest occurrences in one or more measured section. The maximum range shown for each species (dashed line), like those provided for several species of *Lotagnostus* by Westrop *et al*. (2011, fig. 1), spans the bio/chronostratigraphic interval to which its age is constrained by associated taxa and/or bracketing superjacent and subjacent faunas in all reported occurrences. The solid black bar within the range of each species (Figure 8) delineates the interval within which the information currently available suggests its actual age probably lies.

The solid, probable range bars for the three *Lotagnostus* species that occur in the *L. rushtoni* Fauna in the Windfall Formation are placed in the *Eoconodontus notchpeakensis* Subzone given the absence of *Cambrooistodus minutus* from all conodont collections extracted from samples of this fauna. However, it is not unusual for a sample processed from the *C. minutus* Subzone to fail to yield the relatively uncommon eponymous species. Consequently, it is possible that one or more of the *L. rushtoni* collections does actually represent the higher subzone. The maximum possible ranges (dashed lines) for all three *Lotagnostus* species are extended to the top of the *Eoconodontus* Zone accordingly. The different lengths of their probable ranges (solid bars) are based on their distribution within the

four *L. rushtoni* collections (Figure 8). The probable range of *Lotagnostus* cf. *L. nolani* is the shortest because it is present only in the USGS collection from float (D3381-CO), which might be the oldest *L. rushtoni* collection as it is the only one that yielded neither *Proconodontus serratus* nor *Cambrooistodus cambricus*. The probable range for *L. morrisoni,* which also occurs in D3381-CO, is slightly longer, consistent with its occurrence in collections 5/22/08C and 5/22/08D. That of *L. rushtoni,* which occurs in all four collections of the *L. rushtoni* Fauna, extends even farther upward. It is the only *Lotagnostus* species in collection D3383-CO, suggesting that this is the youngest collection of that fauna.

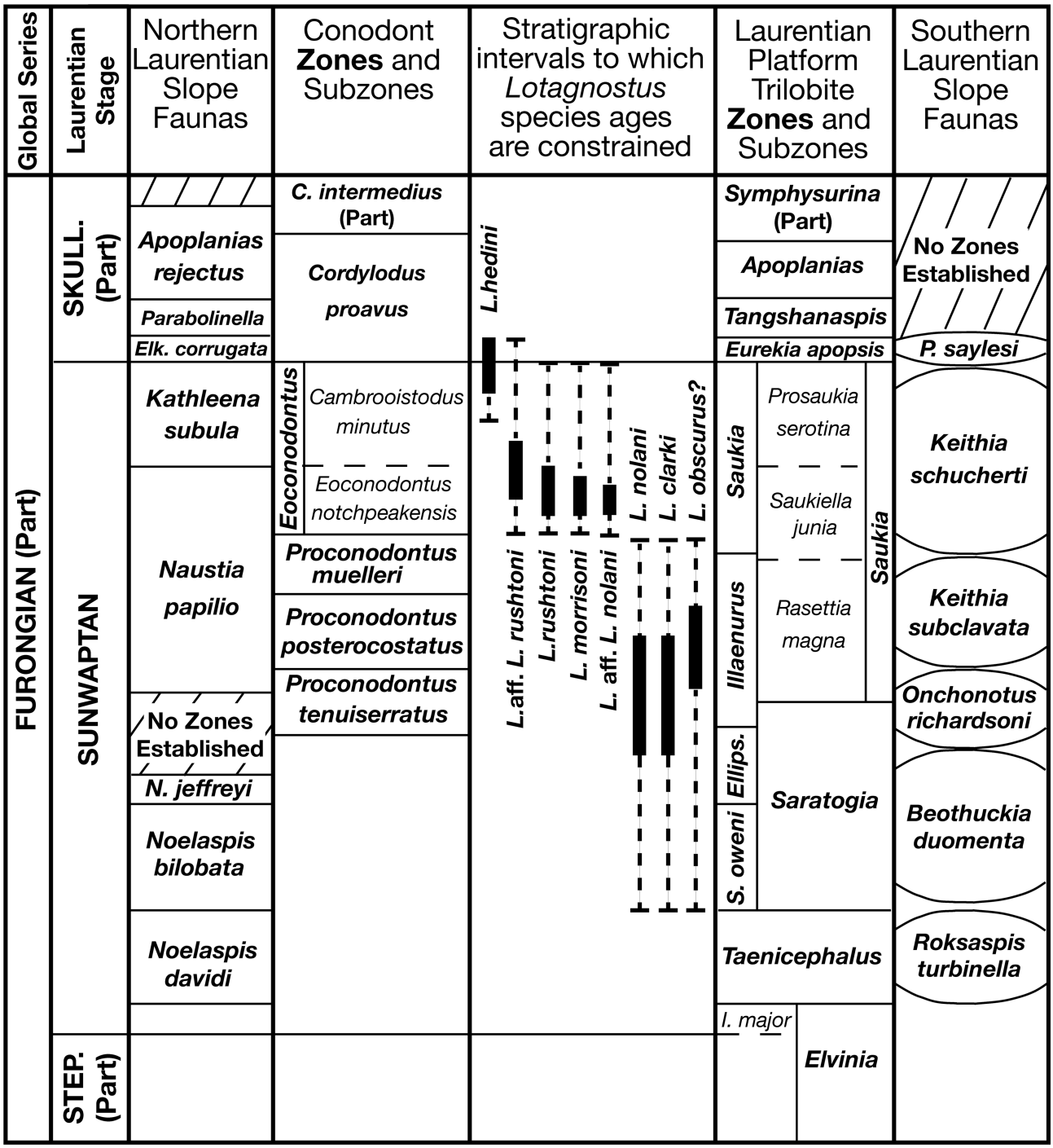

FIGURE 8. Estimated distribution of *Lotagnostus* species within the trilobite and conodont zonations. Probable range (black bar) delineates interval within which occurrences of a species probably lie. Maximum range (dashed lines) denotes full possible range. Abbreviations: *C., Corbinia*; *Elk., Elkanaspis*; *Ellips., Ellipsocephaloides*; *I., Irvingella*; *N., Noelaspis*; *P., Phylacterus*; *S., Stigmacephalus*; Skull., Skullrockian; Step., Steptoean; Trem., Trempealeauan. Zonal successions from: 1) Westrop, 1995; 2) Miller *et al.,* 2003, 2015; 3) Westrop, 1986; 4) Ludvigsen *et al.,* 1989.

Ranges for 2 other *Lotagnostus* species that occur in the *Eoconodontus* Zone elsewhere are included in Figure 8: *Lotagnostus* aff. *L. rushtoni* and *Lotagnostus hedini.* Eight of the 9 specimens assigned herein to *L.* aff. *L. rushtoni* (see Systematic Paleontology), previously reported as *L. hedini* (Ludvigsen *et al*., 1989; Taylor *et al*., 1991), were collected from the "Main Zone" of the Gorge Formation in Highgate Gorge, Vermont. Taylor *et al.* (1991) demonstrated that strata assigned to the "Main Zone" in earlier studies span most, if not all, of the *Eoconodontus* Zone, as well as basal strata of the *Cordylodus proavus* Zone. The maximum possible range for *L.* aff. *L. rushtoni* is drawn accordingly (Figure 8). However, most of the trilobites and agnostoids reported by Taylor *et al.* (1991) were recovered from Unit A18 (= Zone 1 of earlier studies), including 3 of the 4 *Lotagnostus* sclerites reported as *L. hedini.* This suggests that the archived specimens of *L.* aff. *L. rushtoni* from Highgate Gorge illustrated by Ludvigsen *et al.* (1989) were collected from that interval, which the conodont data presented by Taylor *et al*. (1991) assign to the *Eoconodontus notchpeakensis* Subzone. For this reason, most of the probable range for *L.* aff. *L. rushtoni* lies within that subzone. Its extension upward into the *C. minutus* Subzone is based on an occurrence in western Newfoundland in a fauna that contains species characteristic of the coeval *Saukiella serotina* Subzone of the *Saukia* Zone. The single specimen of *L.* aff. *L. rushtoni* illustrated herein (Plate 6.14) that is not from the Gorge Formation is a pygidium recovered by J.F. Taylor from a clast in Bed 19 of the Green Point section (Cooper *et al*., 2001). The same clast yielded *Bowmania americana*, an uppermost Sunwaptan species restricted to the *S. serotina* Subzone and equivalent units in various areas of North America (Longacre, 1970; Stitt, 1971; Ludvigsen, 1982; Westrop, 1995). Although the probable range shown for *L.* aff. *L. rushtoni* overlaps with those of the three species in the *L. rushtoni* Fauna in the Windfall, the imprecise placement for all four species within the *Eoconodontus* Zone makes it impossible to establish for certain the age of *L.* aff. *L. rushtoni* relative to the three Windfall species. It might be older, younger, or comparable in age to those species that inhabited the opposite (northern) margin of the paleocontinent.

Although the possible range for *Lotagnostus* aff. *L. rushtoni* (Figure 8) extends upward into the basal Skullrockian, there is no compelling evidence that the species occurs in rocks that young. No macrofossils unequivocally younger than Sunwaptan have ever been recovered from the "Main Zone" at Highgate Gorge, and no collection of the basal Skullrockian *Phylacterus saylesi* Fauna from the limestone conglomerates of the northern Appalachians contains that species (Ludvigsen *et al.*, 1989). The *Phylacterus saylesi* Fauna does contain a species of *Lotagnostus,* but it displays the strong constriction of the pygidial acrolobe typical of *Lotagnostus hedini* and was assigned, although with uncertainty, to that species by Westrop *et al*. (2011). We concur both with their synonymy for *L. hedini* and with the stratigraphic range they provide specifically for what they identify as *Lotagnostus hedini?* in the *P. saylesi* Fauna*,* restricting it to the basal strata of the Laurentian Skullrockian Stage, i.e., the *Eurekia apopsis* Zone and its equivalents.

The range for *Lotagnostus hedini* in Figure 8 is based on all reported occurrences of the species, particularly those in Asia (Lu *et al*., 1984; Lu & Lin, 1984, 1989; Apollonov *et al*., 1988), where associated conodont faunas facilitate precise correlation into the Laurentian biostratigraphy. Thorough summaries of the areas and stratigraphic intervals where it has been reported were provided by Westrop *et al*. (2011), and more recently by Tortello *et al.* (2018), the latter utilizing the relatively narrow range for *L. hedini* to more precisely constrain the age of the *Parabolina frequens argentina* Zone in the Cordillera Oriental of Argentina. Only one correction is required to those summaries; they mistakenly place the range of *L. hedini* in Kazakhstan in the *Euloma limitaris-Taoyuania* Zone of that region, the base of which is confirmed by associated conodonts to coincide with the base of the *Cordylodus proavus* Zone. That horizon is the top of the subjacent *L. hedini* Zone of Apollonov *et al*. (1988), who note the importance of that boundary as the horizon at which *Lotagnostus* and numerous other genera disappear. The *L. hedini* Zone spans approximately the upper half of the *Eoconodontus alisonae* Zone, the eponymous species of which ranges through the entire *Cambrooistodus minutus* Zone and uppermost beds of the *Eoconodontus notchpeakensis* Subzone in the Gorge Formation (Taylor *et al.,* 1991). In Kazakhstan, therefore, *L. hedini* is restricted to the beds below the coincident base of the *C. proavus* and *Euloma limitaris-Taoyuania* zones. Lu *et al*. (1984), however, reported *C. proavus* from the uppermost strata of the *L. hedini* Zone in western Zhejiang, confirming that *L. hedini* ranges upward into the lower part of the *C. provaus* Zone in that region. The contrast in age of the uppermost strata of the *L. hedini* Zone in Zhejiang and Kazahkstan suggests that the base of the *Euloma limitaris-Taoyuania* Zone in Kazakhstan marks an unconformity where the uppermost part of the range of *L. hedini* has been lost to erosion and/or nondeposition.

Content, Age, and Correlation of the *Lotagnostus nolani* Fauna. The older *Lotagnostus*-dominated fauna in the Windfall Formation (Figure 4) includes the following species, listed in decreasing order of abundance: *Lotagnostus clarki* **n. sp.**, *Lotagnostus nolani* **n. sp.**, *Mendoparabolina nyensis* (Taylor, 1976), *Bienvillia eurekensis* **n. sp.**, *Neoagnostus parki* **n. sp.**, *Lotagnostus* cf. *L. obscurus*, *Rhaptagnostus* cf. *R. convergens*, *Homagnostus*? sp., *Micragnostus* cf. *M. intermedius,* and *Machairagnostus* cf. *M. corrugata*. The age of this fauna is much less precisely constrained than that of the *L. rushtoni* Fauna. None of the 3 samples (2935g total) processed for conodonts yielded any diagnostic taxon to allow assignment to an established upper Cambrian zone. Therefore, the conodont data from Ninemile Canyon establish only that the *L. nolani* Fauna is older than the *Eoconodontus* Zone. The olenid trilobites in the fauna allow some inference as to how much older.

In assessing the age of the type material of *Lotagnostus obscurus* (Palmer, 1955) from the Windfall Formation, Westrop *et al.* (2011) used its association with *Bienvillia* to suggest that it is no older than the *Onchonotus richardsoni* Fauna of Newfoundland, which is the oldest of the five Sunwaptan faunas described by Ludvigsen *et al*. (1989) that contains that olenid genus. Palmer (1968) reported *Bienvillia* as a component of his Franconian-2 fauna in eastern Alaska, which Ludvigsen *et al*. (1989) correlated with the next older *Beothuckia duomenta* Fauna. Although this would suggest an earlier appearance of the genus on the northern Laurentian slope, Palmer (1968, p. B14) assigned the single collection that contains *Bienvillia* (D3709-CO) and the collection below it (D4355-CO) to the Franconian-2 fauna with some reservation. In particular, he noted that they lack *Drumaspis* and contain different species of *Onchonotus* and *Richardsonella* than the collections from lower in the Hillard Limestone that definitely represent the Franconian-2 Fauna. Subsequent identification by Ludvigsen *et al.* (1989) of one of those species (*Richardsonella* sp. 3) as *R. megalops*, a species characteristic of the *O. richardsoni* Fauna, casts further doubt on the assignment of those two collections to the Franconian-2 fauna. Another indication of a younger age is that these collections constitute the only occurrences of "*Lauzonella" tripunctata* (synonymized by Ludvigsen *et al*. [1989] with *Dikelocephalina? broeggeri*) in the Franconian-2 Fauna; all others are in collections assigned to the Trempealeauan-1 Fauna, in association with *Tatonaspis alaskensis*. Similar, mid-Sunwaptan ages for the lowest established occurrences of *Bienvillia* on both sides of Laurentia do not, of course, preclude an older occurrence in the Windfall, given that *B. eurekensis* is a new species. It is possible that the significance of *B. eurekensis* in the *Lotagnostus nolani* Fauna is not that it constrains the age of the fauna to that of *Onchonotus richardsoni* Fauna*,* but that it extends the known range of *Bienvillia* downward into older strata.

The Hales Limestone

The *Hedinaspis-Charchaqia* Fauna. The other olenid in the *Lotagnostus nolani* Fauna, *Mendoparabolina nyensis,* provides additional constraints on the age of the fauna by reinforcing a correlation established by *L. nolani* itself with the stratigraphically restricted *Hedinaspis-Charchaqia* Fauna (*HC* Fauna) described by Taylor (1976) from the basal strata of the Hales Limestone in the nearby Hot Creek Range. The holotype of *M. nyensis* (Taylor, 1976) is not only from the same collection (D7130-CO) from the Hales in the Hot Creek section (Figure 9) as the intact specimen of *L. nolani* illustrated (as *L. trisectus*) by Taylor & Cook (1976, text-fig. 29E), it resides on the same small slab of rock (Plate 16.1). The thin (~7m) stratigraphic range of the *HC* Fauna, defined by the concurrent ranges of *Hedinaspis regalis* and *Charchaqia norini*, constitutes only a small part of the much thicker interval (~75m) designated by Taylor (1976, text-fig. 2) as the *Hedinaspis* local range zone, which extends upward to the highest occurrence of *Hedinaspis* sp. As noted in previous studies (e.g. Peng, 1984, 1992; Peng *et al*., 2015), the association with *H. regalis* and *C. norini* strongly supports correlation of the strata containing *L. nolani* in Nevada with the *Lotagnostus punctatus* Zone in China.

Regrettably, identification of the equivalent interval in the biostratigraphy of the Laurentian platform and upper slope is more problematic. Like the *Lotagnostus nolani* Fauna in the Windfall Formation, the *HC* Fauna in the Hales contains no endemic Laurentian taxa, and its age currently can only be estimated through use of faunas that occur in overlying and underlying strata. The age constraints those bounding faunas provide are detailed in the following section. The long-standing and continuing uncertainty as to what horizon within the Laurentian platform biostratigraphy is equivalent in age to the base of Asian *L. punctatus* Zone is illustrated well by the correlation diagram provided by Peng (1992, fig. 5). In that figure, the base of the *L. punctatus* Zone in the column for western Zhejiang based on the work of Lu & Lin (1980, 1984, 1989) projects to a horizon within the upper Steptoean (basal

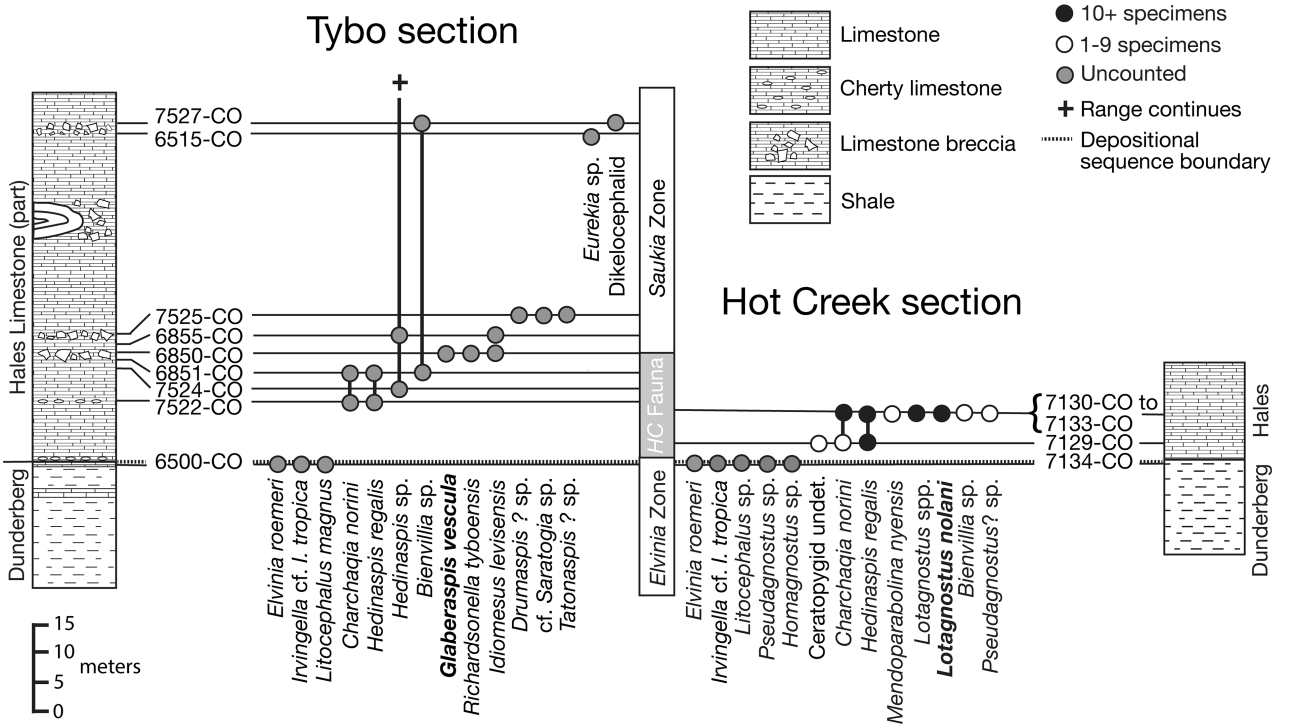

FIGURE 9. Revised trilobite and agnostoid species range chart, Tybo and Hot Creek sections, Hot Creek Range, Nevada (after Taylor, 1976, text-fig. 3). Abbreviation: *HC* Fauna = *Hedinaspis-Charchaqia* Fauna.

Jiangshanian) *Elvinia* Zone in the North American column. In the column representing the succession in northwestern Hunan, the study area of Peng (1992), it is placed significantly higher to align with a horizon in the Sunwaptan (uppermost Jiangshanian) *Illaenurus* Zone in North America. Given that the appearance of the same three species (*L. punctatus, H. regalis,* and *C. norini*) defines the base of the *L. punctatus* Zone in both Zhejiang and Hunan, we consider it highly unlikely that the age of this boundary differs significantly between these adjacent provinces in China as suggested in the correlation figures provided by Lu & Lin (1989, table 9) and Peng (1992) or, for that matter, between Asia and the slope deposits of the Hales as suggested by Landing *et al*. (2011). Our expansion and reappraisal of the biostratigraphic data from the Hot Creek Range (Figure 7), along with a reinterpretation of the nature and significance of the Dunderberg-Hales formation boundary, has resolved some of these issues. It has not, however, refined the correlation into the Laurentian platform biostratigraphy sufficiently to identify the particular zone in which the horizon equivalent in age to the base of the *L. punctatus* Zone lies, or the zone(s) that contain strata equivalent to those that yield the *HC* and *L. nolani* faunas.

Depositional Setting and Claim of Early Jiangshanian Age for *HC* Fauna. The Hales Limestone figured prominently in a series of seminal papers on deep water carbonate facies and associated trilobite faunas, the latter separated into well-preserved *in situ* basinal assemblages of lower slope taxa and "allochthonous" assemblages comprising disarticulated remains of shallow water species transported downslope from shallower water settings (Cook & Taylor, 1975, 1977; Taylor, 1976, 1977). The *HC* Fauna at the base of the Hales is an *in situ* basinal assemblage preserved in very thinly bedded lime mudstone deposited at the base of the northern Laurentian slope. Unlike the Catlin Member at Ninemile Canyon, which is bounded below by the Ninemile Fault (Merriam, 1963), the lower slope deposits that contain the *HC* Fauna in the Hot Creek Range are part of an intact stratigraphic succession. There the Hales lies in depositional (although not necessarily conformable) contact on the underlying Dunderberg Shale. Consequently, trilobites from limestone interbeds at the top of the Dunderberg place a maximum age on the *HC* Fauna and, by extension, the *Lotagnostus nolani* Fauna of the Windfall.

Updated species range charts for the faunas through the relevant stratigraphic interval in the Tybo and Hot Creek sections of Taylor (1976) are provided in Figure 9. The following taxa were identified in the collections of the *HC* Fauna from the Hot Creek section, listed in decreasing order of abundance: *Hedinaspis regalis, Lotagnostus nolani, Lotagnostus* sp., *Charchaqia norini, Mendoparabolina nyensis, Bienvillia* sp., *Pseudagnostus?* sp., and Ceratopygid

indet. Trilobites in the limestone beds at the top of the Dunderberg include characteristic taxa of the lower part of the Laurentian *Elvinia* Zone, establishing the maximum possible age of latest Steptoean (= earliest Jiangshanian) for the *Lotagnostus* species in the *HC* and *L. nolani* Faunas. The close proximity of the lowest collection of the *HC* Fauna to the uppermost *Elvinia* Zone collection in the Hot Creek section of Taylor (1976), where they are separated by less than 2 meters (Figure 9), was likely the impetus for correlation of the *Lotagnostus punctatus* Zone with some part of this uppermost Steptoean zone by Lu & Lin (1989). Landing *et al*. (2011) cited that specific occurrence in the Hot Creek section of the *HC* Fauna only a short distance above a fauna with *Irvingella angustilimbata* (re-identified by Westrop & Adrain [2016] as *Irvingella* cf. *I. tropica,* and so labelled in Figure 9) as evidence for an early Sunwaptan or even latest Steptoean age for the *HC* Fauna. A separate occurrence suggesting an even closer stratigraphic association of these two faunas noted by E. Landing (written comm.) is a report by Palmer (1965) of an *Elvinia* Zone collection (USGS collection D1471-CO) made at a locality in the Tybo area from "...about 10 feet above the base of the Hales …". That is precisely the distance above the base of the Hales that M.E. Taylor's field notes (of July 8, 1971) specify for the lowest collection of the *HC* Fauna (Collection D7129-CO) in the Hot Creek section.

Confirmation of an early Jiangshanian age for the *HC* Fauna in the Hales would be, at the very least, highly problematic for those promoting *Lotagnostus americanus* as the defining taxon for the base of Cambrian Stage 10, given their estimate of late Sunwaptan (latest Jiangshanian) for the horizon in Laurentian successions equivalent in age to the base of the *L. americanus* Zone (*L. punctatus* Zone of earlier papers) in China (Peng & Babcock, 2005; Peng *et al*., 2012, 2014). In defense of that estimate, Peng *et al*. (2015) argued that the early Jiangshanian trilobites (e.g. *Irvingella angustilimbata*) reported in association with the *HC* Fauna in the Hales are redeposited sclerites from allochthonous platform faunas that were reworked into late Jiangshanian deposits. To establish whether there is any co-occurrence in a single collection of the *HC* Fauna with early Jiangshanian taxa, we borrowed all collections from the Hot Creek section, as well as the *Elvinia* Zone collection (D1471-CO) Palmer (1965) reported from 10 feet above the base of the Hales, for examination and additional processing. Taylor (1976) had illustrated neither the *Elvinia* Zone taxa nor the agnostoids in the *HC* Fauna.

Collection D7134-CO is the *Elvinia* Zone collection that Taylor (1976, text-fig. 3) reported from the very base of the Hales in the Hot Creek section, less than 2m below the lowest beds that yielded the *HC* Fauna. After additional processing, this collection comprises 43 trilobite sclerites and 27 agnostoid specimens. As reported by Taylor (1976), the trilobites include characteristic late Steptoean genera such as *Irvingella, Elvinia,* and *Litocephalus.* Although other genera are present, none represents a stratigraphically higher level of the Cambrian to support the interpretation that the basal Jiangshanian bioclasts have been reworked. The same is true of collection D1471-CO, which now consists of 59 trilobite sclerites and 12 agnostoid specimens. It contains the same diagnostic *Elvinia* Zone genera and no trilobite taxa characteristic of younger zones. Although both collections contain numerous agnostoid specimens, all are assignable to either *Pseudagnostus* or *Homagnostus*; *Lotagnostus* is not represented. Similarly, reprocessing of the collections of the *HC* Fauna from the Hales in the Hot Creek section produced no *Elvinia* Zone taxa to support the claim of sedimentary reworking of older bioclasts. While it is possible, or even likely that some mixing of faunas of different age occurred during deposition of the limestone conglomerates from which Taylor (1976) described the allochthonous faunas of the *Saukia* Zone higher in the Hales Limestone, there is no evidence that the *Elvinia* Zone faunas were re-deposited into sediments younger than early Jiangshanian. With no direct association of diagnostic taxa of both the *Elvinia* Zone and *HC* Faunas in any collection, the evidence for an early Jiangshanian occurrence of *Lotagnostus* in the Hales is reduced to the proximity of older Jiangshanian faunas in subjacent and/or overlying strata.

Age Constraints for *HC* Fauna from overlying strata. It was not only the proximity to subjacent *Elvinia* Zone faunas that suggested a possible middle to early Jiangshanian age for the *HC* Fauna in the Hales at the outset of our study. Collections a short distance above the highest occurrence of the *HC* Fauna in the Tybo Canyon section of Taylor (1976, text-fig. 2; Figure 9 herein), which provide a minimum age for *Lotagnostus nolani,* include a collection from approximately 21m above the base of the Hales that contains two trilobite genera that invite assignment to the lower Sunwaptan. Taylor (1976) identified two taxa in collection D7525-CO as "cf. *Saratogia"* and "*Drumaspis*? sp". Both genera characterize faunas below the *Illaenurus* Zone and, like the close proximity to *Elvinia* Zone faunas, this might have played a role in correlation of the base of the *L. punctatus* Zone with uppermost Steptoean strata in earlier studies. These identifications were, however, clearly tentative, and information from more recent work reveals that two species Taylor (1976) illustrated from a slightly lower collection confirm that D7525-CO cannot

be that old. *Idiomesus levisensis* is one of the species Taylor (1976, pl. 3, figs 12,13) illustrated from collection D6850-CO, which was recovered from approximately 3m below collection D7525-CO. *Idiomesus levisensis* is one of several species of that genus that succeed one another up-section through the Sunwaptan Stage, and it is restricted to the uppermost part of the *Illaenurus* Zone (Ludvigsen & Westrop, 1986, fig. 7). *Idiomesus infimus* represents the genus in the lower half (or more) of the *Illaenurus* Zone. What Taylor (1976, Pl. 3, Fig. 21) identified as "?*Leiocoryphe* sp. A" in D6850-CO is referred to in more recent papers as *Glaberaspis vescula* (Stitt, 1971). That species of *Glaberaspis* is a reliable indicator of proximity to the base of the *Eoconodontus* conodont Zone, occurring only in the uppermost strata of the *Illaenurus* Zone and perhaps very basal beds of the overlying *Saukiella junia* Subzone of the *Saukia* Zone (Miller *et al*., 2015, fig. 7). Collection D6850-CO is, therefore, unequivocally late Sunwaptan in age and, therefore, D7525-CO cannot be as old as early Sunwaptan.

Re-interpretation of the Dunderberg-Hales boundary as major sequence boundary. The re-assignment of collection D6850-CO in the Tybo Canyon section to the top of the *Illaenurus* Zone or base of the overlying *Saukia* Zone, combined with the confirmation of an early Jiangshanian (*Elvinia* Zone) age for collection D6500-CO at the top of the Dunderberg in the same section, prompted a re-evaluation of the depositional history of the Dunderberg-Hales boundary interval. Using the scale provided for the Tybo Canyon measured section by Taylor (1976), we determined that the stratigraphic distance between collections D6500-CO (lower *Elvinia* Zone) and D6850-CO (uppermost *Illaenurus* Zone) is only 18.2m. That same biostratigraphic interval spans more than 350m of strata in the coeval carbonate platform deposits of the Egan Range a short distance away in eastern Nevada (Taylor & Cook, 1976, text-fig. 2). The thicknesses reported from Alberta (Chaba Creek section of Westrop, 1986) and Oklahoma (Stitt, 1971) are only slightly thinner, in the 250m to 300m range, but those sections also start in the uppermost *Elvinia* Zone rather than in its lower part. The true thicknesses are, therefore, likely to be even closer to that in the Egan range.

The age and depositional setting of the Dunderberg-Hales succession in the Hot Creek Range provide a straightforward explanation for the exceptionally thin interval separating lower *Elvinia* Zone and *Saukia* Zone faunas in that area. We attribute the greatly attenuated thickness to an unconformity at the formation boundary and/or extreme condensation of the basal 17 to 18m of the Hales due to starved basin deposition through the latest Steptoean and early Sunwaptan. Slope and basinal environments frequently experience sediment starvation when major transgressions provide accommodation space on the shelf and arrest downslope transport of sediment from the shelf margin to deep-water environments. It is more than reasonable to invoke that process for the interval involved at the base of the Hales, as it coincides with the major transgression that expanded marine deposition shoreward across much of Laurentia during the deposition of the basal strata of the Sauk III supersequence that compose the upper part of the *Elvinia* Zone and lower part of the *Taenicephalus* Zone (Taylor *et al*., 2012).

Our interpretation of the formation contact as a major depositional sequence boundary that records the onset of starved basin conditions is supported by a marked contrast in lithologies between the uppermost Dunderberg and basal Hales strata. As noted by Taylor (1976), the boundary between the two formations coincides with a change in color of shale partings from olive green below to dark gray or black above. The bioclastic limestone beds above and below the boundary are strikingly different, not only in the taxonomic makeup of the fauna, but also in color, texture, and state of preservation of the fossils. The *in situ* fauna described from the base of the Hales consists of small specimens, some still articulated, sparsely distributed, and slightly flattened (Plate 16.8, 16.9) on parting surfaces of very thin beds of dark lime wackestone to fine grainstone. The thin to medium beds that contain the *Elvinia* Zone fauna consist of light brown, coarse bioclastic grainstone in which much larger, disarticulated trilobite and agnostoid sclerites occur in abundance, distributed throughout each bed. This contrast in color, texture, and taphonomy is helpful in this situation, because it makes it possible to confidently distinguish material from the limestone beds deposited in the early Jiangshanian (lower *Elvinia* Zone) that lie below the sequence boundary from that collected above it, which accumulated under more dysoxic conditions. Accordingly, we assign the uppermost bed that yielded collection D1734-CO in the Hot Creek section to the Dunderberg (Figure 9), rather than considering it the basal bed of the Hales as Taylor (1976, text-fig. 3) did. Collection D1471-CO, collected by Palmer in 1953 from the Tybo Canyon area (but not from the Tybo Canyon section measured much later by Taylor [1976]) is identical in all respects to collection D1734-CO, and strikingly different in lithology from all the collections of the *HC* Fauna. The contrast in those physical characteristics further reinforces the evidence provided by the lower *Elvinia* Zone fauna it contains (and the absence of *Hedinaspis, Charchaqia* and *Lotagnostus)* that it was collected from a bed below the sequence boundary, not above it.

Consequently, in our opinion the biostratigraphic data from the Hot Creek Range do not confirm an early Jiangshanian occurrence of *Lotagnostus.* The stratigraphic proximity of the *HC* Fauna to *Elvinia* Zone faunas is the product of its occurrence within a severely condensed interval directly above a major sequence boundary. In fact, the data from the Hot Creek range alone actually do little to constrain the age of the *Hedinaspis-Charchaqia* Fauna, confirming only that it is no older than middle Steptoean (lower *Elvinia* Zone) and no younger than upper Sunwaptan (uppermost *Illaenurus* Zone). The strongest evidence for the middle to late Sunwaptan age shown for the species of the *Lotagnostus nolani* Fauna by their probable range bars (Figure 8) is provided by the stratigraphic succession documented by Peng (1992) in northern Hunan. Despite well-founded concerns expressed by Westrop & Adrain (2016) regarding the limited information available for many species assigned in earlier studies to *Irvingella angustilimbata,* particularly those promoting its utility as an auxiliary index for the base of the Jiangshanian (e.g, Peng *et al*., 2012), equivalence of the Laurentian *Elvinia* Zone with at least some part of the *Agnostotes clavatus-I. angustilimbata* Assemblage Zone of Peng (1992) remains likely. As previously noted, we also consider the correlation of the *HC* Fauna in the Hales with the *Lotagnostus punctatus-Hedinaspis regalis* Zone reasonable. Given those equivalences, the occurrence of approximately 250m of strata assigned to three zones and an unnamed interval between the *A. clavatus-I. angustilimbata* and *L. punctatus-H. regalis* Zones in northwestern Hunan elevates the probable range into the mid-Sunwaptan (Figure 8). It remains uncertain, however, as to whether the correlative strata lie within the lower part of the *Illaenurus* Zone or an older zone in the Lower Sunwaptan.

Deficiencies of *Lotagnostus* for defining the base of Cambrian Stage 10

Contrary to the claim of Peng *et al.* (2015, p. 302) that "…*Lotagnostus americanus* provides the same favorable characteristics as other agnostoids such as *Ptychagnostus atavus, Lejopyge laevigata, Glyptagnostus reticulatus,* and *Agnostotes orientalis* ...", multiple studies on Laurentian occurrences of *Lotagnostus*, including our own, have established that it lacks several of the indispensable attributes that made those four species suitable for defining the bases of global Cambrian stages. First of all, the taxonomy of *Lotagnostus* is far more controversial. Secondly, in addition to the strongly divergent opinions among specialists regarding the acceptable range of morphologic variation within *L. americanus*, which in our view is best restricted to the holotype for the reasons already noted and discussed in greater detail in Systematic Paleontology, *Lotagnostus* was not as broadly distributed environmentally. Unlike the four agnostoids already in use as indices for global stages, whose environmental tolerances allowed them to occupy shallower waters where they were preserved in association with the endemic taxa of many paleocontinents, *Lotagnostus* in Laurentia was largely restricted to very deep/cold waters of lower slope and basinal settings (Figure 6). We know not only within which zone the First Appearance Datum (FAD) of those other agnostoid species lie in Laurentia, but where within those zones, often to subzone level. In contrast, neither the fauna from the Hales, nor our rich faunas from the Windfall Formation, contain any taxa that constrain the position of the equivalent horizon in shallow Laurentian successions to less than approximately half a stage Figure 8). This is an unacceptable level of imprecision on one of the major Cambrian paleocontinents for a global stage boundary. Selection of a *Lotagnostus*-based GSSP for the base of Cambrian Stage 10 despite these shortcomings would be particularly unfortunate given the availability of an alternative horizon that does not suffer from such deficiencies; the FAD of the conodont *Eoconodontus notchpeakensis* (Landing *et al*., 2011; Miller *et al*., 2011, 2015).

Systematics

Repositories. Types and illustrated specimens collected by J.F. Taylor and Loch are housed in the Carnegie Museum of Natural History (CM), Pittsburgh, Pennsylvania or National Collection of Invertebrate and Plant Fossil Types (GSC) in Ottawa, Canada. Re-illustrated specimens from collections of The Natural History Museum, London bear the prefix NHM. Trilobites collected by M.E. Taylor and conodonts illustrated herein are reposited at the Smithsonian National Museum of Natural History (USNM): conodont specimens from collections 5/22/08C and 5/22/08D are assigned USNM locality numbers USGS CO-12121 and USGS CO-12122, respectively.

Methods and Terminology. Trilobite specimens were inked and whitened with magnesium oxide in preparation for photography. Abundance data are provided in a cranidia-pygidia-librigenae (C-P-L) format. Measurements

used in morphologic comparisons were made digitally on enlarged images, utilizing dimensions acquired with a calibrated microscope ocular. Ratio values are calculated means; minimum and maximum values are presented parenthetically. Morphologic terms used are those recommended by Whittington (1997) with additional reference to Robison (1982) and Shergold *et al.* (1990) for aspects of agnostoid morphology. Usage of open nomenclature follows that recommended by Bengtson (1988) wherein "cf." denotes possible but uncertain assignment to the species designated, and "aff." is used to identify a similar but definitely separate species.

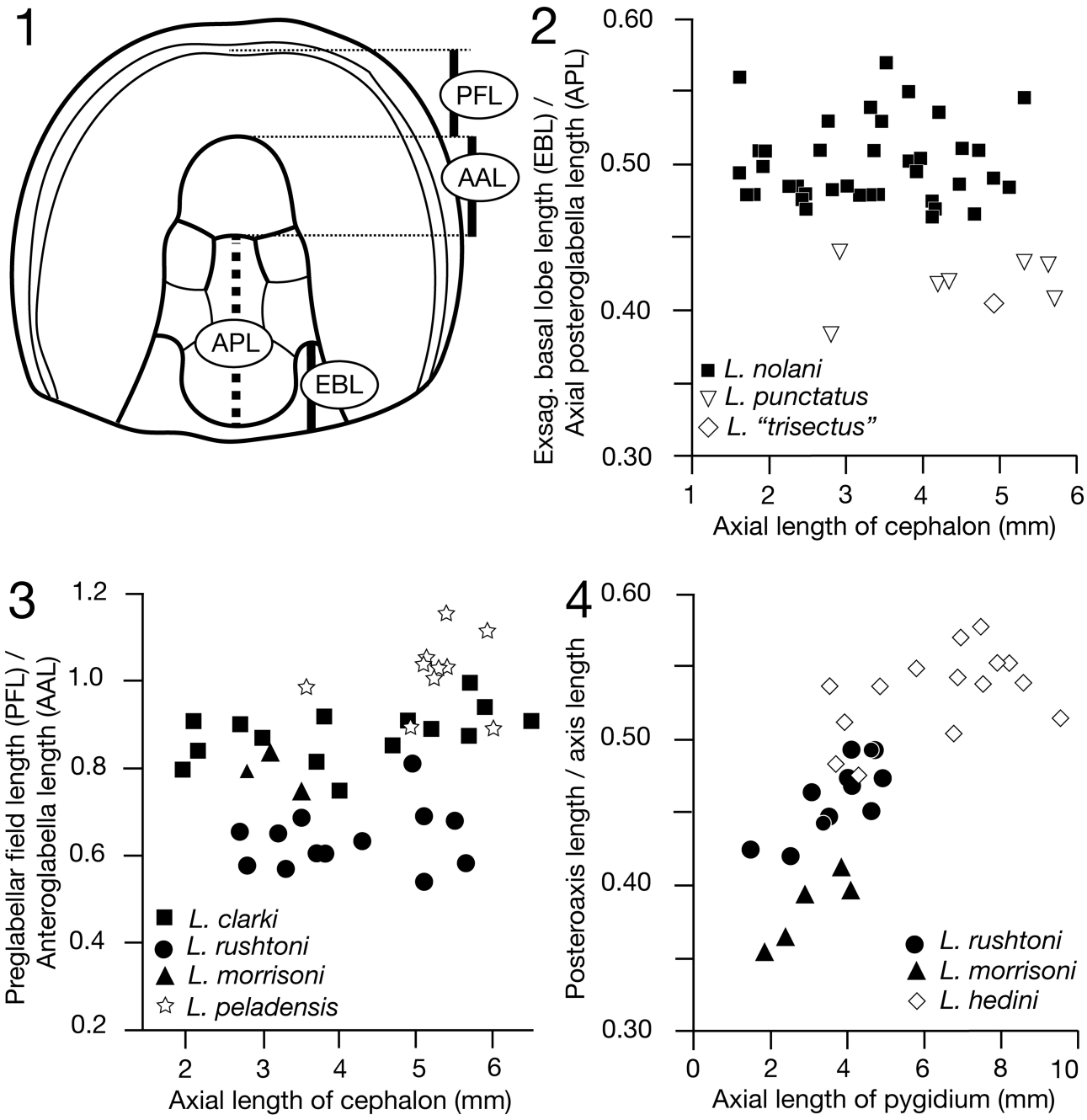

FIGURE 10. Morphometric comparisons of some *Lotagnostus* species. (1) Dimensions measured on cephala. Abbreviations: AAL, Axial Anteroglabella Length; APL, Axial Posteroglabella Length; EBL, Exsaggital, Basal lobe Length; PFL, Preglabellar Field Length. (2) Scatter plot of EBL/APL ratio versus length of the cephalon for 3 species of *Lotagnostus*. *L. "trisectus"* refers to species identified by that name from Sweden in previous studies. (3) Scatter plot of PFL/AAL ratio versus length of the cephalon for 4 species of *Lotagnostus*. (4) Graphic comparison of posteroaxis length/length of axis as a function of pygidial length (excluding articulating half ring) for 3 species of *Lotagnostus*.

In describing the partitioning of the pygidial axis in *Lotagnostus,* we interpret the furrows that bound the central lobe of the tripartite M1 as forward extensions of the longitudinal furrows that trisect M2, rather than following Westrop & Landing (2016) and Tortello (2018), who suggested that they represent the anterior deflection of F1 to intersect the articulating furrow. We note that *Innitagnostus* Opik (1967, text-fig. 12, pl. 58, figs 3–4), another member of the Subfamily Agnostinae, exhibits a complete, transaxial F1 furrow while the anterior lobe still appears trisected. Moreover, F1 shallows over the midline in larger pygidia of *L. rushtoni* (e.g. Plate 12.11).

Length ratios for basal glabellar lobes: The utility of the length of basal glabellar lobes for discrimination of species within *Lotagnostus* has been debated at length. Some (Ludvigsen *et al*., 1989; Rushton (2009); Westrop *et al*., 2011) consider it a useful character while others (Peng *et al*., 2015) dismiss the variation in that feature as primarily taphonomic. In their critique, Peng *et al*. (2015, fig. 10) utilized a ratio designated the BLL:PGL, calculated by dividing the total length of the basal lobe by the length of the posteroglabella. In the present study, we employed a superior metric referred to herein as the EBL/APL ratio, which compares the lengths of the basal lobe and posteroglabella measured along different lines (Figure 10.1). The Exsagittal Basal lobe Length (EBL) is the distance from the anterior-most point (the tip) of the basal lobe to the posterior margin (back of the basal lobe) measured parallel to the midline. It differs from the Basal Lobe Length (BLL) of Peng *et al*. (2015, fig. 10) in being measured along an exsagittal line, rather than spanning the total length from the anteriormost to posteriormost points regardless of whether they lie along the same line parallel to the midline. The Axial Posteroglabella Length (APL) is the distance along the midline from the center of F3 to the glabellar culmination. For specimens with a node at the glabellar termination, the measurement was to the base of the node. It differs from the Posteroglabellar Length (PGL) of Peng *et al*. (2015) in being measured along the midline, rather than exsagittally from the back of the basal lobe to the intersection of F3 with the axial furrow.

The EBL/APL ratio (Figure 10.2) is typically higher than the BLL/PGL ratio for the same cephalon because the denominator is greater, due to 1) the anterior convexity of F3, which places its junction with the axial furrow junction farther forward than where it crosses the midline and 2) the most posterior point at the back of the basal lobe commonly lying some distance behind the glabellar culmination. Conversely, the length of the basal lobe measured exsagittally (EBL) is commonly somewhat less than the total length, not constrained to a line parallel to the axis (PGL), but that difference is small compared to the difference between the APL and PGL.

The EBL/APL ratio has several advantages over the BLL/PGL ratio. First, it is based on two totally independent lengths of basal lobe and posteroglabella, whereas the length of the posteroglabella in the PGL is commonly in part controlled by the length of the basal lobes. The PGL also can be affected by the *position* of the basal lobes if they are situated far enough back that their posterior margins lie behind the glabellar culmination. This relationship becomes more problematic when, as is commonly the case, the basal lobes are displaced by compaction and/or tectonic deformation. Such displacement does not distort the EBL/APL ratio. An advantage of the EBL over the BLL is that measurement of the latter is problematic in some agnostoids whose basal lobes merge adaxially with the occipital band behind the axis with no clearly defined boundary between those two elements. Consequently, a specific, posteriormost point on the back of the basal lobe is not determinable.

Phylum Arthropoda Siebold & Stannius, 1845

Class Trilobita Walch, 1771

Order Olenida Adrain, 2011

Family Olenidae Burmeister, 1843

Subfamily Oleninae Burmeister, 1843

Discussion. We follow Henningsmoen (1957) and Ludvigsen (1982) in considering the Subfamily Triarthrinae Ulrich *in* Bridge, 1930 as a junior subjective synonym of the Oleninae Burmeister, 1843.

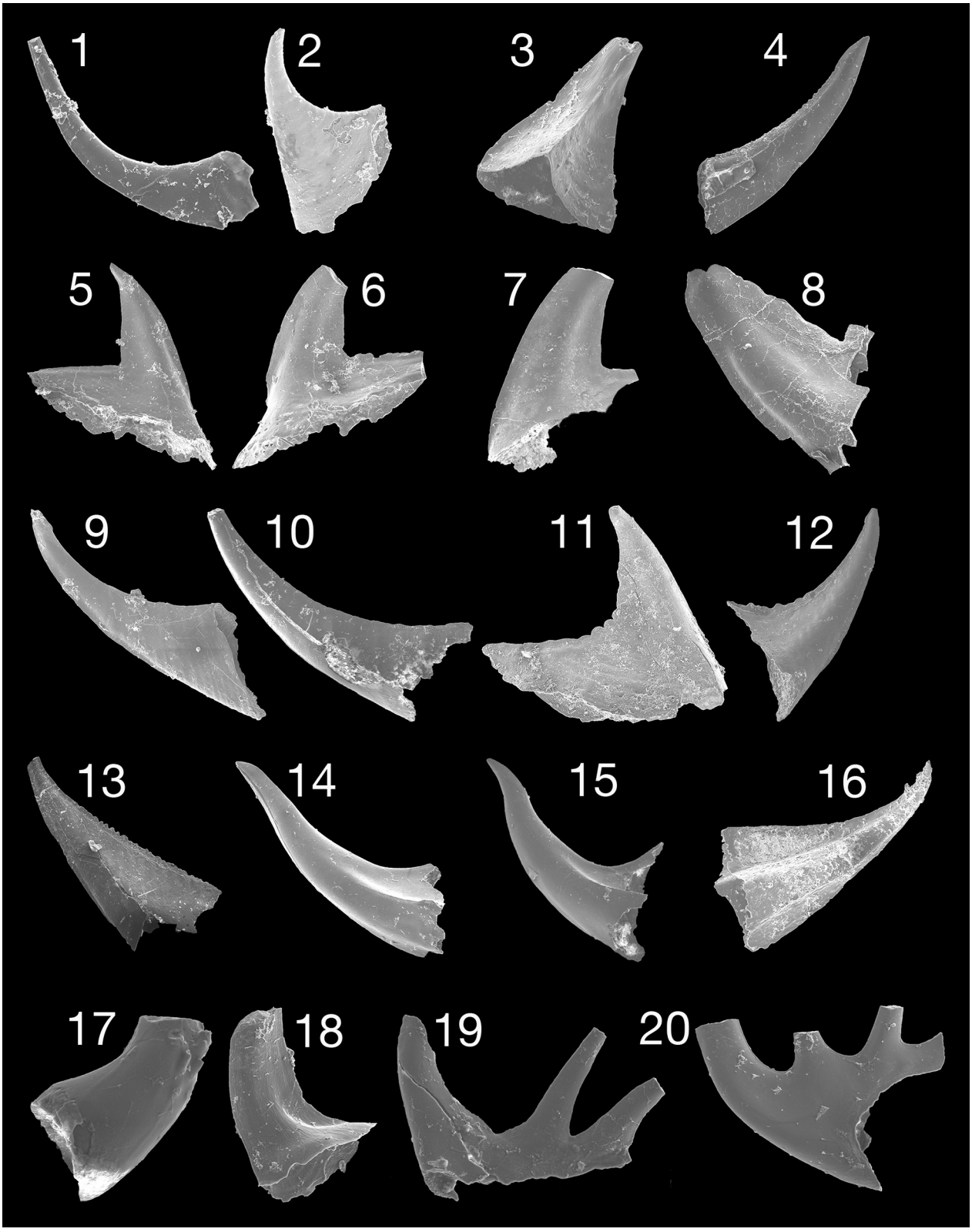

.....Plate legend provided on the next page

PLATE 2. SEM photomicrographs of selected conodonts from the Windfall Formation, Ninemile Canyon section, Eureka County, Nevada. Illustrated specimens reposited in the Paleontology Department collections, Smithsonian National Museum of Natural History (USNM). Conodont specimens from collections 5/22/08C and 5/22/08D are assigned USNM locality numbers USGS CO-12121 and USGS CO-12122, respectively. Specimens recovered from J.E. Repetski's collections identified as "JR". Specimens from M.E. Taylor's USGS collections identified as "Dxxxx-CO" with "D" for Denver catalog and "-CO" for Cambrian-Ordovician catalog numbers. 1. *Eoconodontus notchpeakensis*. USNM 775557, lateral view, x157, D3383-CO, *Eoconodontus* Zone. 2. *Prooneotodus gallatini*. USNM 775567, lateral view, X57, CO-12122, *Eoconodontus* Zone. 3. *Furnishina furnishi*. USNM 775558, posterior view, x104, CO-12121, *Eoconodontus* Zone. 4. *Proconodontus tenuiserratus bicostatus* Szaniawski and Bengtson. USNM 775559, lateral view, x77, D3383-CO, *Eoconodontus* Zone. 5-8. *Cambrooistodus cambricus*, all posterior views, *Eoconodontus* Zone. 5. USNM 775550, x45, CO-12122. 6. USNM 775551, x48, CO-12122. 7, USNM 775552, x 56, CO-12121. 8, USNM 775553, x26, D3383-CO. 9, 10. *Proconodontus muelleri,* both *Eoconodontus* Zone. 9. USNM 775561, lateral view, x44, CO-12122. 10. USNM 7755562, lateral view with long, longitudinal fracture, x69, CO-12121. 11-13. *Proconodontus serratus,* all lateral views, *Eoconodontus* Zone. 11. USNM 775563, x50, CO-12122. 12. USNM 775564, x37, CO-12122. 13. USNM 775565, x39, D3383-CO. 14, 15. *Proconodontus* **n. sp.**, lateral views, *Eoconodontus* Zone. 14. USNM 775554, x73, CO-12122. 15. USNM 775555, x49, CO-12121. 16. *Diaphanodus* **n. sp.**? USNM 775568, lateral view, x64, CO-12122, *Eoconodontus* Zone. 17. *Hirsutodontus hirsutus*. USNM 775556, lateral view, x238, JR 6-18-76F, *Cordylodus proavus* Zone. 18. *Utahconus utahensis*. USNM 775566, lateral view, x132, JR 6-18-76H, *Cordylodus lindstromi* Zone. 19. *Cordylodus andresi*. USNM 775560, lateral view, x210, JR 6-18-76F, *Cordylodus proavus* Zone. 20. *Cordylodus lindstromi*. USNM 775569, lateral view, x146, JR 6-18-76H, *Cordylodus lindstromi* Zone.

Bienvillia Clark, 1924

Type species. *Dikelocephalus*? *corax* Billings, 1865, by original designation, from the Lévis Formation, Quebec, Canada.

Emended diagnosis. Olenine with moderately inflated glabella with well impressed S1 and S2 lateral glabellar furrows, S3 and S4 faintly impressed to absent, S3 not reaching axial furrow, and S4 directed anteriorly adaxially; occipital node present; preglabellar field convex and declined from axial furrow, very short anterior border; anterior branch of facial suture convergent anterior to palpebral lobe. Modified from Rasetti (1944), C. Poulsen (*in* Harrington (1959), and Ludvigsen and Tuffnell (1983).

Other species. *Bienvillia angelini* (Linnarsson, 1869); *B. shinetonensis* (Lake, 1913); *B. rectifrons* (Harrington, 1938); *B. tetragonalis* (Harrington, 1938); *B.*? *australis* (Rusconi, 1951a); *B. terranovica* Rasetti, 1954; *B. parchaensis* (Harrington & Leanza, 1957); *B. stikta* Fortey, 1974; *B. grandis* Robison & Pantoja-Alor, 1968; *B.* cf. *B. corax* Ludvigsen *et al.,* 1989; *B. eurekensis* **n. sp.**

Bienvillia eurekensis n. sp.

(Plate 3)

Diagnosis. A species of *Bienvillia* with a subrectangular glabella with evenly rounded anterolateral corners, a long preglabellar field that is equal in length (sag.) to that of the occipital ring, and S1 lateral glabellar furrows that do not connect across the axis.

Etymology. Named after Eureka County, Nevada.

Material and occurrence. Holotype CM 41320 is a cranidium from collection 5/22/08B; assigned specimens include 4 cranidia CM 41321-41324, 1 pygidium CM41326, and 1 librigena CM 41325 from collection 5/22/08B; and 3 cranidia USNM 775713–775715, 1 pygidium USNM 775717, and 1 librigena USNM 775716 from USGS collection D3362-CO. *Lotagnostus nolani* Fauna: collections 5/22/08B (139-1-9) and D3362-CO (12-1-4) from the Windfall Formation at Ninemile Canyon, Nevada.

Description. Cranidium subtrapezoidal in outline; of moderate size compared to associated polymeroids, up to 6mm in length; moderate in convexity (sag., tr.). Prominent subrectangular glabella with evenly rounded anterolateral corners, glabellar length exclusive of occipital ring 60% of total cranidial length (59-65%); glabellar length (sag.) 83% (79-89%) of maximum glabellar width (tr.); slightly keeled in some specimens, moderately convex (tr.) to stand in moderate relief above adjacent fixigenae, slightly convex (sag.) to descend gently into preglabellar furrow.

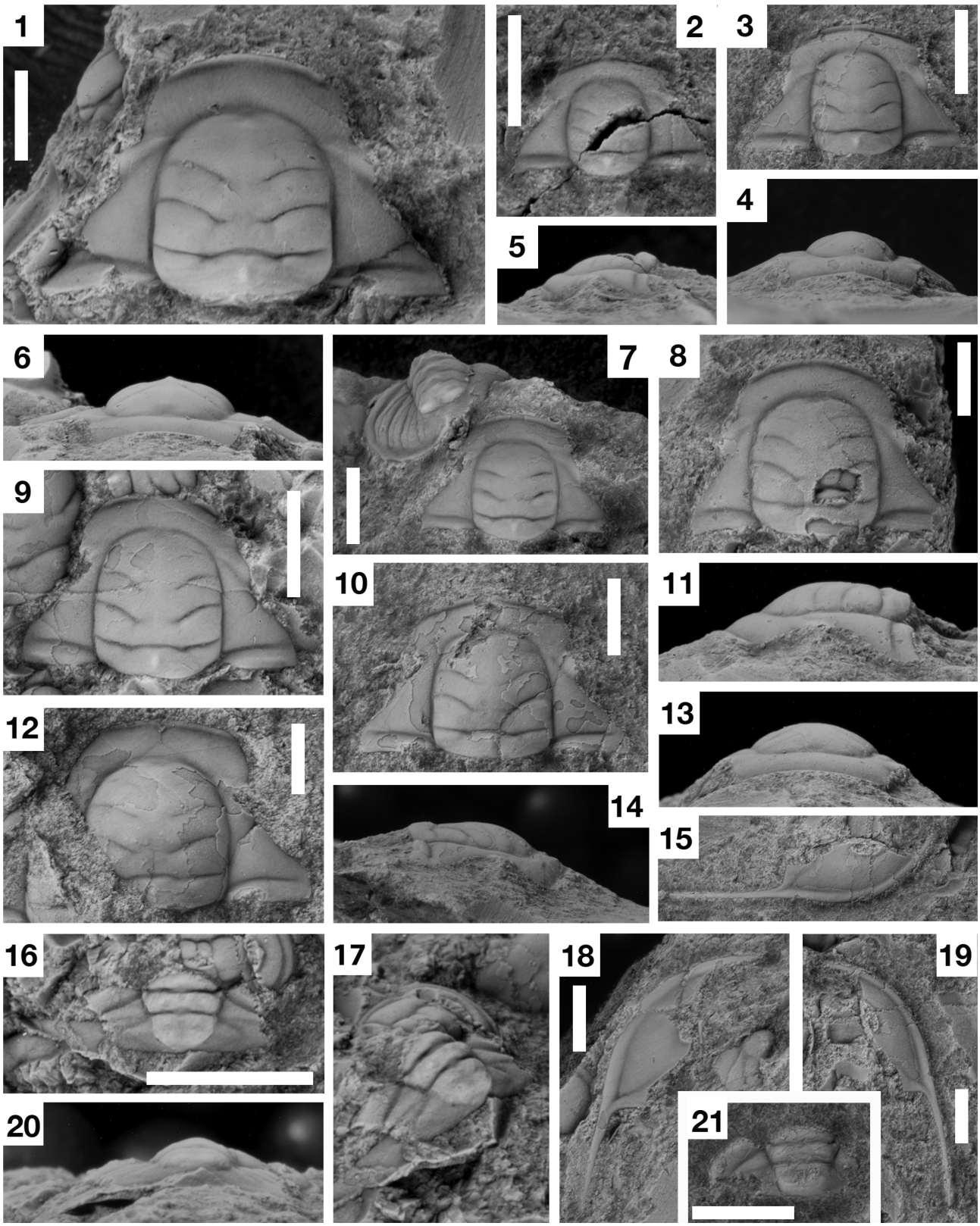

PLATE 3. *Bienvillia eurekensis* **n. sp.** Each white scale bar represents 2mm. 1, 6. Cranidium, holotype**,** CM 41320, from 5/22/08B, dorsal and anterior views. 2, 5. Cranidium, CM 41321, from 5/22/08B, dorsal and left lateral views. 3, 4. Cranidium, USMN 775713, from D3362-CO, dorsal and anterior views. 7. Cranidium, CM 41322, with *Mendoparabolina nyensis,* from 5/22/08B, dorsal view. 8, 11, 13. Cranidium, CM 41323, from 5/22/08B, dorsal, left lateral, and anterior views. 9. Cranidium, CM 41324, from 5/22/08B, dorsal view. 10, 14. Cranidium, USMN 775714, from D3362-CO, dorsal and right lateral views. 12. Cranidium, USMN 775715, from D3362-CO, dorsal view. 15, 19. Right librigena, CM 41325, from 5/22/08B, external and dorsal views. 16, 17, 20. Pygidium CM 41326, from 5/22/08B, dorsal, posterior oblique and posterior views. 18. Left librigena, USMN 775716, from D3362-CO, dorsal view. 21. Pygidium, USMN 775717, from D3362-CO, dorsal view.

Axial furrows moderately impressed, subparallel along glabella, curved adaxially from occipital furrow to posterior margin forming rounded posterolateral extremity to occipital ring. Preglabellar furrow moderately impressed, slightly shallowing and widening across midline. Four pairs of lateral glabellar furrows: S1 well impressed, slightly shallowed abaxially, curved, slightly greater than 33% maximum glabellar width, terminate adaxially in short (tr.), transverse segment; S2 well impressed, slightly shallowed abaxially, curved, approximately 33% maximum glabellar width; S3 absent or very faintly impressed, slightly curved, short (tr.), 10-15% of maximum glabellar width, positioned in front of proximal half of S2; S4 absent or very faintly impressed, nearly straight, short, 15-20% of maximum glabellar width, directed antero-laterally at approximately 20 degrees from transverse line from intersection with axial furrow opposite proximal end of eye ridge. Occipital furrow tripartite with central, anteriorly convex, slightly shallower and wider (sag.) segment constituting 40% of width (tr.); lateral segments well impressed, directed slightly anteriorly abaxially, nearly reaching the axial furrow. Occipital ring moderate in length (sag.), 18% (16-22%) of cranidial length; low, slightly elongate occipital node of moderate size centered near midlength (sag.). Anterior margin an even curve viewed dorsally, low anterior arch in anterior view. Anterior border a narrow (sag.), upturned rim, less than 5% of cranidial length, very gently tapering abaxially; anterior border furrow faintly to moderately impressed, shallowing across midline. Preglabellar field moderate in length (sag.), 18% (16-19%) of cranidial length; moderately convex dorsally. Preocular area narrow (tr.), slightly convex, moderately declined toward anterolateral corners. Faint radiating genal caecae cover preglabellar field and preocular area. Low eye ridge intersects axial furrow opposite S4 glabellar furrow; merges distally with short, slightly upturned palpebral lobe; length (exsag.) of palpebral lobes 33% of glabellar length exclusive of L0, centered slightly anterior to distal end of S2, end posteriorly near midlength of L2, at approximate mid-length of glabella. Palpebral areas narrow, 25-33% of glabellar width at palpebral lobe midlength, short (exsag.), 25% of cranidial length; slightly declined (tr., exsag.). Posterior area triangular in outline, long (exsag.), approximately 33% cranidial length; slightly convex, moderately declined; bear straight, moderately impressed posterior border furrow. Anterior branch of facial sutures gently curved and slightly convergent from palpebral lobes to anterior border furrow, then sharply turned adaxially. Posterior branch of facial suture divergent from posterior end of palpebral lobes at approximately 45 degrees.

Librigenae crescentic in outline with long, slender genal spine approximately the length (exsag.) of the genal field; prominent, adaxially tapering anterior extension of border slightly longer than the length (exsag.) of the eye; lateral margin curved anterior to posterior end of palpebral lobe, continues straight posteriorly. Genal field narrow (tr.), slightly convex dorsally, slightly declined. Lateral border narrow (tr.) increasing slightly in width toward genal angle; posterior border narrows abaxially; lateral and posterior border furrows broad, faintly impressed, slightly deeper where they intersect at approximately 60º angle.

Pygidium known only from fragmentary material; transverse, more than three times as wide (tr.) as long. Moderately tapered pygidial axis with articulating half-ring, two axial rings, terminal axial piece; articulating and first inter-ring furrow moderately impressed, second inter-ring furrow very faintly impressed separating poorly defined second ring and terminal axial piece; terminal axial piece with two faint lateral knobs; axis extends to pygidial margin. Pleural fields with moderately impressed anterior pleural furrow, faintly impressed second pleural furrow, both directed slightly posteriorly. Very faint interpleural furrows roughly perpendicular to midline.

Discussion. The association of cranidia and librigenae for *Bienvillia eurekensis* is straightforward given the smooth surfaces on the fixigenae and the genal field of the librigena. The associated pygidium is the only other polymeroid pygidium available from collection 5/22/08B. Several other species assigned to *Bienvillia* possess pygidial axes with two rings and a terminal axial piece, consistent with the association of sclerites from the Windfall.

Taylor (1976, p. 689, pl. 2, figs 10–11) illustrated *Bienvillia* sp. from the Hales Limestone from the nearby Eureka mining district, Eureka County, Nevada. *Bienvillia eurekensis* differs from Taylor's illustrated specimens in exhibiting a glabella with anterolateral corners that are more rounded, larger palpebral lobes which extend posterior to S2, and an S1 that is discontinuous across the axis.

Bienvillia eurekensis **n. sp.** differs from the type species, *B. corax* (Billings, 1865; see Ludvigsen *et al.*, 1989, p. 15, pl. 4, figs 18–22), in having a subrectangular glabella rather than one that is ovate and which bears S1 and S2 furrows that are incomplete across the axis rather than transglabellar. Furthermore, the preglabellar field in *B. eurekensis* is long, subequal in length to the occipital ring; the preglabellar field of *B. corax* is shorter than the occipital ring.

Tortello (2014, p. 303, fig. 6.3, 6.4) reillustrated *Bienvillia*? *australis* (Rusconi, 1951a, p. 3, fig. 3a–3c) from the Furongian of Argentina. The cranidium of *Bienvillia eurekensis* differs from that of *B.*? *australis* in having a

subrectangular glabella, rather than one that is markedly tapered, a longer preglabellar field, and a S1 furrow that is not continuous across the axis. The pygidia of these species are more distinct: the axis of *B.*? *australis* has three axial rings, rather than two, and does not extend to the posterior margin.

The remaining species previously assigned to *Bienvillia* are all Tremadocian or younger in age (Rasetti, 1954; Harrington & Leanza, 1957; Robison & Pantoja-Alor, 1968; Fortey, 1974; Ludvigsen & Tuffnell, 1983). All but one of these younger species display significantly shorter (sag.) preglabellar fields than *B. eurekensis.* The exception, *B. terranovica* Rasetti (1954), differs from *B. eurekensis* in having only faintly impressed glabellar furrows, a much shorter (sag.) occipital ring that tapers rapidly abaxially, weakly developed eye ridges, and broader (tr.) librigenae that lack a distinct border furrow.

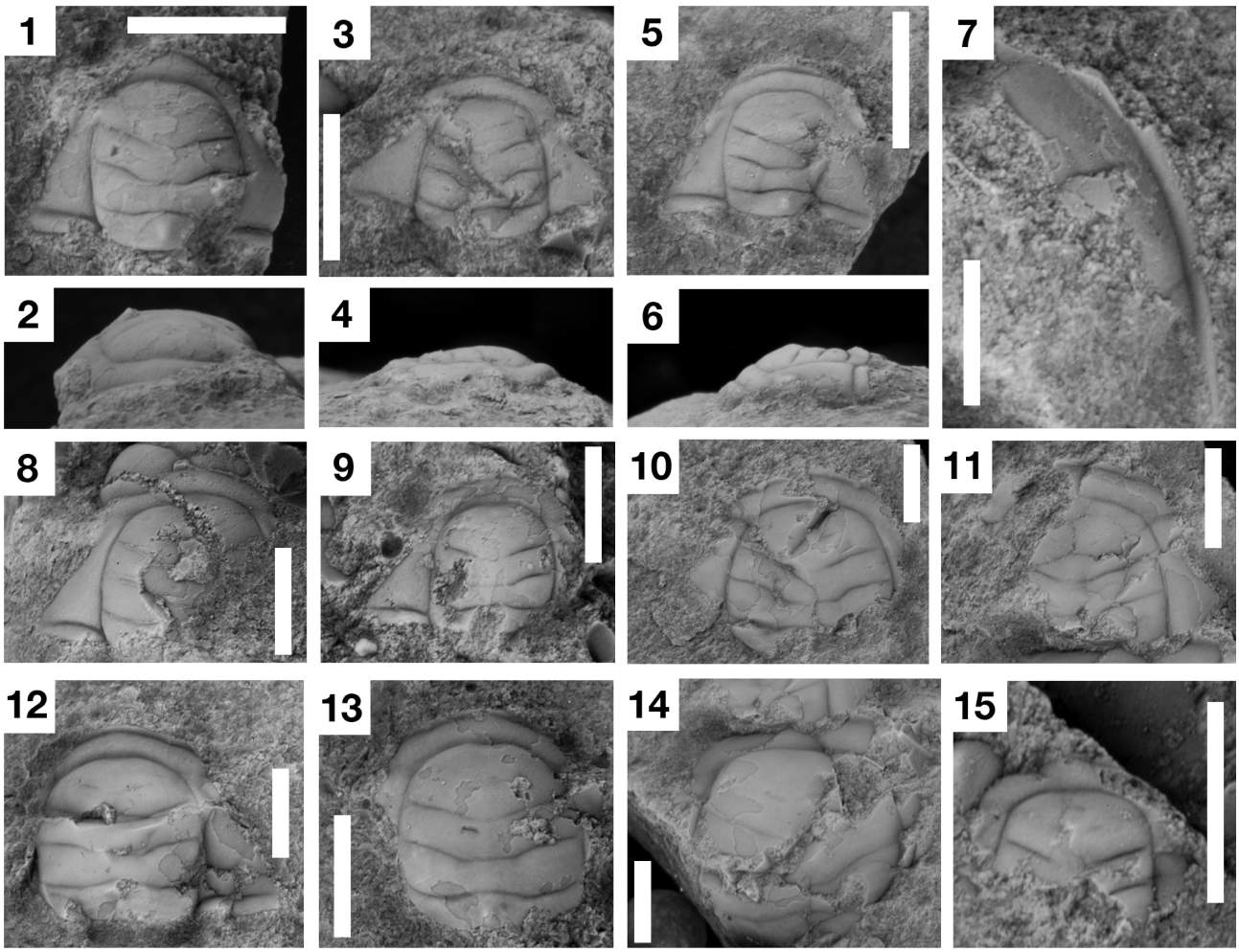

PLATE 4. *Bienvillia* sp. All cranidia except 7 (librigena). Each white scale bar represents 2mm. 1-2. USMN 775718, from D3383-CO, dorsal and anterior views. 3-4. CM 41327, from 5/22/08C, dorsal and right lateral views. 5-6. CM 41328, from 5/22/08D, dorsal and left lateral views. 7. Right librigena, CM 41329, from 5/22/08C, dorsal view. 8. CM 41330, from 5/22/08C, dorsal view. 9. CM 41331, from 5/22/08C, dorsal view. 10. CM 41332, from 5/22/08D, dorsal view. 11. CM 41333, from 5/22/08D, dorsal view. 12. CM 41334, from 5/22/08D, dorsal view. 13. CM 41335, from 5/22/08D, dorsal view. 14. CM 41336, from 5/22/08D, dorsal view. 15. CM 41337, from 5/22/08C, dorsal view.

***Bienvillia* sp.**
(Plate 4)

Material and occurrence. *Lotagnostus rushtoni* Fauna: 5/22/08C (11-0-1), 5/22/08D (15-0-0), and D3383-CO (3-0-0) from Ninemile Canyon, Nevada.

Discussion. The species of *Bienvillia* in the *Lotagnostus rushtoni* Fauna differs from *B. eurekensis* in displaying a shorter preglabellar field and S1 furrows that are connected across the axis. *Bienvillia* sp. is most similar to

B. corax, displaying most of the characteristic features of the holotype cranidium, which was well illustrated by Ludvigsen *et al.* (1989, pl. 4, fig. 18). The shape and position of the four pairs of glabellar furrows are similar, although the S4 furrows are even more weakly developed than those of the holotype, and are not discernible at all on most specimens. Like the holotype, the better preserved cranidia of *Bienvillia* sp. have a bluntly pointed anterior margin, and a preglabellar field that is longest (sag.) at the midline and tapers slightly abaxially. However, *Bienvillia* sp. displays a shorter (sag.) and more convex preglabellar field and a more quadrate glabella that is nearly parallel-sided and less evenly rounded anteriorly. The other cranidia identified as *B. corax* by Ludvigsen *et al.* (1989, pl. 4, figs 19–22) show significant variation in these features, much of it clearly ontogenetic, and collectively provide a broad species concept in which the Windfall species could be accommodated. However, the trend in ontogenetic variation suggested by their material is opposite to that displayed by the specimens of *Bienvillia* sp. in the Windfall. In *Bienvillia* sp., the smaller cranidia display more quadrate, parallel-sided and anteriorly truncate glabellae, as compared to somewhat more circular and anteriorly rounded glabellae in larger sclerites from the same collection. In contrast, the glabellae of the smallest cranidia of *B. corax* figured by Ludvigsen *et al.* (1989) are more circular than the larger cranidia, a trend well illustrated by the two cranidia they illustrate from the same collection (Ludvigsen *et al*., 1989, pl. 2, figs 19, 22). Given these differences, and the relatively small number and poor quality of the compacted and deformed cranidia from the Windfall, we consider it best to leave the species in the *Lotagnostus rushtoni* Fauna in open nomenclature.

An older species designated *Bienvillia* cf. *B. corax* by Ludvigsen *et al.* (1989) in their *Onchontus richardsoni* Fauna resembles our younger species in the Windfall in the shape and proportions of the glabella. However, *B.* cf. *B. corax* differs from both the Windfall species and *B. corax* in the transverse (as opposed to oblique) orientation of the F3 furrows, and better development of a palpebral ridge. Additionally, *B.* cf. *B. corax* displays neither the pointed anterior margin nor the lengthening (sag.) of the preglabellar field sagitally seen in those younger species. The position of the intersection of the occipital furrow and the axial furrow also differs. In *Bienvillia corax* and *Bienvillia* sp., that junction lies well in front of the proximal end of the posterior border furrow. On *B.* cf. *B. corax* cranidia, the occipital furrow does not curve forward as strongly as it approaches the axial furrow, so the intersection lies barely in front of the posterior border furrow.

Subfamily PLICATOLININAE Robison & Pantoja-Alor, 1968

Discussion. Robison & Pantoja-Alor (1968) erected the Subfamily Plicatolininae to include three genera: *Plicatolina* Shaw, 1951; *Plicatolinella* Robison & Pantoja-Alor, 1968; and a third undescribed and unnamed genus from the western United States. Robison & Pantoja-Alor (1968) emphasized low cranidial convexity, a quadrate glabella bearing 4 pairs of lateral glabellar furrows, and short anterior border and preglabellar field as defining characteristics for the new subfamily. The pygidial margin was either entire (*Plicatolina*) or bilobed (*Plicatolinella* and the unnamed genus). *Mendoparabolina* Rusconi, 1951a exhibits these characters and is included in the subfamily. Taylor (1976) transferred the genus *Westergaardites* Troedsson, 1937 into the subfamily. Benedetto (1977) erected *Paraplicatolina*, with *P. acantha* as the designated type species, and included it in the Plicatolininae. *Paraplicatolina acantha*, however, has a subtrapezoidal glabella and apparently lacks S4 lateral glabellar furrows: the assignment bears further consideration.

Mendoparabolina Rusconi, 1951a

Type species. *Mendoparabolina pirquinensis* Rusconi, 1951a, by monotypy, from El Relincho Formation, Cerro Pelado, Mendoza, Argentina.

Emended diagnosis. The diagnosis of Tortello (2014, 2018) is accepted, with the addition of the sigmoid shape of the S1 and S2 lateral glabellar furrows previously noted by Rusconi (1951a).

Other species. *Mendoparabolina brevicauda* Rusconi, 1955a; *M. nyensis* (Taylor, 1976).

Discussion. Rusconi (1951a) sketched the original cranidium and associated pygidium of *Mendoparabolina pirquinensis,* the type species**.** Subsequently, Shergold *et al.* (1995, p. 246; Jell and Adrain, 2003) suggested that *Mendoparabolina* is a junior subjective synonym of *Bienvillia* Clark, 1924. Tortello (2014, p. 301–303, figs 6.1, 6.2,

4.5–4.25) photographically illustrated the type material and additional specimens from the El Relincho Formation, Mendoza, Argentina. Based upon the more complete knowledge of *M. pirquiensis*, Tortello (2014) resurrected *Mendoparabolina*.

Mendoparabolina nyensis (Taylor, 1976)

(Plate 5; Plate 16.1, 16.10, 16.11)

1976 *Plicatolina nyensis* Taylor, p. 687–688, pl. 3, figs 16–18.

Diagnosis. A species of *Mendoparabolina* with a short, horizontal, caecate preglabellar field; prominent constriction of the glabella where impingement by eye ridge offsets axial furrow inward directly in front of S4; a pronounced axial notch in the front of the glabella, S3 glabellar furrows oriented perpendicular to the midline; and a transverse pygidium with a strongly bilobed posterior margin in larger specimens.

Material and occurrence. *Lotagnostus nolani* Fauna: collection 5/22/08B (136-64-5) and D3362-CO (6-7-2) from Ninemile Canyon, Nevada; *Hedinaspis-Charchaqia* Fauna: collections D7129-CO (cephalon and partial thorax), D7130-CO (4-2-0), and D7133-CO (4-0-0) from the Hales Limestone in the Hot Creek section, Nevada.

Description. Cranidium large among associated sclerites, up to 1cm in length; subtrapezoidal in outline. Prominent glabella; subrectangular in outline, glabellar length exclusive of occipital ring 60-70% of cranidial length (sag.), glabellar width (tr.) at occipital furrow equals 85-90% of glabellar length exclusive of occipital lobe; moderately convex transversely with weakly developed keel; very weakly convex from posterior margin to S2, moderately convex (sag.) forward of S2 as frontal lobe descends to preglabellar field. Axial furrows moderately impressed, mostly straight, subparallel to slightly divergent, tightly sinuous at intersection with eye ridge; preglabellar furrow moderately impressed, broadly curved to merge evenly with axial furrows, slightly recurved sagittally, slightly lengthening the preglabellar field in front of shallow notch in front of the glabella. Four pairs of lateral glabellar furrows: S1 moderately impressed, deepest near mid-length (tr.); sinuous; distal half gently curved and directed slightly posteriorly adaxially, inner half anteriorly concave, extends 75% of the way from axial furrow toward midline; S2 moderately impressed, slightly curved, anteriorly convex, intersection with axial furrow nearly perpendicular, terminates adaxially at same distance from axial furrow as S1; S3 short (tr.), slightly to moderately impressed, straight to very gently curved, oriented perpendicular to midline, opposite or slightly behind intersection of eye ridge with axial furrow; proximal end in line (exsag.) with adaxial termination of S2, extending abaxially half way to axial furrow; S4 lightly impressed, narrow, and straight, anteriorly directed at 65° angle from intersection with axial furrow at posterior edge of eye ridge; extends half way to midline. Occipital ring subcrescentic in outline; long (sag.), 17-19% of cranidial length, longest medially where occipital furrow recurves; low, slightly elongate occipital node occupies posterior half of ring, very faintly impressed furrow extends from anterior end of node diagonally toward posterolateral corners of ring. Occipital furrow moderately to deeply impressed distally, faintly impressed medially; sinuous, directed slightly posteriorly from intersection with axial furrow, extends 75% of way to midline where it is recurved to cross axial line in anteriorly convex arc; most specimens exhibit bifurcation of furrow at distal ends of the arc to form faintly impressed, posteriorly directed furrows that fail to reach posterior margin or axial furrows. Anterior margin as broad even curve. Anterior border a narrow (sag.), upturned rim that tapers gently abaxially, disappearing in front of preocular area where suture descends into border furrow. Border furrow narrow (sag.) and moderately impressed in smaller specimens, shallower and broader in larger sclerites. Anterior branch of facial suture trends slightly posteriorly from midline, traverses anterior border at oblique angle, and turns inward in tight curve to intersect distal end of eye ridge; posterior branch of facial suture diverges from posterior edge of palpebral lobe at 45° angle, broadly curved to intersect posterior margin at 85°. Preglabellar field short (sag.), 10-20% of cranidial length, longer abaxially although slightly lengthened at midline due to curvature in preglabellar furrow; subhorizontal in orientation. Preocular area subhorizontal, moderate in length (exsag.), wide (tr.), extending beyond palpebral lobes. Radiating genal caecae cover preglabellar field and preocular areas. Eye ridge well developed, directed slightly posteriorly from axial furrow, merging distally with short palpebral lobes that extend from distal end of S4 to slightly behind intersection of S2 with axial furrow. Palpebral areas narrow (tr.), subhorizontal; postocular areas long, extend to approximately cranidial midlength between S1 and S2; slightly convex, subhorizontal adaxially to slightly declined distally; finely granulate prosopon on some specimens; moderately impressed posterior border furrow widens and shallows distally.

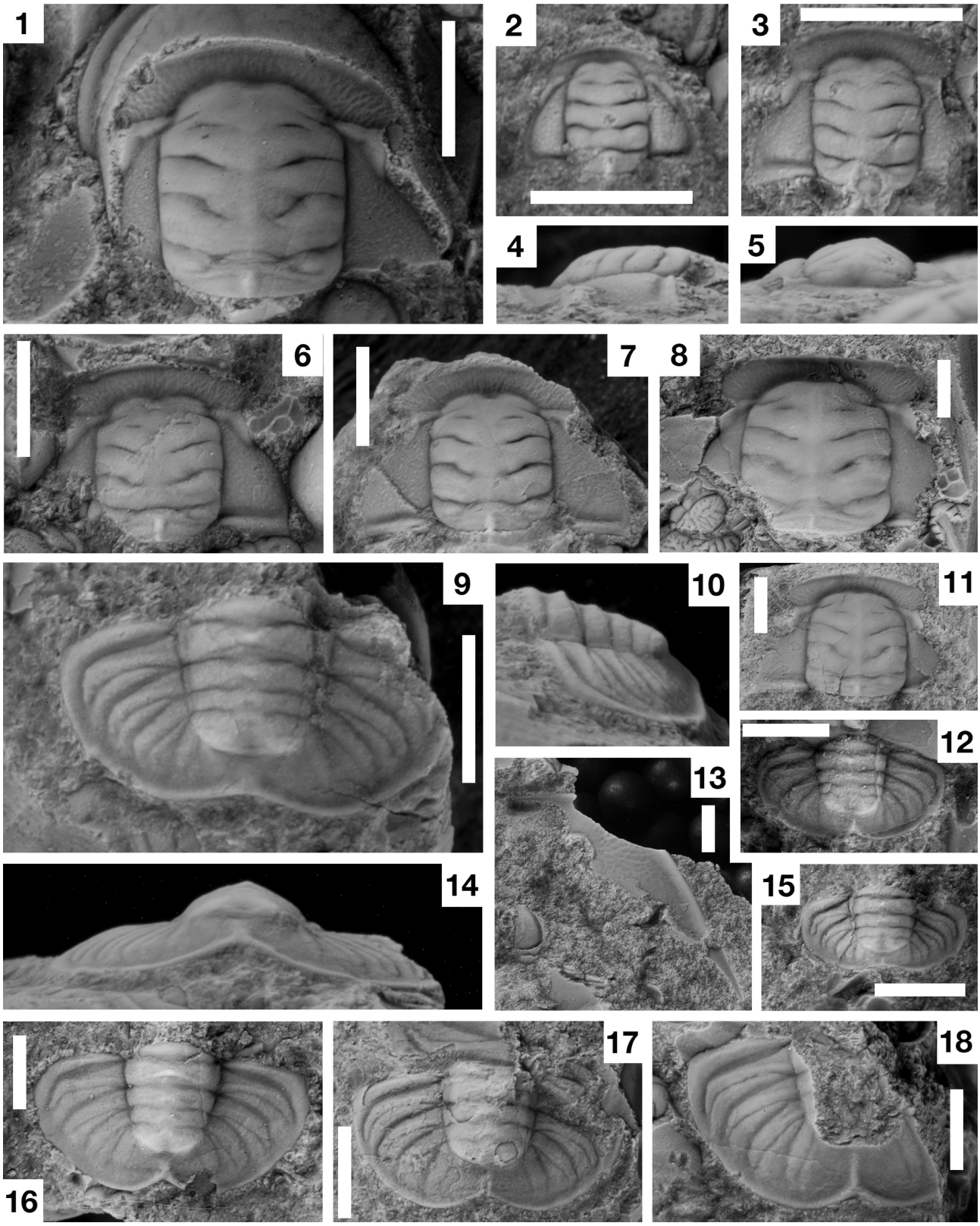

PLATE 5. *Mendoparabolina nyensis* (Taylor, 1976). Each white scale bar represents 2mm. 1. Cranidium, CM 41338, from 5/22/08B, dorsal view. 2. Cranidium, CM 41339, from 5/22/08B, dorsal view. 3-5. Cranidium, CM 41340, from 5/22/08B, dorsal, left lateral, and anterior views. 6. Cranidium, CM 41341, from 5/22/08B, dorsal view. 7. Cranidium, CM 41342, from 5/22/08B, dorsal view. 8. Cranidium, CM 41343, from 5/22/08B, dorsal view. 9, 10, 14. Pygidium, CM 41344, from 5/22/08B, dorsal, lateral, and posterior views. 11. Cranidium, USMN 775719, from D3362-CO, dorsal view. 12. Pygidium, CM 41345, from 5/22/08B, dorsal view. 13. Right librigena, USMN 775720, from D3362-CO, dorsal view. 15. Pygidium, CM 41346, from 5/22/08B, dorsal view. 16. Pygidium, CM 41347, from 5/22/08B, dorsal view. 17. Pygidium, USMN 775721, from D3362-CO, dorsal view. 18. Pygidium, CM 41348, from 5/22/08B, dorsal view.

Librigenae subcrescentic in outline; lateral margin as broad, even curve; long, gently tapering anterior extension; lateral border narrow, smooth, uniform in width (tr.), defined by inflection at distal edge of genal field; genal field traversed by radiating genal caecae that fade posteriorly, narrow genal spine roughly 75% length of genal field (exsag.).

Pygidium large in comparison to associated sclerites, up to 5.6mm in length (sag.); transverse with axial pygidial length only 50% of maximum pygidial width; slightly convex (tr.) to moderately convex (sag.); pygidial margin as even curve from anterolateral corner to axial line, interrupted in small specimens by minute, blunt marginal spines at distal tips of two anteriormost pleurae; shallow embayment in posterior margin behind axis in small specimens becomes narrower (tr.), prominent notch in larger specimens, rendering pygidum bilobed with axial length (sag.) approximately 90% of maximum length (exsag.); narrow (tr.) postaxial ridge extends forward from notch, diminishing in height anteriorly, more pronounced in larger specimens; narrow, convex border along posterior half to third of pygidium, increasing in width (sag.) behind axis in larger specimens; border furrow ill defined by distal ends of pleurae. Axis long, 80-90% of pygidial length (sag.) and broad, approximately 33% of maximum pygidial width at anterior end; slightly tapered, width at posteriormost inter-ring furrow 70-75% width at articulating furrow; composed of 3 progressively shorter (sag.) axial rings and lunate terminal piece that bears two lateral nodes separated by faint medial furrow; axial rings with faint transverse ridge on posterior half of ring. Inter-ring furrows straight, weakly impressed, shallowed axially. Axial furrows straight, slightly convergent; moderately impressed opposite anterior two axial rings, faintly impressed opposite third ring, as break in slope around terminal axial piece. Pleural fields tapered posteriorly, slightly convex (tr.), slightly declined (tr.), moderately declined post-axially. Four pairs of pleurae defined by faintly impressed interpleural furrows; anterior pair straight, nearly transverse through proximal two thirds, turned posteriorly through outer third, cross 80% of width of pleural field (tr.) terminating just inside lateral border; second interpleural furrows long, as broad curve, slightly posteriorly directed; remaining furrows shorter, posteriormost furrow strongly directed posteriorly. Anteriormost pleural furrows moderately impressed, anterior side more steeply declined than posterior; more strongly directed posteriorly than adjacent interpleural furrow, turns at two-thirds length to converge on interpleural furrow; remaining pleural furrows as broad curves, progressively shorter and more posteriorly directed.

Discussion. Taylor (1976) described *Plicatolina nyensis* from the Hales Limestone at Hot Creek Canyon, Nevada, illustrating three cranidia and a partial cephalon and thorax. Among the olenids recovered from the Windfall Formation at Ninemile Canyon, Nevada, is a species that conforms with *P. nyensis* in the length, orientation, and caecate prosopon of the preglabellar field, in the shape and orientation of the glabellar furrows, the divergent anterior branch of the facial suture, the structure of the occipital ring, and almost every other feature. The cranidia from the Hales illustrated by Taylor (1976) differ from those of the Windfall in only two respects. The S1 furrow in the former appears transglabellar, whereas S1 furrows on Windfall specimens are separated medially. Furthermore, the palpebral lobes on the Windfall specimens are slightly longer (exsag.), extending posteriorly a short distance beyond where those of the Hales terminate opposite the distal end of S2. While examination of borrowed material from the Hales confirmed the minor difference in length of the palpebral lobes, the apparent contrast in form of S1 proved to be a preservational artefact. Material from the Hales is poorly preserved with most sclerites displaying some fracturing from compaction of the enclosing lime mudstone. Additionally, many of the specimens are internal molds that do not reliably replicate the features of the dorsal surface of the sclerites. This is the case with the illustrated holotype of *P. nyensis* (Taylor, 1976, pl. 3, fig. 16). A latex peel of the counterpart of the holotype, illustrated herein (Pl. 16, fig. 1), more accurately captures the features of the dorsal surface and confirms that S1 is not transglabellar. With the differences in cranidial morphology thereby reduced to a slightly more posterior position for the back of the palpebral lobe, we consider the Windfall specimens conspecific with those of the Hales. Additional support for this conclusion was provided by a pygidium (Pl. 16, fig. 11), virtually identical to those associated with *P. nyensis* cranidia in the Windfall (e.g., Pl. 5, figs. 12, 15), that was recovered through re-processing of the Hales collection (7130-CO) that provided the holotype.

With this recovery, the *Plicatolina nyensis* cranidia in both the Hales and the Windfall are associated with a transverse pygidium that bears distally curved pleurae and a bilobed posterior margin. This species is confidently transferred from *Plicatolina* Shaw, 1951 to *Mendoparabolina* based upon the quadrate glabella; the 4 pairs of glabellar furrows, especially the sinuous S1 and S2 furrows and the S3 that fails to intersect the axial furrows; the short, caecate, horizontal preglabellar field; the divergent anterior facial sutures; and the bilobate posterior pygidial margin in moderate to larger specimens.

The Windfall pygidia exhibit two obvious ontogenetic progressions. First, minute spines present opposite the terminal axial piece on the smallest specimens (Plate 5.15) are lost during ontogeny. Further, in the smallest specimens the posterior margin is an even curve, becoming progressively more embayed with a distinct bilobed appearance evident in larger specimens.

Mendoparabolina nyensis (Taylor, 1976) compares very closely with *M. piriquensis* (Rusconi, 1951a; Tortello, 2014) in glabellar shape and proportions, the shape of the S1 and S2 lateral glabellar furrows, and the orientation of the preglabellar field. The cranidia of *M. nyensis*, however, differ from the latter in the transverse orientation of the S3 glabellar furrow and in a slightly longer preglabellar field relative to the glabellar length, although the preglabellar fields in *M. piriquensis* may be incomplete or incompletely prepared. The pygidia of the two species are very similar in the composition of the axes, the shape of the pleurae, the rim-like border, and the bilobed margin in the larger specimens. That of *M. nyensis,* however, is relatively shorter (sag.). With the length measured sagitally and the articulating half-ring excluded, the length of the *M. nyensis* pygidium is only 43.5% (38-44.6%) of the maximum pygidial width, as opposed to 55% (46.3-64.5%) for *M. piriquensis*.

The pygidium of *Mendoparabolina brevicauda* (Rusconi, 1955b; Tortello, 2018, fig. 4) is similar to that of *Mendoparabolina nyensis* in the nature of the axis and the pleurae. The degree of embayment along the posterior margin is more significant in *M. nyensis* when comparing specimens of similar sizes (Tortello, 2018, fig. 4h). The cranidium of *M. brevicauda*, however, is markedly different from *M. nyensis*. The cranidium is more rounded at the anterolateral corners, exhibits an evenly curved preglabellar furrow, has S3 and S4 glabellar furrows that are more faintly impressed, a longer preglabellar field, and the anterior lobe of the glabella, when seen in lateral view, that is less convex. In these characters the cranidium assigned to *M. brevicauda* conforms more closely to *Bienvillia* and contrasts with *Mendoparabolina*: the association of sclerites of *M. brevicauda* might bear reappraisal.

The cranidium of *Plicatolina dunbari* Ludvigsen & Westrop (*in* Ludvigsen *et al.*, 1989, p. 15–16, pl. 5, figs 4–6) closely compares to those of *Mendoparabolina nyensis* in the shape of the glabella and the shape and arrangement of the lateral glabellar furrows. *P. dunbari* differs, however, in having a longer anterior border, a shorter preglabellar field, and a nearly straight posterior branch of the facial suture. The pygidium of *P. dunbari* has an evenly curved posterior margin and the distal ends of the pleurae are not as sharply turned.

The pygidium of *Plicatolinella ocula* (Robison & Pantoja-Alor, 1968, p. 794, pl. 103, figs 24–26, pl. 104, figs 1–4) is bilobed as in *Mendoparabolina nyensis*; however, the posterior end of the axis is less well defined, lacking the post-axial ridge highlighted by Tortello (2018). The cranidium of *P. ocula* exhibits large, posteriorly placed palpebral lobes at the distal end of long eye ridges that result in long, broad palpebral areas which contrast with the short, narrow palpebral areas of *M. nyensis*. Furthermore, the S3 furrows in *P. ocula* intersect the axial furrows, unlike the detached S3 furrows in *M. nyensis*.

The small pygidium of *Simuloenus quadrisulcatus* Palmer, 1968 (p. 56, pl. 8, figs 1–4) is weakly bilobed and bears pleurae that are curved distally, as seen in *Mendoparabolina*. The pygidium of *S. quadrisulcatus*, however, bears only 2 axial rings. The form and details of the cranidium of *S. quadrisulcatus* closely resemble those of *M. nyensis* in the presence of the 4 pair of glabellar furrows, small palpebral lobes set close to the glabella, the short preglabellar field, and oblique furrow crossing the occipital ring. However, the axial furrows in *S. quadrisulcatus* are moderately convergent resulting in a subtrapezoidal glabella, unlike the subrectangular glabella of *M. nyensis,* and the anterior border is convex, rather than upturned.

Family Ceratopygidae Linnarsson, 1869

Subfamily Hedinaspininae Peng, 1992

Hedinaspis Troedsson, 1951

Type species. *Hedinia regalis* Troedsson, 1937, by original designation from Xianxiang, China.

Hedinaspis sp.
(Plate 7.19)

Discussion. A single, very fragmentary pygidium was recovered in collection 5/22/08C in the *Lotagnostus rushtoni* fauna from the Windfall Formation, Ninemile Canyon, Nevada. The distal half to two-thirds of six pleurae with very broad (exsag.) pleural furrows are bounded in front and behind by narrower, strongly convex bands of roughly equal width. Posterior bands of the anteriormost pleurae extend for very short distance posterolaterally as short, blunt terminal spines. The distinctive form of the pleurae allows for certain assignment to *Hedinaspis* but the specimen is too fragmentary for more precise identification. Uncertainty as to which part(s) of the skeleton the specimen represents is made all the more difficult by the typically obscure boundary between the thorax and pygidium noted in previous studies of *Hedinaspis* (e.g. Troedsson, 1937; Lu & Lin, 1989).

Ceratopygid indeterminate
(Plate 16, figs 13, 17)

Discussion. Two relatively large specimens in collection D7129-CO from the Hot Creek section of the Hales Limestone represent a non-spinose ceratopygid species. The flat, semi-elliptical pygidium with a tapering axis that extends nearly to the posterior margin, and long frontal area on the cranidium resemble those of some species of *Pseudoyuepingia* (e.g. *P. elongata* Lu & Lin, 1989). However, the cranidium is too fragmentary for confident assignment to genus.

Class Uncertain

Order Agnostida Salter, 1864b

Family Agnostidae M'Coy, 1849

***Lotagnostus* Whitehouse, 1936**

Type species. *Agnostus trisectus* Salter, 1864a, by original designation from the White-Leaved Oak Shale, Malvern, England.

Other species. *Lotagnostus americanus* (Billings, 1860); *L. trisectus* (Salter, 1864b); *L. ponepunctus* (Matthew, 1901); *L. germanus* (Matthew, 1901); *L. asiaticus* Troedsson, 1937; *L. hedini* (Troedsson, 1937); *L. peladensis* (Rusconi, 1951a); *L. verrucosus* Rusconi, 1951a; *L. obscurus* Palmer, 1955; *L. atenuatus* (Rusconi, 1955a); *L. punctatus* Lu, 1964; *L. ergodes* (Shergold, 1971); *L. irretitus* (Shergold, 1975); *L. spectabilis* Xiang & Zhang, 1985; *L. shergoldi* Tortello *in* Esteban & Tortello, 2007; *L. salteri* Westrop & Landing, 2016; *L. matthewi* Westrop & Landing, 2016; *L. nolani* **n. sp.**; *L. clarki* **n. sp.**; *L. rushtoni* **n. sp.**; *L. morrisoni* **n. sp.**

Discussion. For most species of *Lotaganostus* only a few specimens have been illustrated from a single bed or thin stratigraphic interval. The resultant lack of information on morphologic variation from such stratigraphically constrained collections has allowed for strongly divergent opinions regarding the range of intraspecific variation within *Lotagnostus* species, and the number of valid species within the genus. Some (Peng & Babcock, 2005; Peng *et al*., 2015) contend that many species described in earlier studies constitute a single, widespread, highly variable species for which *Lotagnostus americanus* (Billings, 1860) is the senior subjective synonym. Others (Rushton, 2009; Landing *et al*., 2011; Westrop *et al*., 2011; Westrop & Landing, 2016) have challenged the extensive synonymy resulting from that broad species concept, in part because of the inadequacy of type material for many species. The abundant material from collection 5/22/08B allows for an assessment of the contrasting hypotheses on the variation of *Lotagnostus*.

In a re-evaluation of the species diversity and biostratigraphic distribution of *Lotoganostus* in North America, Westrop *et al.* (2011) recommended restriction of the type species, *L. trisectus,* to its type area in Avalonian Britain, arguing that the loss of critical morphologic information resulting from compaction in shale rendered comparison with less deformed material recovered elsewhere highly problematic. Having discovered in the present study the importance of features such as the steepness and variation in slope of the pleural fields and genae for discrimination of *Lotagnostus* species, we endorse that recommendation. Although the compacted condition of the holotype of *L. punctatus* from China could be offered as justification for similar geographic restriction of that species, the

availability of non-compacted specimens preserved in limestone from the same area and formation allows for effective comparison and eliminates the need for such limitation.

The problem of small sample sizes also lies at the heart of conflicting interpretations regarding the material assigned to *Lotagnostus asiaticus* (Troeddson, 1937) offered in previous studies. In response to criticism by Landing *et al.* (2010) regarding lack of evidence of intraspecific variation within individual collections, Peng *et al.* (2015) cited co-occurrence of weakly and strongly scrobiculate morphs within the collections from which that species was described, as well as from a single bed of the Siyanshan Formation in China sampled by Lu & Lin (1980). However, Westrop & Landing (2016) noted that co-occurrence alone does not confirm that the two morphs are conspecific and, given the absence of evidence of intergradation, argued that they represent separate, sympatric species. The absence of transitional forms between the strongly scrobiculate and largely effaced *Lotagnostus* specimens in our large collections from the Windfall Formation strongly supports the latter interpretation. Consequently, we follow Westrop & Landing (2016) in considering *L. asiaticus* a valid, weakly scrobiculate species, and exclude the strongly scrobiculate specimens of the type suite. Those sclerites represent a different species, like *L. punctatus,* which might ultimately prove to be the appropriate assignment for coarsely scrobiculate material previously assigned to *L. trisectus* from Australia (Bao & Jago, 2000), Kazakhstan (Ergaliev, 1983), Siberia (Pegel, 2000), and Sweden (Westergard, 1922) as well.

Lotagnostus americanus (Billings, 1860)

(Plate 6, figs 1–3)

1860 *Agnostus americanus*; Billings, p. 303, fig. 1a only [fig. 1b = *L.* aff. *L. clarki*].
1865 *Agnostus americanus* Billings, 1860; Billings, p. 395, fig. 372a only [fig. 372b = *L.* aff. *L. clarki*].
1944 *Agnostus americanus* Billings, 1860; Rasetti, p. 233, pl. 36, fig. 2 only [fig. 1 = *L.* aff. *L. clarki*].
1989 *Lotagnostus americanus* (Billings, 1860); Ludvigsen & Westrop *in* Ludvigsen *et al.*, p. 12, pl. 1, fig. 15, only [fig. 16 = *L.* aff. *L. clarki*, fig. 17 = *L.* sp. indet.].
non 1995 *Lotagnostus americanus* (Billings, 1860); Westrop, p. 15, pl. 1, figs 17–20 [=*L.* sp. indet.]
2005 *Lotagnostus americanus* (Billings, 1860); Peng & Babcock, p. 110–113, figs 2.2, 2.4 only [2.3 = *L.* aff. *L. clarki*].
non 2008 *Lotagnostus americanus* (Billings, 1860); Lazarenko *et al.,* pl. 23, figs 1, 2, 5, 5a.
non 2009 *Lotagnostus americanus americanus* (Billings, 1860); Rushton, p. 276, fig. 1J–O.
2011 *Lotagnostus americanus* (Billings, 1860); Westrop *et al.*, p. 578–584, fig. 5A–C only [figs. 5D-G, 6 = *L.* cf. *L. clarki*].
non 2012 *Lotagnostus americanus* (Billings, 1860); Ahlberg & Terfelt, fig. 4a–f.
2015 *Lotagnostus americanus* (Billings, 1860); Peng, Babcock, Zhu, Ahlberg, Terfelt, & Dai, fig. 5H–J only [fig. 5G = *L.* aff. *L. clarki*].

Discussion. Rushton (2009) discussed the selection of Billings' (1860) pygidium as the holotype. Only eleven specimens identified as *L. americanus* from the Lévis Formation have been illustrated: the holotype and two other pygidia, six cephala, and one enrolled skeleton. All but three of the eleven specimens came from one boulder, designated Boulder 37 by Rasetti (1944). Unfortunately, those three specimens are the holotype (Plate 6.1-6.3) and two topotype cephala. They came from elsewhere in the Lévis Formation and, in describing the species, Billings (1860) noted that he could not say for certain that the cephala represented the same species as the holotype. What is even more problematic with respect to the type material for *L. americanus* is that none of the pygidia illustrated from Boulder 37 displays the pitted surface texture on the distal areas of the pleural fields, the short scrobiculae on the proximal areas, or the very steep slope of the pitted distal areas that characterize the holotype. One pygidium (Rushton, 2009; fig. 1M) is nearly the same size as the holotype, making it implausible to attribute those differences to ontogenetic variation. In fact, the steep slope of the pitted distal areas of the pleural field gives the holotype an appearance unlike that of any other pygidium assigned to *L. americanus*, with the proximal, scrobiculate part of the pleural field appearing wider (tr.) than the pitted distal portion at the level of F2 in dorsal view. This can be clearly seen in Peng & Babcock (2005, fig. 2) where the holotype is one of sixteen pygidia included in the collage. On all other pygidia attributed to *L. americanus* in that figure, the pitted distal part of the pleural field appears as wide or wider than the scrobiculate inner part at F2. The uniqueness of the holotype, combined with the uncertainty of association with the topotype cephala or any other sclerites from the Lévis Formation, renders it unsuitable as a standard in our opinion and we here restrict *Lotagnostus americanus* to the holotype.

The affinities of the remaining *Lotagnostus americanus* specimens from the Lévis are uncertain. They most closely resemble *Lotagnostus clarki* **n. sp.** from the Windfall Formation. While the pygidia are indistinguishable from those of

L. clarki, there are noteworthy differences in the shapes and relative proportions of the glabellar lobes in the two species. Therefore, the Lévis specimens are left in open nomenclature here as *Lotagnostus* aff. *L. clarki*, which is discussed below.

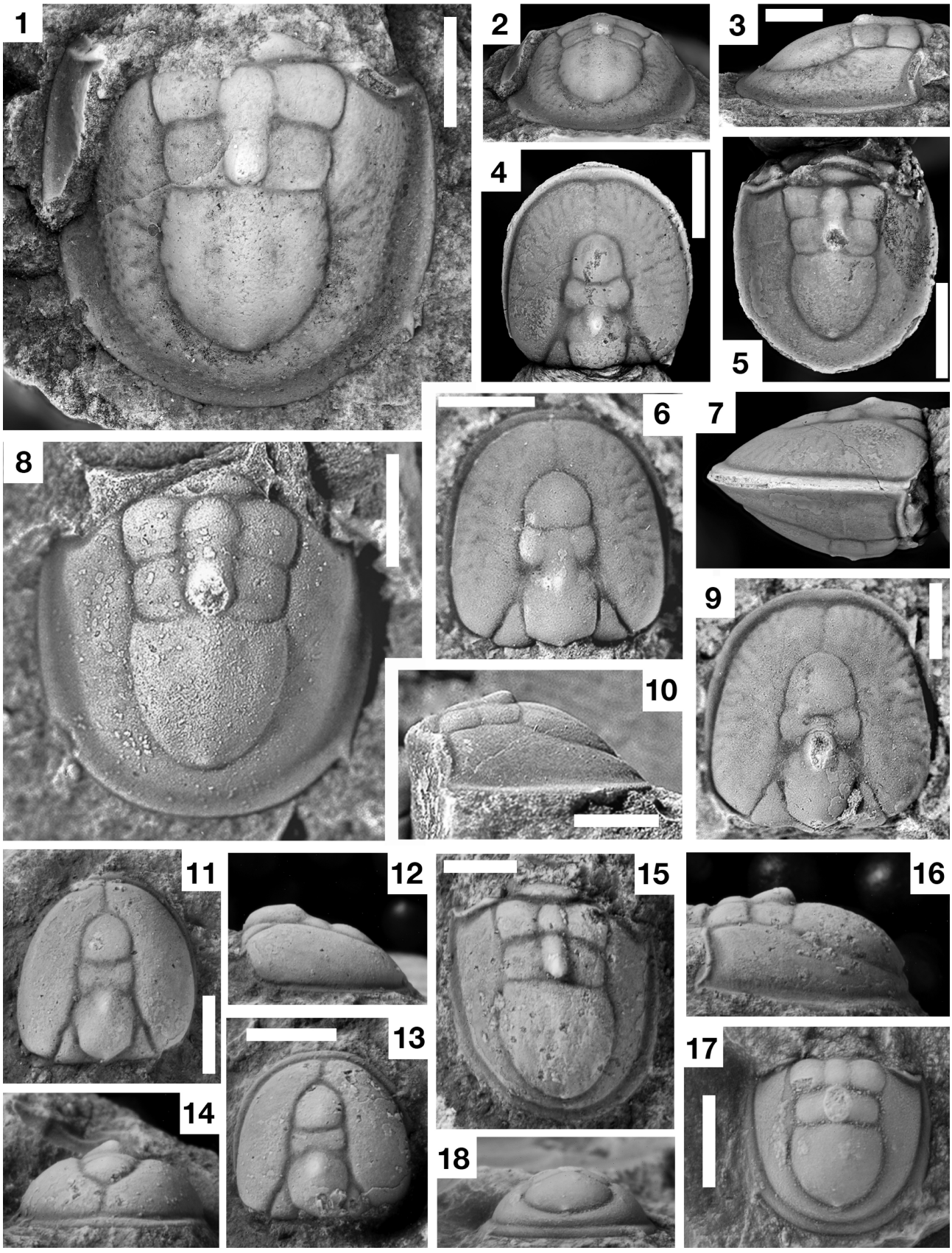

.....Plate legend provided on the next page

PLATE 6. *Lotagnostus* spp. Each white scale bar represents 2mm. 1-3. *Lotagnostus americanus* (Billings, 1860). Pygidium, GSC 859, holotype**,** dorsal, posterior oblique, and right lateral views (previously illustrated as Ludvigsen, Westrop, and Kindle, 1989, pl. 1, fig. 15; Westrop *et al.*, 2011, fig. 5A-C.; Peng *et al*., 2015, fig. 5G-I). 4-10. *Lotagnostus* aff. *L. clarki*. 4, 5, 7. Carapace, GSC 134619, dorsal, dorsal, right lateral views (previously illustrated as Westrop *et al*., 2011, fig.6A-D). 6. Cephalon, NHM It 21180, dorsal view (previously illustrated as Rushton, 2009, fig. 1L). 8. Pygidium, NHM It 21184, dorsal view (previously illustrated as Rushton, 2009, fig. 1M). 9. Cephalon, NHM It 21181, dorsal view (previously illustrated as Rushton, 2009, fig. 1J). 10. Pygidium, NHM It 21185, left lateral view (previously illustrated as Rushton, 2009, fig. 1N). 11-18. *Lotagnostus* aff. *L. rushtoni.* 11-12. Cephalon, GSC 70590, dorsal and lateral views, from Gorge Formation, Vermont, (previously illustrated as Ludvigsen, Westrop, & Kindle, 1989, pl. 1, fig. 2). 13-14. Cephalon, GSC 70575, dorsal and lateral views, from Gorge Fm., Vermont, (previously illustrated as Ludvigsen, Westrop, & Kindle, 1989, pl. 1, fig. 5). 15-16. Pygidium, GSC 70582, dorsal and lateral views, from Gorge Fm., Vermont, (previously illustrated as Ludvigsen, Westrop, & Kindle, 1989, pl. 1, fig. 8). 17-18. Pygidium, GSC 142849, dorsal and posterior views, from Cow Head Group, Green Point, Newfoundland, Canada, x8.4.

Lotagnostus cf. *L. obscurus* Palmer, 1955

(Plate 7.1–7.3, 7.7–7.9, 7.13–7.15)

cf. 1955 *Lotagnostus obscurus*, Palmer, p. 92, pl. 19, figs 5–7 only [fig. 10 = *L*. sp. indet].
non 2011 *Lotagnostus* cf. *L. obscurus* Palmer, 1955; Westrop *et al.*, p. 24, figs 10A-Q.

Material and occurrence. *Lotagnostus nolani* Fauna: collection 5/22/08B (4-3), D3362-CO (2-0) from the Windfall Formation at Ninemile Canyon, Nevada.

Discussion. Ludvigsen & Westrop (*in* Ludvigsen *et al*., 1989) placed *Lotagnostus obscurus* in synonymy with *Lotagnostus americanus* (Billings, 1865), a decision perpetuated in a few subsequent papers (Westrop, 1995; Peng & Babcock, 2005). However, Westrop *et al.* (2011) restudied and re-illustrated the type specimens of *L. obscurus* and resurrected *L. obscurus* as a separate, largely effaced species. Peng *et al.* (2015) agreed with this decision as do we. However, unlike previous authors, we exclude the second pygidium illustrated by Palmer (1955, pl. 19, fig. 10) from *Lotagnostus obscurus*. This pygidium has well-impressed furrows, displays evidence of trisection of the pygidial axis, and lacks the conspicuous elevation and strong sagittal convexity at the anterior end displayed by the holotype. It strongly resembles a pygidium of *Lotagnostus* sp. from the Hales (Plate 16.16), but displays a narrower intranotular axis, narrower border furrow of more constant width, and lacks the constriction of the acrolobe displayed by that species.

Two nearly effaced cephala in collection D3362-CO resemble *Lotagnostus obscurus* in the outline of their acrolobe, very strong transverse convexity, elevated and very strongly convex (sag.) posterior end, and the shape of the anteroglabella. They differ, however, in possessing longer basal lobes and a prominent occipital band that extends posteriorly well behind the glabellar culmination. Additionally, while the structure of the axis in the associated Windfall pygidia appears consistent with *Lotagnostus obscurus* (Westrop *et al*., 2011, fig. 7D–F, reillustrated the holotype pygidium) the pygidial outline appears more quadrate, the border widens opposite the posteroaxis as the margin of the pleurae appears to straighten, the convexity is less (although the specimen looks dorsoventrally compressed resulting in the longitudinal fracture), and the posterior margin looks more quadrate than rounded. Given the small number of specimens available to evaluate the significance of these differences, we consider the assignment of our material to that species uncertain.

Westrop *et al*. (2011) similarly reported an effaced species of *Lotagnostus* from the Windfall Formation in the Cherry Creek Range in eastern Nevada as *Lotagnostus* cf. *L. obscurus.* It differs from the species identified by that name herein from the Antelope Range in numerous features of both the cephalon and pygidium. The species from the Cherry Creek Range has smaller basal lobes and a longer (sag.) preglabellar field, which constitutes 26% of the length of the cephalon, as compared with only 20% in the species from the Antelope Range. The former species also has a proportionally shorter posteroaxis that makes up only 50% of the length (sag.) of the pygidial axis, in contrast to that of the Antelope Range species which composes 60%. Consequently, the axial node on the species from the Cherry Creek Range lies very near the midlength of the pygidial axis, rather than well in front of it. It also displays a smoothly rounded anterior margin on the cephalon and posterior margin on the pygidium, whereas those margins on the Antelope Range species are more transverse, and the sclerite shape slightly quadrate.

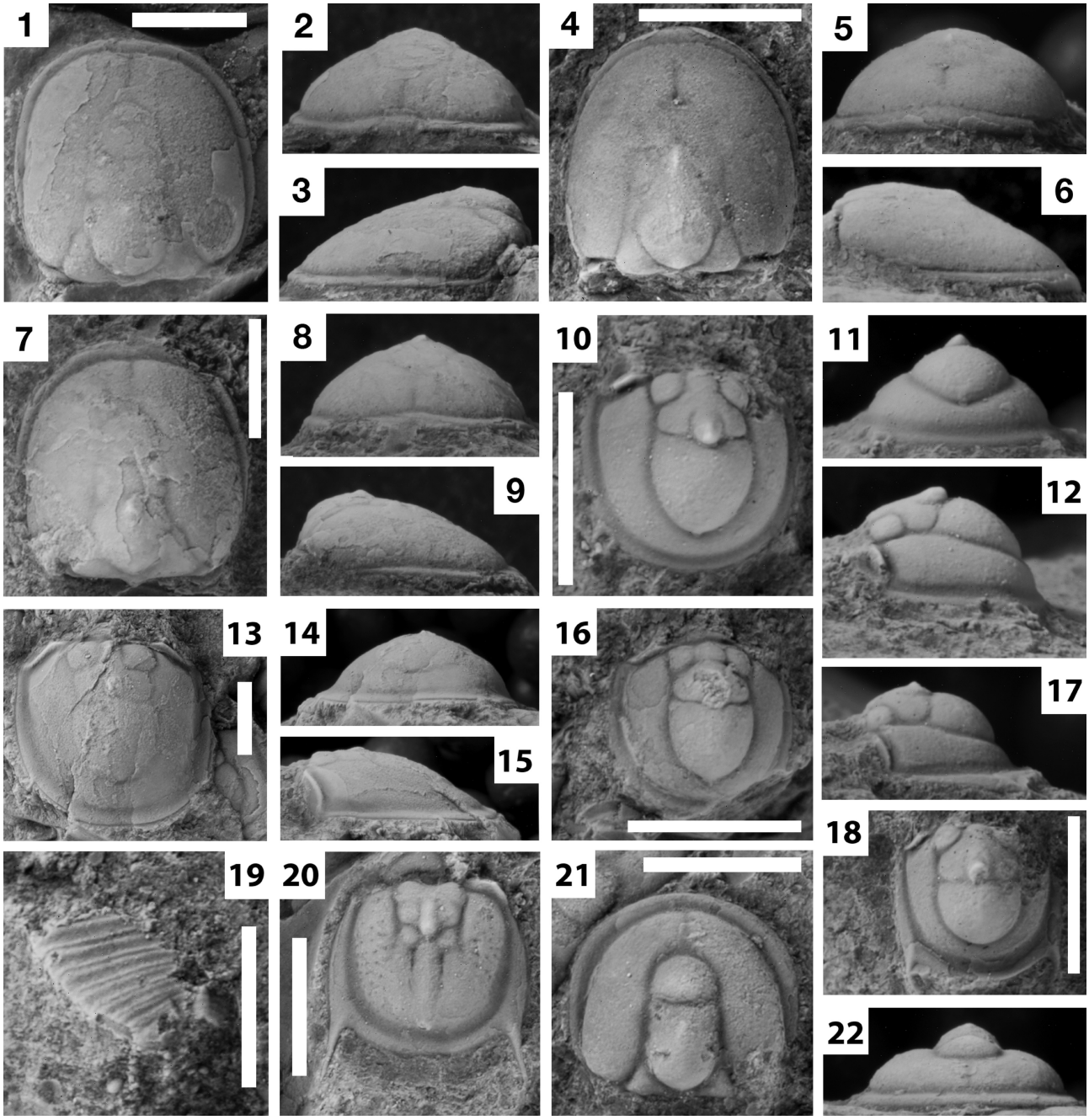

PLATE 7. Miscellaneous Windfall taxa. Each white scale bar represents 2mm. 1-3. *Lotagnostus* cf. *L. obscurus*. USMN 775722, cephalon, from D3362-CO, dorsal, anterior, and left lateral views. 4-6. *Rhaptagnostus* cf. *R. convergens*. Cephalon, CM 41350, from 5/22/08B, dorsal, anterior, and right lateral views. 7-9. *Lotagnostus* cf. *L. obscurus.* Cephalon, CM 41351, from 5/22/08B, dorsal, anterior, and right lateral views. 10-12. *Homagnostus* ?. Pygidium, CM 41356, from 5/22/08B, dorsal, posterior, and left lateral views. 13-15. *Lotagnostus* cf. *L. obscurus.* Pygidium, CM 41353, from 5/22/08B, dorsal, posterior, and left lateral views. 16. *Homagnostus*? sp. Pygidium, CM 41401, from 5/22/08B, dorsal view. 17-18. *Micragnostus* cf. *M. intermedius*. Cephalon, CM 41358, from 5/22/08B, left lateral and dorsal views. 19. *Hedinaspis* sp. Fragmentary thoracic and/or pygidial fragment, CM 41359, from 5/22/08C, dorsal view. 20. *Machairagnostus* cf. *M. corrugatu*s. Pygidium, CM 41349, from 5/22/08B, dorsal view. 21-22. *Homagnostus*? sp. Cephalon, CM 41357, from 5/22/08B, dorsal and anterior views.

***Lotagnostus nolani* n. sp.**
(Plate 1.1–1.5, 1.11–1.16, Plate 8.1–8.17, Plate 9, Plate 16.1–16.7)

1976 *Lotagnostus trisectus* (Salter, 1864a); Taylor & Cook, text-fig. 29F.

Diagnosis. Strongly scrobiculate *Lotagnostus* with M2 lateral lobes depressed and subdivided, long basal lobes (EBL/APL ratio greater than 0.45; Figure 10.2), and elongate, slightly asymmetrical glabellar node anteriorly positioned on the front half of M2; median preglabellar furrow in larger specimens weakly impressed, shallowing anteriorly, and does not intersect the border furrow; posteroaxis conspicuously trisected with notular axis bounded by faintly to moderately impressed notular furrows that connect deep notulae; pleural field divided into a subcircular, nearly horizontal proximal area with widely spaced, radially oriented short scrobiculae that is surrounded by more downsloping distal areas with densely spaced, irregular pits.

Etymology. Named after Thomas B. Nolan in recognition of his accomplishments as former Director of the United States Geological Survey (see Leopold & Baker, 1996).

Material and occurrence. Holotype CM 41360 is a cephalon from collection 5/22/08B: assigned specimens include 10 cephala CM 41301–41305, 41361–41365 and 11 pygidia CM 41306–41309, 41366–41372 from collection 5/22/08B; and 2 cephala USNM 775724–775725 and 2 pygidia USNM 775727–775728 from collection D3362-CO. *Lotagnostus nolani* fauna: collections 5/22/08B (267-255) and D3362-CO (17-15). from the Windfall Formation at Ninemile Canyon, Nevada; *Hedinaspis-Charchaqia* Fauna: collections D7130-CO (13-13), D7132-CO (0-2) and D7133-CO (6-2) from the Hales Limestone at the Hot Creek section, Nevada.

Description. Cephalon semiovate in outline; sagittal length approximately equal to maximum width (93-105%); moderately convex (sag., tr.). Genae slightly convex (sag., tr.), moderately inclined in anterior view. Axial furrows moderately impressed; nearly straight, moderately convergent from posterior margin to F2, bowed outward slightly along M3, gently convergent along anterior lobe. Glabella long (sag.) 73% of cephalic length (69–79%), approximately one-third of cephalic width at M3 (29-35%); stands in low relief above adjacent genae in larger specimens, more strongly convex (tr.) and stands higher in relief in smaller specimen. Basal lobes subtriangular; long (exsag,), approximately one third (27–37%) of glabellar length; anterior ends lie at or behind posterior end of glabellar node, posterior ends extend slightly beyond glabellar culmination; basal furrow angled to appear concave adaxially. Narrow (sag.) occipital band visible closely behind glabellar termination in dorsal view. F1 a slight expansion of axial furrow or very short, anterolaterally directed notch extending inward from axial furrow just posterior to anterior end of basal lobes. M1 hexagonal on specimens with slot-like F1; glabellar culmination bluntly pointed with small terminal node. M2 trisected; lateral lobes depressed, subdivided into multiple, small, subelliptical lobes separated by faint furrows; elongate, slightly asymmetrical axial node centered on front half of lobe. F2 a short (tr.) and wide (exsag.) notch in side of glabella extending adaxially half way to midline. M3 trisected on larger specimens by faintly impressed, anteriorly convergent, longitudinal furrows extending from F2 to F3; longer (exsag.), lateral lobes subelliptical and slightly inflated. F3 transglabellar, moderately impressed, straight to gently concave anteriorly in smaller specimens, tripartite in larger specimens with transverse central segment and lateral segments in front of lateral lobes of M2 directed anterolaterally abaxially to intersection with axial furrow. Anteroglabella accounts for slightly less than a third (29–34%) of glabellar length (sag.); broad, length equals only 83% (75–93%) of maximum width (tr.); subpentagonal with anterolateral corners rounded; bluntly pointed anteriorly. Median preglabellar furrow faintly impressed, shallowing anteriorly, failing to reach border furrow in some larger specimens; straight in small specimens, more irregular, blending with scrobiculae in larger sclerites. Anterior cephalic margin typically as even curve although several specimens slightly indented medially. Convex border of very gently tapered from midline to posterolateral angle; border furrow well impressed, equal in width to border. Scrobiculae distributed uniformly across genae, well impressed distally in all specimen sizes shallowing adaxially to appear less strongly impressed adjacent to axial furrows, particularly in small specimens.

Pygidium semiovate in outline, nearly equant, width at M2 slightly greater (97–107%) than length; moderately convex (sag., tr.); axis stands in low relief above pleural field in posterior view; pleural field separated into a subhorizontal circular area adjacent to axial furrow from F1 to slightly behind posteroaxis marked by widely spaced, short, radially arranged scrobiculae, surrounded by more steeply inclined area with closely spaced, deep, irregular pits; boundary between scrobiculate and pitted areas sharp. Slope of pitted area very steep posterior to F2, more moderately inclined along anteroaxis. Articulating half-ring short, crescentic. Articulating furrow broad (sag.), well-impressed, narrowed distally; curved backward slightly medially. Axis long, 84% (77–92%) of pygidial length

exclusive of articulating half-ring; slightly convex (sag., tr.) with exception of axial node, slightly constricted at M2. Axial furrows slightly sinuous, moderately impressed along anteroaxis, slightly shallower around posteroaxis. Anterior axial lobe strongly trisected; M1 lateral lobes slightly inflated, M2 lateral lobes very slightly inflated, slightly shorter than M1; medial lobe confluent from M1 to M2, narrower than lateral lobes, bearing axial node posteriorly. F1 well impressed, slightly curved, directed slightly anteromedially; discontinuous, interrupted medially by confluent central lobes of M1 and M2. Transaxial F2 moderately impressed, nearly straight, transverse; moderately impressed subsidiary furrows extend from F2 to connect with F1 to circumscribe M1-M2 medial lobe. Posteroaxis long (sag.), 57% (52–62%) of axial length, slightly convex, slightly declined (sag.), broadest (tr.) slightly anterior to lobe midlength, maximum width variable, average 105% (94–113%) of posteroaxis length; trisected by faintly impressed notular furrows, very faint along anteriormost 20% of lobe; furrows diverge slightly from F2 to approximately a third of the length of lobe, intranotular axis achieving its maximum width at this point, converge slightly posteriorly; intranotular axis slightly convex, stands in low relief above extranotular areas; well impressed notulae present, best expressed along posteriormost 80% of lobe; terminal node commonly absent. Border short (sag.), convex. Short posterolateral spines level with or behind the terminus of posterior lobe. Border furrow uniformly well impressed, broad, slightly narrower at anterolateral corners; wider and shallower in largest specimens.

Discussion. Strongly scrobiculate species with virtually identical pygidia to that of *Lotagnostus nolani* have been reported, by various species names (e.g. *L. punctatus* and *L. trisectus,* among others)*,* from Asia, Australia, South America, and Sweden. *L. nolani* is set apart from all these species by its higher (>0.45) EBL/APL ratio (Figure 10.2), and more anterior placement of the asymmetrical glabellar node, which is centered on the anterior half of M2 such that the base of its steeper anterior slope lies in line with the posterior ends of the anterolateral lobes of M3. Similarly high EBL/APL ratios have been confirmed only in *Lotagnostus trisectus,* which is now restricted to Avalonian Britain, and *L.* aff. *L. nolani* from the *Lotagnostus rushtoni* Fauna in the Windfall (discussed below). Although *L. trisectus* cephala yield comparably high EBL/APL ratios, none of the topotype pygidia of *L. trisectus* illustrated by Rushton (2009) displays prominent scrobiculae and pits on the pleural fields like those of *L. nolani.* It is possible that what Rusconi (1951b) described as *Goniagnostus verrucosus* from Argentina, and Shergold *et al.* (1995) subsequently re-assigned to *L. trisectus* has a similarly high EBL/APL ratio, but matrix concealing the posterior margin of the single cephalon on which this species is based makes accurate measurement of the ratio impossible. Moreover, the well-preserved glabellar node is centered at the midlength of M2, rather than on the front half as on *L. nolani*. Comparison of pygidial morphology between the two species is not possible at present because the pygidium of *L. verrucosus* is unknown. Until additional material can be described and illustrated, we feel it is best to treat *Lotagnostus verrucosus* and *L. nolani* as separate species. Despite some flattening and resultant fractures, the specimens from the Hales Limestone assigned here to *Lotagnostus nolani* retain the defining features of this species, fortifying correlation of the *L. nolani* and *Hedinaspis-Charchaqia* Faunas. The three figured cephala (Pl. 16, figs 1-5) all display the forwardly placed glabellar node, depressed and subdivided lateral lobes of M2, and long basal lobes that yield an EBL/ABL ratio over .45.

The flattened condition of the holotype of *Lotagnostus punctatus* (Lu, 1964, pl 5, fig. 5; Peng *et al*. 2015, fig. 9B) precludes recovery of some critical features, such as shape and position of the glabellar node. However, uncompacted cephala recovered from limestone in the same formation (Peng *et al*., 2015, figs 9D, 9H) confirm a more posterior placement of the node and lower EBL/APL ratios than in *L. nolani.* The sclerites from Sweden identified as *L. trisectus* by Westergård (1922), and used to illustrate that species by Shergold & Laurie (1997), actually compare more closely with *L. punctatus* in position of the glabellar node and EBL/APL ratio (Fig. 10.2). Two of the four species of *Lotagnostus* reported by Westrop & Landing (2016) from Avalonian strata in Nova Scotia also strongly resemble *L. nolani* but are readily distinguished by their lower EBL/APL ratios, less elongate and more posteriorly positioned glabellar node, and several other features. The cephalon of *Lotagnostus salteri* differs in having the glabellar node situated opposite the anterior tips of the basal lobes, more weakly impressed and usually discontinuous longitudinal furrows on M3, and fewer and shallower scrobiculae on the genal fields than *L. nolani*. Although the pygidia of the two species are very similar, most *L. salteri* pygidia display a proportionally shorter posteroaxis and slightly broader (tr.) intranotular axis. *Lotagnostus ponepunctus* (Matthew, 1901) differs from *L. nolani* in having fewer and more weakly impressed scrobiculae on the genal fields and a deeper and more continuous median preglabellar furrow that intersects the anterior border furrow. Its pygidium has much shallower scrobiculae and pits on the pleural fields, and a constricted acrolobe in larger specimens.

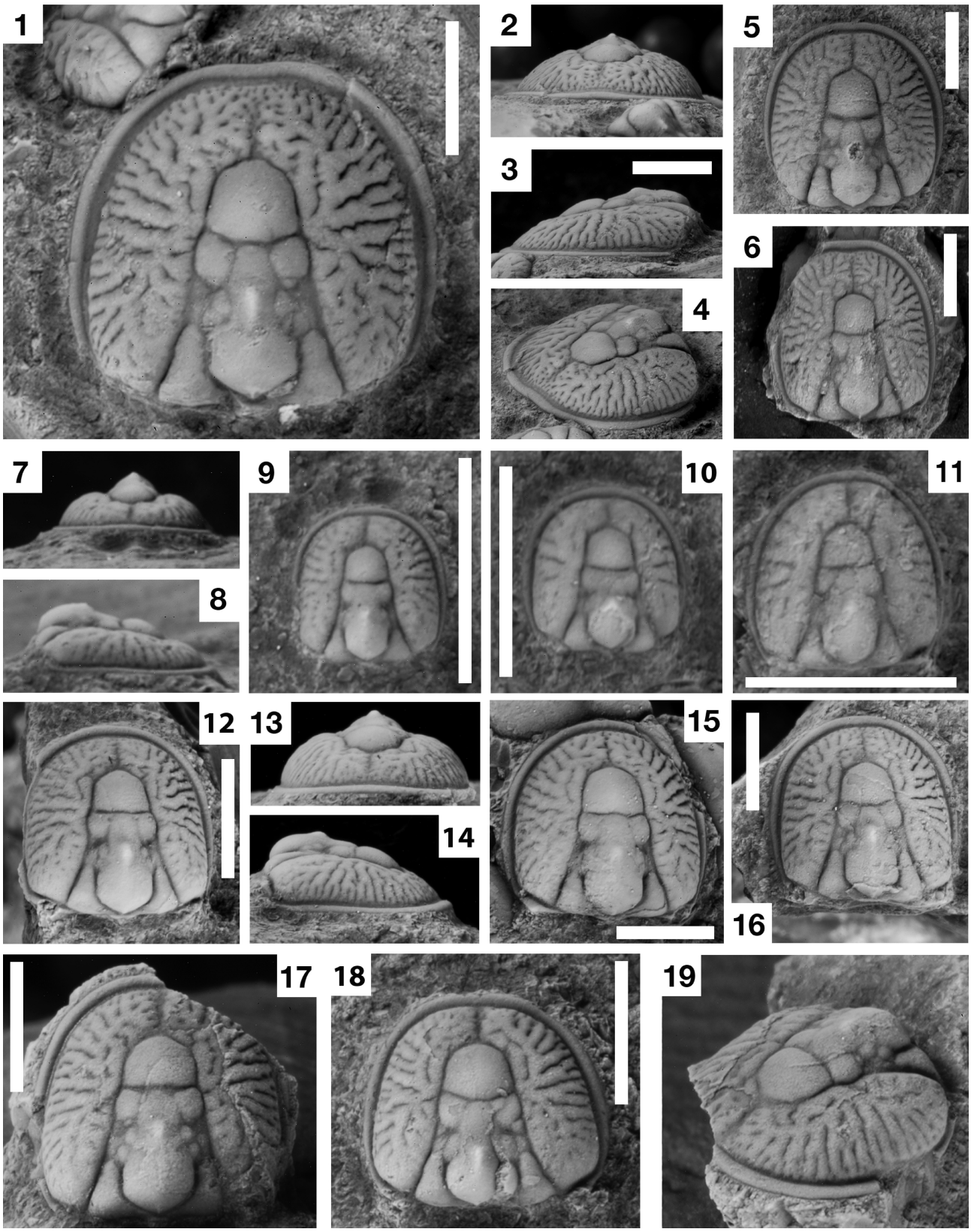

PLATE 8. Cephala of *Lotagnostus nolani* **n. sp.** and *Lotagnostus* aff. *L. nolani.* Each white scale bar represents 2mm. 1-17. *Lotagnostus nolani* **n. sp.** 1-4. Holotype, CM 41360, from 5/22/08B, dorsal; anterior, left lateral, and anterior oblique views. 5. CM 41361, from 5/22/08B, dorsal view. 6. CM 41362, from 5/22/08B, dorsal view. 7-9. USMN 775724, from D3362-CO, anterior, right lateral, and dorsal views. 10. CM 41301, from 5/22/08B, dorsal view. 11. CM 41302, from 5/22/08B, dorsal view. 12-14. CM 41363, from 5/22/08B, dorsal, anterior, and right lateral views. 15. CM 41364, from 5/22/08B, dorsal view. 16. CM 41365, from 5/22/08B, dorsal view. 17. USMN 775725, from D3362-CO, dorsal view. 18-19. *Lotagnostus* aff. *L. nolani.* USMN 775726, from D3381-CO, dorsal and anterior oblique views.

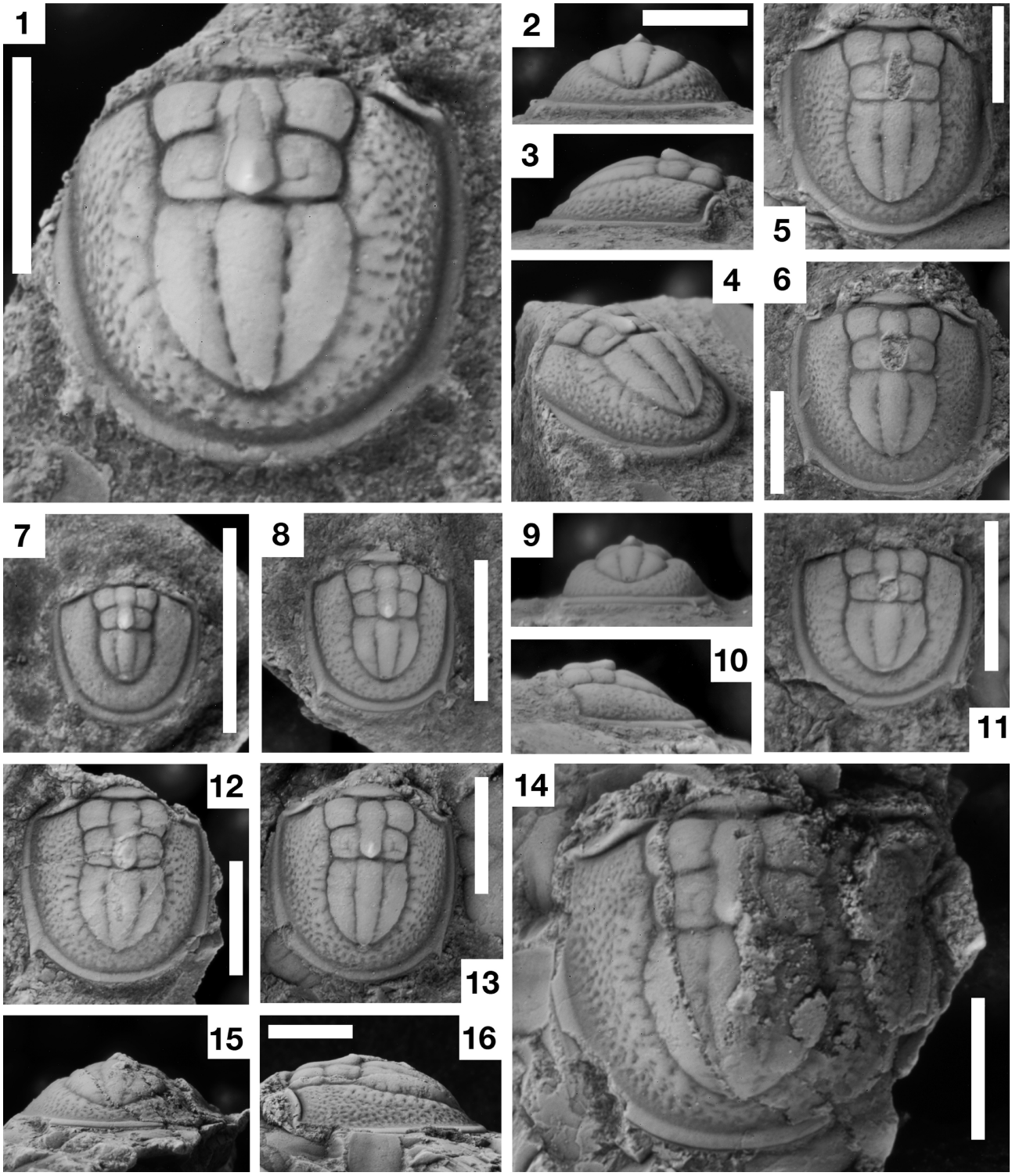

PLATE 9. Pygidia of *Lotagnostus nolani* **n. sp.** Each white scale bar represents 2mm. 1-4. USMN 775727, from D3362-CO, dorsal, posterior, right lateral, and posterior oblique views. 5. CM 41366, from 5/22/08B, dorsal view. 6. CM 41367, from 5/22/08B, dorsal view. 7. USMN 775728, from D3362-CO, dorsal view. 8-10. CM 41368, from 5/22/08B, dorsal, posterior, and left lateral views. 11. CM 41369, from 5/22/08B, dorsal view. 12. CM 41370, from 5/22/08B, dorsal view. 13. CM 41371, from 5/22/08B, dorsal view. 14-16. CM41372, from 5/22/08B, dorsal, posterior, and left lateral views.

Lotagnostus* aff. *L. nolani
(Plate 8.18–8.19)

Material and occurrence. *Lotagnostus rushtoni* Fauna: collection D3381-CO (2-1); 5-22-08D (1-1) from the Windfall Formation at Ninemile Canyon, Nevada.

Discussion. Strongly scrobiculate *Lotagnostus* sclerites are rare in collections of the *L. rushtoni* Fauna, and all but two cephala were too small or fragmentary for meaningful comparison with *L. nolani* and similar species. However, those cephala differ from those of *L. nolani* in having a more posteriorly positioned glabellar node situated at the rear of M2, centered in line with or just in front of the anterior tips of basal lobes. The largest and best preserved cephalon also displays a significantly lower ratio (Figure 10.3) between preglabellar field length (PFL) and anteroglabella length (AAL). In *L. nolani* the PFL/AAL ratio averages 0.81, with the lowest recorded value being 0.63. That of the best *L*. aff. *L*. *nolani* cephalon is 0.62.

***Lotagnostus clarki* n. sp.**
(Plate 1.6–1.10, 1.17–1.22, Plate 10, Plate 11)

Diagnosis. Genae of large cephala covered by weakly to moderately impressed scrobiculae; pygidia and small cephala non-scrobiculate; M2, at maximum width (tr.) behind glabellar node, is significantly wider than M1 and slightly wider than M3; longitudinal furrows that converge and shallow anteriorly trisect M3, defining elliptical lateral lobes in larger specimens; trisection of pygidial posteroaxis absent or very faint, with sides of intranotular axis defined only by minor change in slope rather than furrows or notulae; pleural field widest (tr.) near midlength of anteroaxis, narrowing (sag.) behind axis; pygidial border furrow in larger specimens widens (tr.) posteriorly from anterolateral corners, then narrows behind posteroaxis to midline.

Etymology. Named after Dr. Joseph C. Clark, our colleague and mentor (Indiana University of Pennsylvania).

Material and occurrence. Holotype CM 41373 is a cephalon from collection 5/22/08B: assigned specimens include 9 cephala CM 41310–41314, 41374–41377 and 10 pygidia CM 41315–41319, 41378–41382 from collection 5/22/08B; and 5 cephala USNM 775729–775733 and 5 pygidia USNM 775734–775738 from collection D3362-CO**.** *Lotagnostus nolani* Fauna: collection 5/22/08B (495-383) and 3362-CO (38-46) from the Windfall Formation at Ninemile Canyon, Nevada.

Description. Cephalon semiovate in outline with maximum width approximately equal (89–105%) to length (sag.); moderately convex (tr.) and slightly convex (sag.). Glabella long, 75% (72–79%) of cephalic length (sag.), glabellar width at F3 30% (27–31%) of maximum cephalic width (tr.); slightly convex (sag. and tr.) standing in low relief above genae. Axial furrows moderately impressed in smallest specimens, faintly impressed in larger specimens; straight and strongly convergent (20º to midline) along basal lobes, slightly convergent to gently angular anterolateral corners of glabella; widest (tr.) from anterior tip of basal lobes to midlength of M3; meet medially at obtuse angle (approximately 120 º). Basal lobes subtriangular in outline, moderately long, 28% (24–36%) of glabellar length; end anteriorly at or just in front of F1; end posteriorly in line with small terminal glabellar node; moderately impressed basal furrows straight anterior to posterolateral corners of M1, turning sharply inward posteriorly to follow bluntly pointed back of M1 to glabellar culmination. Occipital band short (sag.). F1 absent, or a very faintly impressed, anteromedially directed furrow extending less than a third of the way to the midline. Slight abaxial shift of axial furrow at F1 expands the posterior half of M2, making it as wide (tr.) or slightly wider than M3; constriction of anterior half of M2 produces narrowest (tr.) part of glabella and widest segment of axial furrow; small, nearly circular glabellar node centered on anterior half of M2. M3 trisected in larger specimens by longitudinal furrows that converge and shallow anteriorly, defining slightly elongate (exsag.), subelliptical lateral lobes. F2 faintly to moderately impressed, anteromedially directed, terminating at posterior ends of longitudinal furrows of M3. F3 transglabellar, moderately impressed, straight to gently concave anteriorly in smaller specimens, tripartite in larger specimens with transverse central segment and lateral segments in front of lateral lobes of M2 directed anterolaterally abaxially to intersection with axial furrow. Anteroglabella accounts for 30% (27-33%) of glabellar length (sag.); subpentagonal in outline with gently angular corners and front. Genae moderately convex and moderately declined (tr.); preglabellar field constitutes 20% (13-23% of cephalic length (sag.), slightly less than width (tr.) of genae laterally; genae smooth in small specimens, weakly scrobiculate in specimens longer (sag.) than 4mm. Median preglabellar furrow moderately impressed, of constant depth and width (tr.), intersects axial

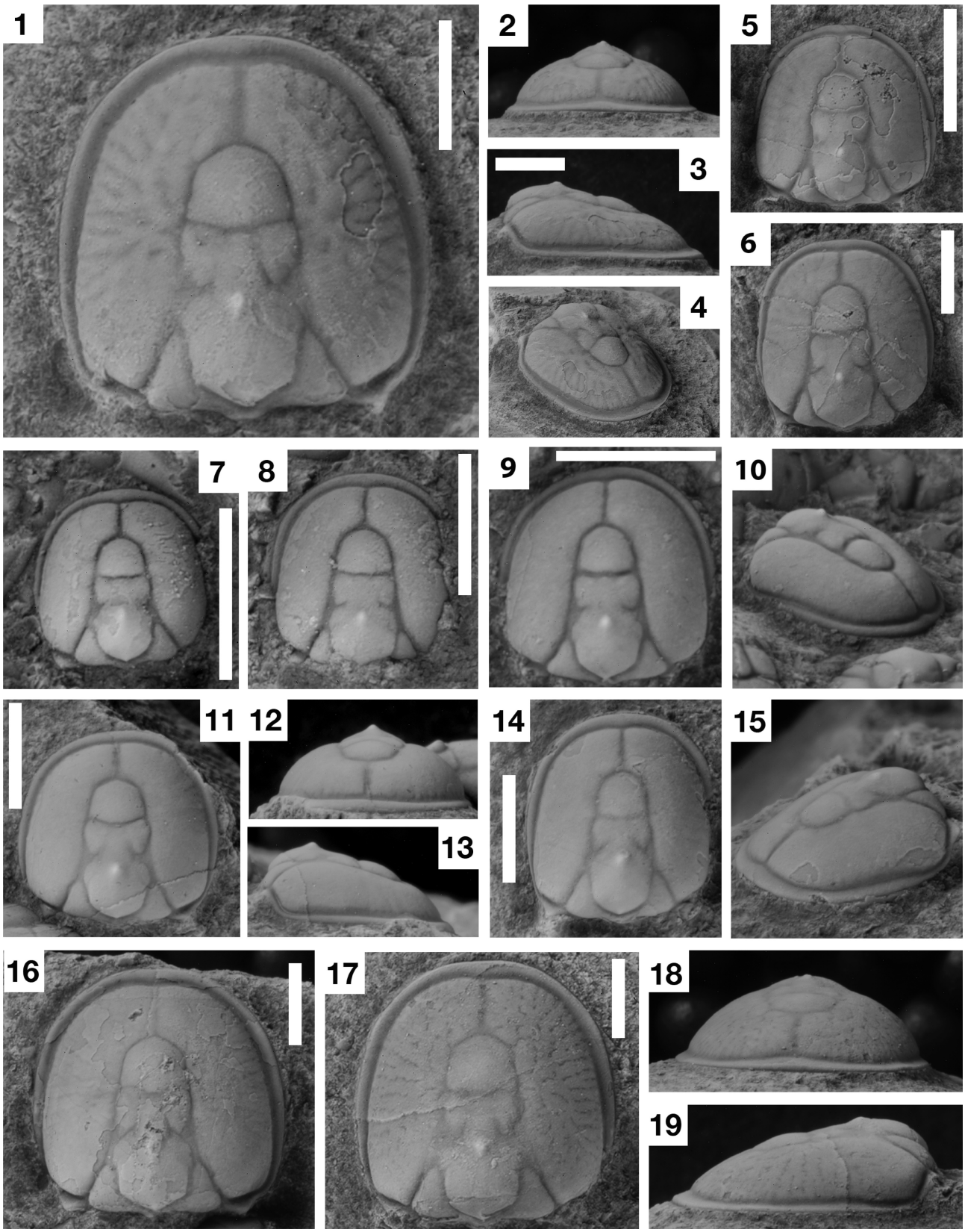

PLATE 10. Cephala of *Lotagnostus clarki* **n. sp.** Each white scale bar represents 2mm. 1-4. Holotype**,** CM 41373, from 5/22/08B, dorsal, anterior, right lateral, and anterior oblique views. 5. USMN 775729, from D3362-CO, dorsal view. 6. USMN 775730, from D3362-CO, dorsal view. 7. CM 41374, from 5/22/08B, dorsal view. 8. CM 41375, from 5/22/08B, dorsal view. 9, 10. USMN 775731, from D3362-CO, dorsal and anterior oblique views. 11-13. USMN 775732, from D3362-CO, dorsal, anterior, and right lateral views. 14, 15. Cephalon, CM 41376, from 5/22/08B, dorsal and anterior oblique views, x9.5. 16. Cephalon, USMN 775733, from D3362-CO, dorsal view, x7.3. 17-19. Cephalon, CM 41377, from 5/22/08B, dorsal, anterior, and left lateral views, x7.0.

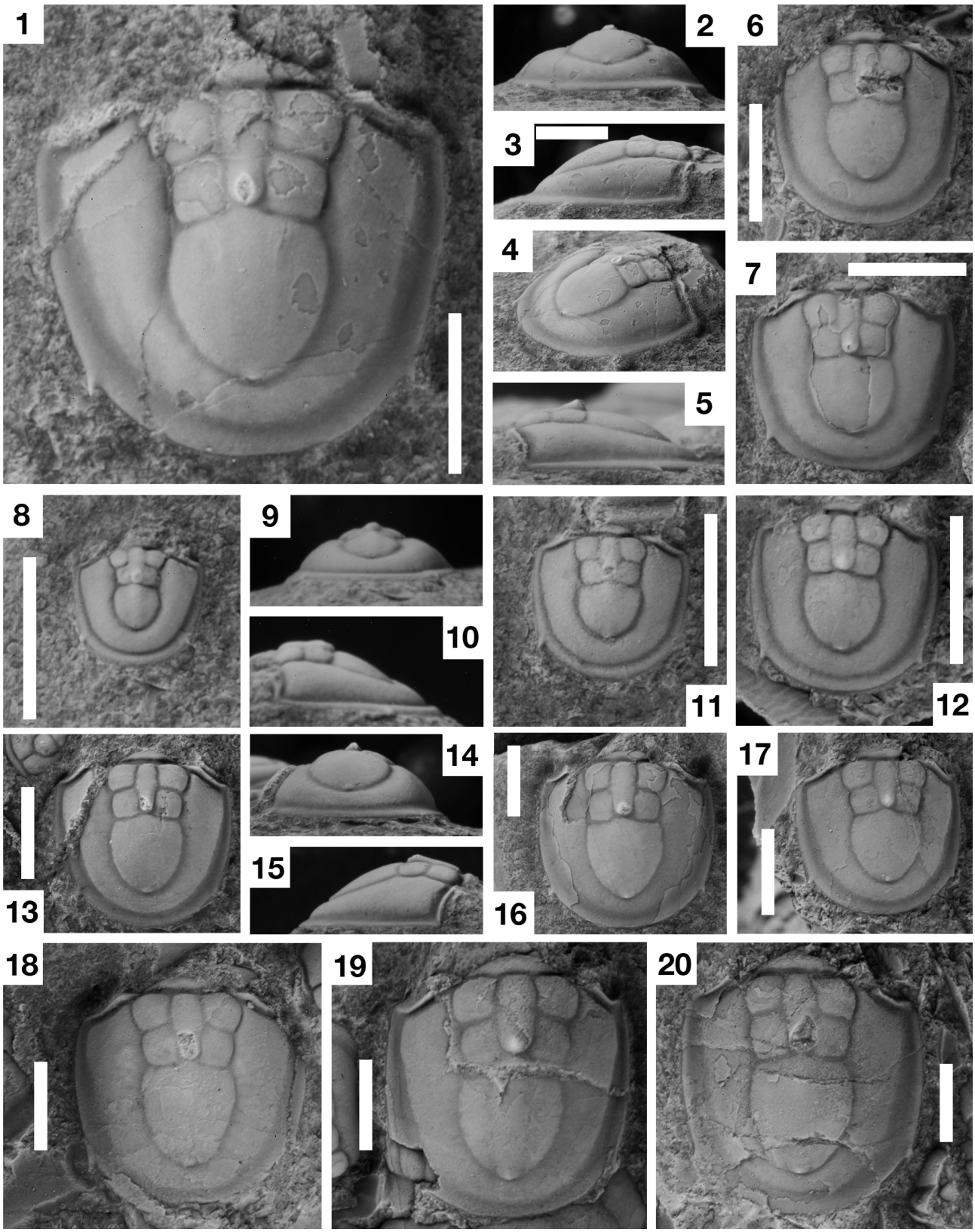

PLATE 11. Pygidia of *Lotagnostus clarki* **n. sp.** Each white scale bar represents 2mm. 1-4. USMN 775734, from D3362-CO, dorsal, posterior, right lateral, and posterior oblique views. 5, 7 USMN 775735, from D3362-CO, left lateral and dorsal views. 6. CM 41317, from 5/22/08B, dorsal view. 8-10. USMN 775736, from D3362-CO, dorsal, posterior, and left lateral views. 11. CM 41316, from 5/22/08B, dorsal view. 12. CM 41378, from 5/22/08B, dorsal view. 13-15. USMN 775737, from D3362-CO, dorsal, posterior, and right lateral views. 16. USMN 775738, from D3362-CO dorsal view. 17. CM 41379, from 5/22/08B, dorsal view. 18. CM 41380, from 5/22/08B, dorsal view. 19. CM 41381, from 5/22/08B, dorsal view. 20. CM 41382, from 5/22/08B, dorsal view.

and border furrows. Border convex, narrow, slightly wider at midline, slightly tapered posteriorly from level of M3. Border furrow well-impressed and narrower than border in small specimens; as wide or slightly wider in large specimens; narrowing posteriorly along posterior third of cephalon; deflected slightly posteriorly at intersection with median preglabellar furrow.

Pygidium semi-elliptical in outline, length (sag.) 92% (87–100%) of maximum width (tr.); moderately convex (sag., tr.); in posterior view axis stands in low relief above moderately declined, slightly convex pleurae; in lateral profile axis slightly declined from axial node in even curve continued by post-axial pleural field. Axis long, 80% (69–85%) of pygidial length exclusive of articulating half-ring; slightly convex (sag., tr.) with exception of axial node; constricted at M2. Articulating half-ring short (sag.), crescentic. Articulating furrow straight, well impressed. Axial furrows moderately impressed, convergent posteriorly from anterior margin, convex laterally over M1, M2, and posteroaxis; slightly shallower around posterior lobe in larger specimens, shallowest medially. Anteroaxis strongly trisected by longitudinal furrows that extend from F2 to articulating furrow; confluent medial lobe of M1 and M2 much narrower (tr.) than lateral lobes of M2, slightly narrower than lateral lobes of M1; M1 lateral lobes slightly inflated, M2 lateral lobes very slightly inflated; asymmetrical axial node at posterior end of confluent medial lobe projects posteriorly to overhang F2. F1 moderately impressed, slightly curved, directed slightly anteromedially from axial furrow across 1/3 width of axis, terminating at intersection with longitudinal furrow. Transaxial F2 moderately impressed, tripartite with narrow (tr.) central segment along posterior margin of confluent medial lobe of anteroaxis, and longer, gently curved lateral segments directed anteromedially from axial furrow. Posteroaxis constitutes 59% (56–61%) of axis length (sag.), slightly convex, slightly declined (sag.); broadest (tr.) slightly anterior to lobe midlength; maximum width variable, averaging 95% (82–118%) of posteroaxis length; small terminal node present; very faint intranotular axis on some specimens, sides defined only by change in slope, except for faintly impressed, very short (exsag.) furrows outlining upturned posterior tip of intranotular axis on a few specimens. Pleural fields narrow (tr.), moderately and evenly convex, slightly declined laterally; typically smooth, rarely very faintly scrobiculate in large specimens; much narrower postaxially in large specimens. Border narrow (sag.), convex, widest medially, tapering steadily toward anterolateral corners. Pair of small posterolateral spines directed posterolaterally and positioned posterior to end of posteroaxis in small specimens; directed posteriorly and located slightly in front of posteroaxis in larger specimens. Border furrow on small specimens uniformly well impressed, nearly constant in width, narrower than border; width and variation in width increase with growth; wider than border in large specimens, widest adjacent to posteroaxis, tapering toward anterolateral corners and behind axis.

Discussion. Many of the specimens of *Lotagnostus peladensis* (Rusconi, 1951a) illustrated by Tortello (2014) strongly resemble *L. clarki,* and some pygidia are nearly identical to those of the latter species. However, large, testate cephala of *L. peladensis* have much shallower furrows, and lack the scrobiculae that characterize *L. clarki* cephala of similar size. Exfoliated cephala of *L. peladensis,* which display more firmly impressed furrows, differ from those of *L. clarki* in having a longer (sag.) preglabellar field that is equal to or greater in length than the anteroglabella (Figure 10.3). In *L. clarki* the length of the preglabellar field is shorter, averaging less than 90% of the anteroglabella length. Another species from Argentina, *L. atenuatus* (Rusconi, 1955b), has weakly scrobiculate genae similar to those of *L. clarki*, but its lateral lobes on M3 are less elongate and are bowed outward to make M3 significantly wider than M2. The pygidium of *L. atenuatus* is readily distinguished from that of *L. clarki* by a prominent intranotular axis bounded by well-impressed notulae.

Lotagnostus asiaticus Troedsson (1937) is the species most similar to *L. clarki* among the species of *Lotagnostus* reported from Asian successions. Using a narrow concept for *L. asiaticus* that includes only weakly scrobiculate specimens similar to the holotype, a full exoskeleton re-illustrated by Peng *et al.* (2015, fig. 4), it is clear that several features that separate these species. Most of the paratypes illustrated by Troedsson as part of the type suite from Xinjiang, China were excluded from the analysis because they are strongly scrobiculate and display very deep furrows, as noted by Westrop & Landing (2016). Aside from the holotype, the specimens we used for comparison with *L. clarki* include (among others) those assigned to *L. asiaticus* from eastern China (western Zhejiang) by Lu & Lin (1980, 1989), and similar specimens from the Wa'ergang section in northwest Hunan (Peng *et al.,* 2015, figs 1, 2). The size series illustrated by Peng *et al.* (2015, fig. 7) was particularly informative regarding the range of variation within *L. asiaticus* as all specimens derived from a single collection level (GC26a) in the Siyanshan section of Lu & Lin (1980, 1989) in Zhejiang. This size series, along with the holotype and similar specimens from the other areas of China, confirms a similar pattern of ontogenetic change for *L. asiaticus* and *L. clarki* in which

scrobiculae are absent from the genae and pleural fields of small specimens and become increasingly prominent with increasing size. However, pygidia of *L. asiaticus* of any size differ from those of *L. clarki* in having gently to moderately impressed notular furrows. Larger pygidia of *L. asiaticus* also display, albeit only faintly, the circular proximal area of the pleural field with radially arranged, short scrobiculae adjacent to the posteroaxis and M2 that occurs in several species of *Lotagnostus,* but not in *L. clarki*. At least three features distinguish *L. asiaticus* cephala from those of *L. clarki.* The former species has a proportionally longer anteroglabella that is more parallel-sided and broadly rounded in front than that of *L. clarki*, whose convergent sides produce a narrower, more angular anterior. Secondly, M2 in *L. asiaticus* is approximately equal in width (tr.) to M1 and significantly narrower than M3. In contrast, M2 is wider than both M1 and M3 on the cephala of *L. clarki.* Finally, on most cephala of *L. clarki,* the anterior border widens (sag.) slightly at the midline along with a slight rearward deflection of border furrow where it intersects the median preglabellar furrow; no such widening or deflection is seen on the cephalon of *L. asiaticus*.

Lotagnostus aff. *L. clarki*

(Plate 6.4–6.10)

1860 *Agnostus americanus* Billings; Billings, p. 303, fig. 1b.
1865 *Agnostus americanus* Billings, 1860; Billings, p. 395, fig. 372b.
1944 *Agnostus americanus* Billings, 1860; Rasetti, p. 233, pl. 36, fig. 1.
1989 *Lotagnostus americanus* (Billings, 1860); Ludvigsen & Westrop *in* Ludvigsen, Westrop, and Kindle, p. 12, pl. 1, fig. 16.
2005 *Lotagnostus americanus* (Billings, 1860); Peng & Babcock, p. 110–113, fig. 2.3.
2009 *Lotagnostus americanus americanus* (Billings, 1860); Rushton, p. 276, fig. 1J–O.
2011 *Lotagnostus americanus* (Billings, 1860); Westrop, Adrain, & Landing, p. 578–584, figs 5D–G, 6.
2015 *Lotagnostus americanus* (Billings, 1860); Peng, Babcock, Zhu, Ahlberg, Terfelt, & Dai, fig. 5G.

Discussion. The restriction of *Lotagnostus americanus* to the holotype necessitates re-evaluation of the remaining material from the Lévis Formation formerly assigned to that species. Although the pygidia are indistinguishable from those of *L. clarki,* the cephala differ in the structure of M2, M3, and the anteroglabella. M2 on *L.* aff. *L. clarki* is equal in width (tr.) to M1 and narrower than M3, whereas M2 on *L. clarki* is wider than both M1 and M3. The lateral lobes of M3 on *L.* aff. *L. clarki* are nearly circular in shape, whereas those of *L. clarki* are more elongate and taper posteriorly. In some specimens of *L.* aff. *clarki* they display greater inflation with the distal sides bowing more strongly outward. The species from the Lévis also appears to have a proportionally longer anteroglabella. The ratio between the axial length of the anteroglabella (AAL) and that of the posteroglabella (APL) obtained from *L. clarki* cephala varied from 0.47 to 0.54, with an average of 0.49. Unfortunately, only three of the seven cephala from the Lévis Formation illustrated by Rushton (2009) and Westrop *et al.* (2011) were preserved well enough for accurate measurement of the AAL/APL ratio. Nonetheless, two of those specimens yielded values (0.56, 0.62) outside the range documented for *L. clarki* cephala.

Lotagnostus rushtoni n. sp.

(Plate 12)

Diagnosis. Non-scrobiculate *Lotagnostus* with narrow, strongly curved anterior margin; glabella long and ogival; lateral lobes of M3 defined only by inflation with no bounding longitudinal furrows; slightly elongate glabellar node sits high on elliptical elevated platform on anterior half of M2; large, inflated basal lobes with convex lateral margins extend well behind glabellar culmination; pygidium with transaxial F1; axial furrows narrow and moderately impressed; broad (tr.) posteroaxis with intranotular area undefined or extremely faint; acrolobe unconstricted; post-axial pleural field narrow (sag.); border furrow wide, deep, constant in width, with sharp boundaries with pleural field and border.

Etymology. Named after A.W.A. Rushton for his meticulous work on Cambrian taxa, among them *Lotagnostus.*

Material and occurrence. Holotype CM 41385 is a pygidium from collection 5/22/08D: assigned specimens include 2 cephala CM 41383–41384 and 1 pygidium CM41386 from collection 5/22/08D; 2 pygidia USNM 775743, 775746 from collection D3381-CO; and 4 cephala USNM 775739–775742 and 2 pygidia USNM 775744–775745

from collection D3383-CO. *Lotagnostus rushtoni* Fauna: collection 5/22/08C (32-40), 5/22/08D (36-34), D3381-CO (0-3) and D3383-CO (9-18) from the Windfall Formation at Ninemile Canyon, Nevada.

Description. Cephalon semiovate in outline with maximum cephalic width equal to cephalic length (97–105%); slightly convex (sag.) to moderately convex (tr.). Glabella long (sag.), 76% (71–81%) of cephalic length; narrow, accounting for approximately a third of cephalic width at M3; slightly convex (tr.), rising only slightly above genae in anterior and lateral views. Axial furrows moderately impressed; strongly convergent (30º angle to midline) from posterior margin to anterior end of basal lobes, parallel to very slightly convergent to poorly defined anterolateral corners of glabella, strongly convergent (45º) to front of glabella. Basal lobes long, 32% (26–35%) of glabellar length; basal furrow moderately impressed, but slightly narrower than axial furrows. Very short (sag.), gently curved, posteriorly convex occipital band. F1 a very shallow (tr.) indentation in side of glabella near anterior tip of basal lobe. Glabellar culmination very bluntly pointed with very faint terminal node. M2 equal in width (tr.) or slightly narrower than M3, with rounded anterolateral corners; prominent, slightly elongate glabellar node centered on inflated, elliptical area on posterior half of M2; F2 moderately impressed abaxially, faintly impressed medially in small specimens, incomplete across axis in larger specimens, directly slightly anteromedially. M3 divided transversely into a shorter (sag.), anteriorly tapering, medial lobe flanked by slightly inflated, elongate, subelliptical lateral lobes; boundaries between medial and lateral lobes defined by change in slope rather than furrows. Transglabellar F3 moderately impressed, slightly to moderately concave anteriorly in larger specimens. Ogival anteroglabella constitutes 33% (31–36%) of glabellar length (sag.). Width of genal field, equal to glabellar width (tr.) at F2, steadily decreases anteriorly to where preglabellar field constitutes only 16% (12–18%) of cephalic length at midline; slope angle of genal field increases abaxially from near-horizontal adjacent to axial furrow to vertical at border furrow, causing genal field to overhang border at posterolateral corners. Genal and preglabellar fields nonscrobiculate. Border narrow, convex, narrowing slightly posteriorly. Border furrow well impressed, uniform in depth and width, slightly narrower than border.

Pygidium semiovate in outline, pygidial length exclusive of articulating half-ring 91% (85–94%) of maximum width (tr.) at F2; moderately convex (sag., tr.). Axis long, 82% (78–85%) of pygidial length; slightly convex (sag., tr.), standing in slight relief above adjacent pleural fields; post-axial pleural field continues gentle posterior slope of posteroaxis in lateral view. Anteroaxis accounts for less than half (42–46%) of length (sag.) of axis. Axial furrows moderately impressed; slightly convergent from anterior margin to F2, bowed outward along M1, less so along M2; bowed outward along sides of ogival posteroaxis. Articulating half ring short (sag.), crescentic; width (tr.) approximately 70% of M1; articulating furrow deep and broad (sag.), narrowing laterally in front of lateral lobes of M1. M1 wider (tr.) than M2 and posteroaxis, trisected by longitudinal furrows into slightly shorter (sag.) and narrower (tr.) medial lobe with gently abaxially convex sides, and inflated lateral lobes with broadly rounded anterolateral corners. F1 transaxial, bowed forward slightly, moderately impressed, shallowing over midline in some specimens. M2 trisected, longitudinal furrows slightly shallower than on M1; medial lobe narrower (tr.) than medial lobe of M1, longer (sag.) and narrower than lateral lobes of M2; large, strongly asymmetrical axial node on posterior half of M2 extends postero-dorsally to overhang F2. Transaxial F2 moderately impressed, transverse to gently anteriorly convex; wider (exsag.) and curved forward slightly at intersection with axial furrows on some specimens, producing rounded posterolateral corners on lateral lobes of M2; shallower and deflected sightly forward over midline at base of axial node. Posteroaxis slightly wider (tr.) than M2; maximum width slightly greater than length (sag.); some specimens display very faint intranotular axis circumscribed by slight change in convexity and flat, terminating in flat, upturned tip. Pleural fields narrow, widest (tr.) at level of slightly constricted M2, narrowing posteriorly to produce short (sag.) post-axial field; moderately convex (tr., sag.); moderately declined post-axially as seen in lateral view; slightly declined from axial furrows increasing to moderately sloping near border furrow. Non-scrobiculate. Border flatly convex, moderate in width, 8% (7–10%) of pygidial length exclusive of articulating half-ring; widest at midline, tapering toward anterolateral corners. Border furrow broad, well impressed with very steep boundaries with pleural field and border; narrows slightly anterior to short posterolateral spines that lie just anterior to end of axis. Shoulder furrow well impressed, narrow (exsag).

Discussion. *Lotagnostus rushtoni* is distinguished from *L. morrisoni,* with which it co-occurs in the Windfall Formation, by the gentler convexity and abaxial slope of the proximal genal and pleural fields, longer and more pointed anteroglabella, transaxial pygidial F1, relatively longer and narrower posteroaxis (Figure 10.4), and absence of notular furrows. All *Lotagnostus clarki* cephala differ from those of *L. rushtoni* in exhibiting a longer preglabellar field, less pointed anteroglabella, and a smaller glabellar node not elevated by inflation of the surrounding area. Larger *L. clarki* cephala are weakly scrobiculate, whereas those of *L. rushtoni* are smooth. The transaxial F1

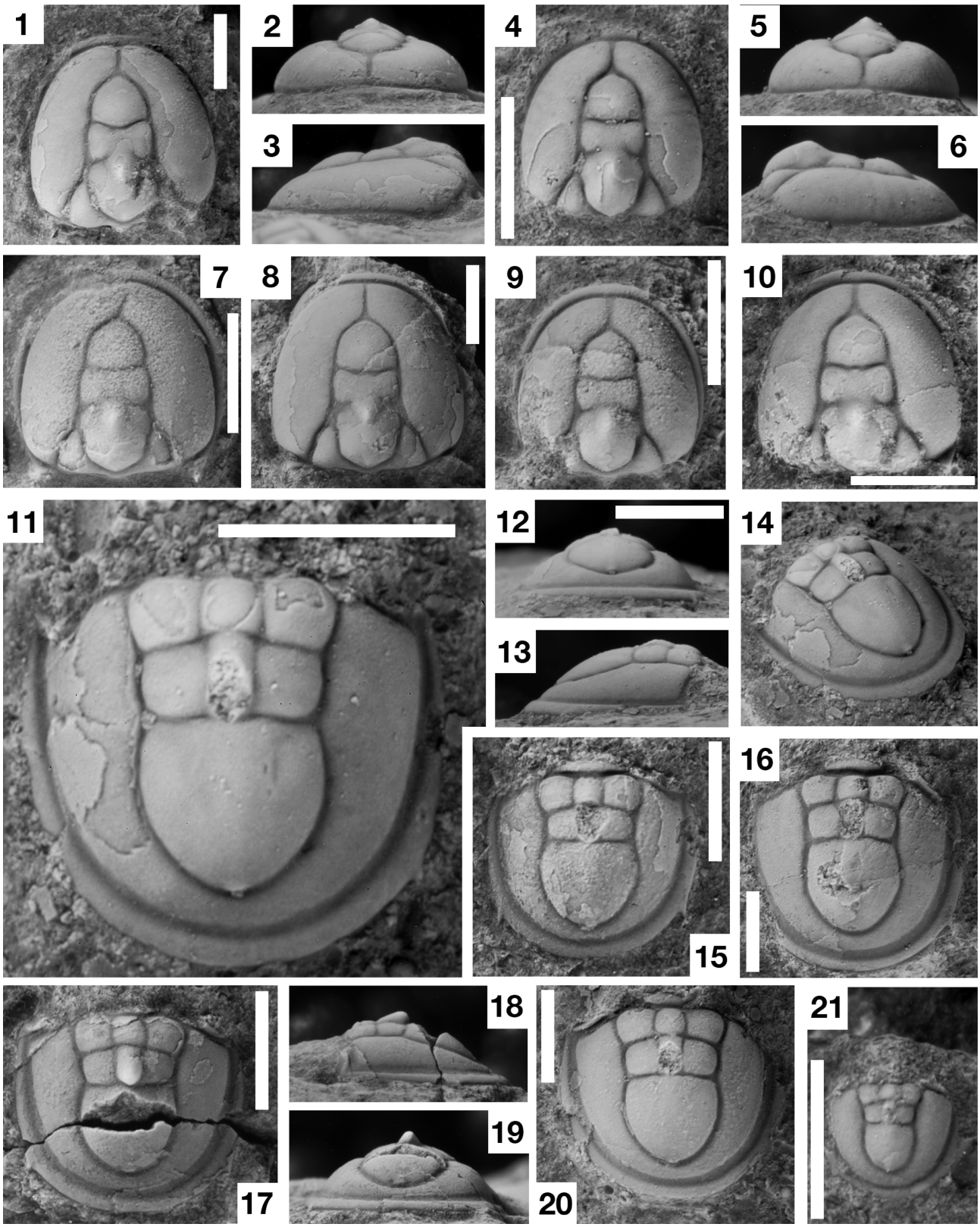

PLATE 12. *Lotagnostus rushtoni* n. sp. Each white scale bar represents 2mm. 1-3. Cephalon, CM 41383, from 5/22/08D, dorsal, anterior, and left lateral views. 4-6. Cephalon, USMN 775739, from D3383-CO, dorsal, anterior, and right lateral views. 7. Cephalon, USMN 775740, from D3383-CO, dorsal view. 8. Cephalon, USMN 775741, from D3383-CO, dorsal view. 9. Cephalon, USMN 775742, from D3383-CO, dorsal view. 10. Cephalon, CM 41384, from 5/22/08D, dorsal view. 11-14. Pygidium, holotype, CM 41385, from 5/22/08D, dorsal, posterior, right lateral, and posterior oblique views. 15. Pygidium, USMN 775743, from D3383-CO, dorsal view. 16. Pygidium, USMN 775744, from D3383-CO, dorsal view. 17-19. Pygidium, USMN 775745, from D3383-CO, dorsal, left lateral, and posterior views. 20. Pygidium, CM 41386, from 5/22/08D, dorsal view. 21. Pygidium, USMN 775746, from 3D3381-CO, dorsal view.

distinguishes all *L. rushtoni* pygidia from those of *L. clarki* and larger sclerites of the former display a deeper, more steep-sided border furrow and wider posterior border.

The transaxial pygidial F1 sets *Lotagnostus rushtoni* apart from all other non-scrobiculate species of the genus except *L. hedini* and *L.* aff. *L. rushtoni.* The latter species is discussed in more detail below. The cephalon of *L. rushtoni* differs from that of *L. hedini* in possessing longer and more inflated basal lobes that extend posteriorly beyond the glabellar culmination; the posterior ends of the basal lobes of *L. hedini* lie in line with, or slightly in front of the glabellar culmination. *L. rushtoni* also has a shorter (sag.) and more tapered glabella. The pygidium differs from that of *L. hedini* in having a proportionally shorter (Figure 10.4) and more broadly rounded posteroaxis, an unconstricted acrolobe, and a deep, symmetrical, trough-like border furrow that is less variable in width, and is narrower than the border posterior to F2.

Lotagnostus aff. *L. rushtoni*

(Plate 6.11–6.18)

1989 *Lotagnostus hedini* (Troedsson, 1937); Ludvigsen & Westrop *in* Ludvigsen, Westrop, and Kindle, pl. 1, figs 1–8 only.

Occurrence. *Keithia schucherti* Fauna in the Gorge Formation, Vermont, and Green Point Formation, Newfoundland.

Discussion. The sclerites assigned to this species are those illustrated from the "Main Zone" of the Gorge Formation as *Lotagnostus hedini* in Ludvigsen *et al.* (1989), but subsequently removed from that species by Westrop *et al.* (2011), as well as three pygidia recovered from a clast in the Bed 19 limestone conglomerate in the Global Stratotype Section for the Cambrian-Ordovician boundary at Green Point, Newfoundland (Cooper *et al.,* 2001). Although conodonts recovered from clasts and matrix confirm a significantly younger, Skullrockian age (*Cordylodus intermedius* Zone, or younger) depositional age for Bed 19, trilobites from the clast that yielded *L.* aff. *L. rushtoni* are all Sunwaptan species characteristic of the *Acheilus monile* Fauna of Fortey (1983) and equivalent *Keithia schucherti* Fauna of Ludvigsen *et al.* (1989). *Lotagnostus* aff. *L. rushtoni* closely resembles *L. rushtoni* but has smaller and less inflated basal lobes, a wider (tr.) and more broadly rounded posteroaxis that is as wide or wider than M1, and is conspicuously bulbous in large specimens. Additionally, the pygidial border furrow is narrower, shallower, and lacks the sharp boundary with the border characteristic of *L. rushtoni.*

Lotagnostus morrisoni n. sp.

(Plate 13)

Diagnosis. Non-scrobiculate species with parts of glabella and pygidial axis that lie slightly below dorsally convex proximal areas of acrolobes; anterior end of glabella and posterior end of pygidial posteroaxis particularly low-lying relative to preglabellar field and postaxial pleurae, respectively. Approximately inner third of acrolobe slopes gently toward axial furrow while distal two-thirds descend steeply abaxially to border furrow. Cephalic acrolobe narrows (sag.) only slightly in front of short (sag.), bluntly rounded anteroglabella. A pair of small, elliptical nodes at posterior ends of lateral lobes of M3 discernible on exfoliated cephala. Small, circular glabellar node sits in line with posterior end of very broad (exsag.) F2. Pygidial F1 discontinuous, terminating adaxially at longitudinal furrow that bounds confluent central lobes of M1 and M2. Relatively short (sag.) posteroaxis weakly trisected with intranotular axis bounded only by change in slope along most of its length, but by weakly impressed notular furrows along posterior-most one fourth to one fifth. Pygidial acrolobe constant in width from midlength of posteroaxis to midline behind axis.

Etymology. Named after Scott Morrison for invaluable assistance in conducting a thorough review of the relevant literature.

Material and occurrence. Holotype CM 41389 is a pygidium from collection 5/22/08D: assigned specimens include 1 cephalon CM 41388 from collection 5/22/08D; 1 cephalon CM 41387 from collection 5/22/08C; and 1 cephalon USNM 775747 and 4 pygidia USNM 775748–775751 from collection D3381-CO. *Lotagnostus rushtoni* Fauna: collections 5/22/08C (1-2), 5/22/08D (1-2) and D3381-CO (10-15) from Windfall Formation at Ninemile Canyon, Nevada.

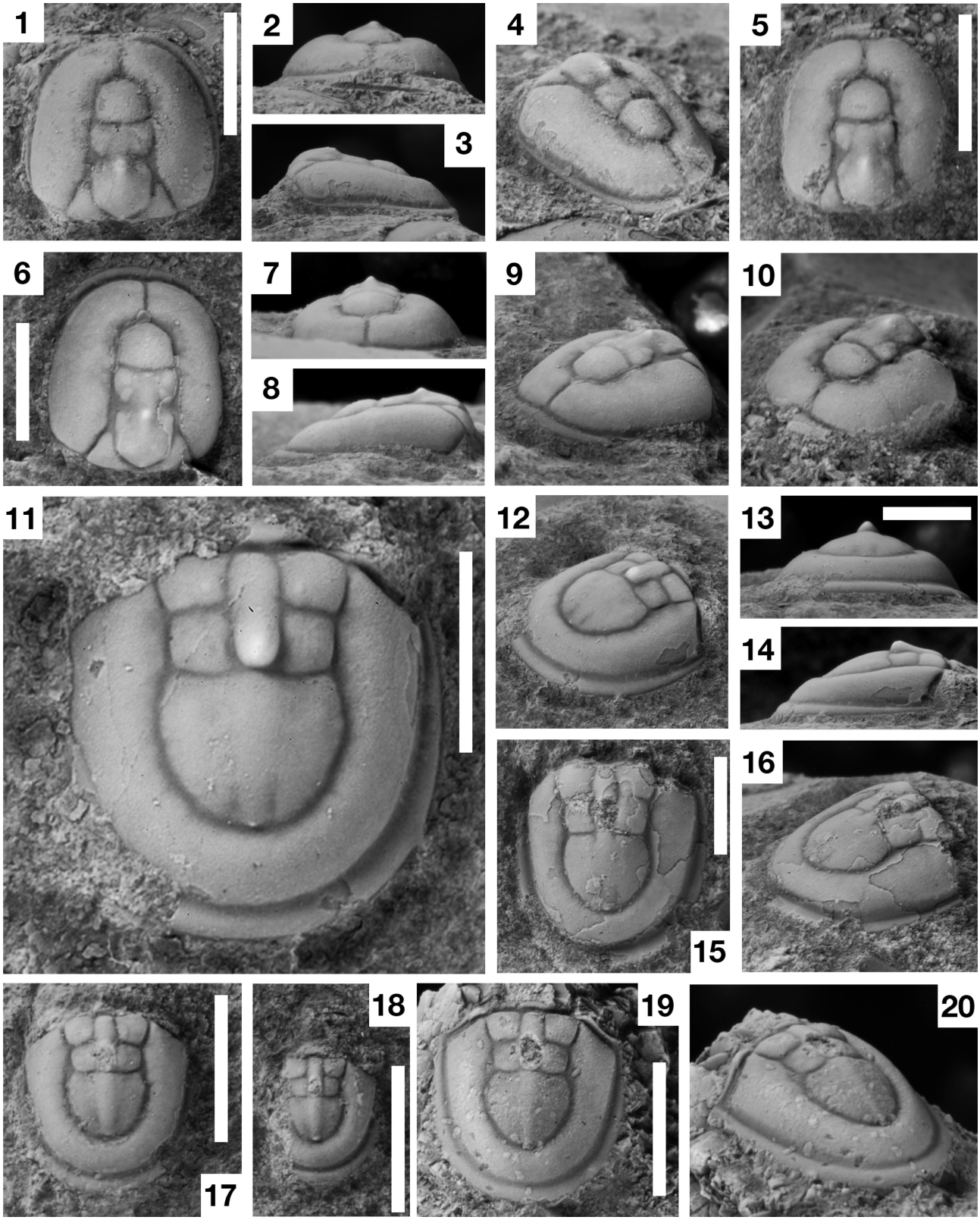

PLATE 13. *Lotagnostus morrisoni* **n. sp.** Each white scale bar represents 2mm. 1-4. Cephalon, USMN 775747, from D3381-CO, dorsal, anterior, right lateral, and anterior oblique views. 5, 10. Cephalon, CM 41387, from 5/22/08C, dorsal and anterior oblique views. 6-9. Cephalon, CM 41388, from 5/22/08D, dorsal, anterior, lateral, and anterior obliqueviews. 11-14. Pygidium, holotype**,** CM 41389, from 5/22/08D, dorsal view; posterior oblique, posterior, and right lateral views. 15-16. Pygidium, USNM 775748, from 3D3381-CO, dorsal and posterior oblique views. 17. Pygidium, USMN 775749, from 3D3381-CO, dorsal view. 18. Pygidium, USNM 775750, from 3D3381-CO, dorsal view. 19-20. Pygidium, USMN 775751, from 3D3381-CO, dorsal and posterior oblique views.

Description. Cephalon semiovate with maximum cephalic width equal to cephalic length (97–105%); strongly convex (sag.) posterior to glabellar node, gently convex from node to anterior margin; moderately to strongly convex (tr.). Glabella moderately long (sag.), accounts for 77% (71–84%) of cephalic length, and a third of cephalic width (tr.) at M3; slightly convex (tr.), barely rises above adjacent pleural fields in anterior and lateral views. Axial furrows broad, moderately impressed; strongly convergent (30º angle to midline) from posterior margin to anterior end of basal lobes, continuing nearly straight until slightly angular turn at anterolateral corners of glabella, converge strongly (60-65º angle to midline) to intersection with median preglabellar furrow. Basal lobes long, 33% (27–35%) of glabellar length; basal furrow moderately impressed, but slightly fainter than axial furrows. Border rim-like, of even width. Border furrow moderately impressed, uniform in depth. Acrolobe semi-circular, maximum width opposite of F2 furrow; moderately convex in lateral and anterior views. Median preglabellar furrow moderately impressed. F1 as slight widening of axial furrows at anterior end of basal lobes; M2 equal in width (tr.) to M1, with small, circular glabellar node centered on anterior half; F2 moderately impressed abaxially, wide (exsag.) and short (tr.), extending only halfway to midline. M3 weakly trisected by very faint longitudinal furrows or change in convexity into wider (tr), anteriorly tapering medial lobe between very slightly inflated, elliptical lateral lobes; smaller, elliptical lobes discernible at posterior ends of lateral lobes on exfoliated specimens. F3 transglabellar, moderately impressed, weakly anteriorly concave. Anteroglabella subpentagonal in outline with rounded anterolateral corners and bluntly pointed front; accounts for 33% (31–36%) of glabellar length. Genae widest (tr.) at F2, narrowing very slightly anteriorly to where preglabellar field accounts for 20% of cephalic length at midline; genae moderately to strongly convex with adaxial third inclined toward axial furrow and distal two thirds descending steeply to border furrow. Adaxial slope of proximal third results in parts of the glabella lying below highest areas of adjacent genal field, imparting a depressed or "sunken" appearance to the anterior third to half of the glabella.

Pygidium semiovate in outline, maximum width (tr.) slightly less (87–100%) than pygidial length exclusive of articulating half-ring; moderately convex (sag., tr.). Axis moderate in length, 70% (67–76%) of pygidial length; slightly convex (sag., tr.), margins lie slightly below height of elevated adjacent pleural fields; widest at M1, slightly constricted at M2, with broadly rounded posteroaxis nearly as wide (tr.) as M3. Axial furrows moderately impressed, slightly shallower along M1, subparallel along M2, abaxially convex along slightly inflated lateral lobes of M1 and posteroaxis. Anteroaxis short (sag.), less than half (42-46%) of length of axis, trisected by moderately impressed longitudinal furrows that create confluent, medial lobe of M1 and M2. F1 and F2 moderately impressed; F1discontinuous, straight, directed slightly anteromedially from axial furrow, terminating at intersection with longitudinal furrows; F2 transaxial, slightly concave forward along posterior margins of M2 lateral lobes, transverse and shallower along base of posteriorly projecting axial node positioned at posterior end of confluent medial lobe. Posteroaxis relatively short (sag.), length only 91% (81-95%) of maximum width; trisected with faint intranotular axis, more clearly defined in smaller specimens; notular furrows restricted to posterior, and in a few specimens anterior, ends of intranotular axis, with remainder delineated only by changes in convexity; faint terminal node present on some specimens. Pleural fields moderately to strongly convex (tr., sag.); moderately declined post-axially in lateral view; in posterior view genae rise from axial furrows before declining steeply to border furrow; proximal third anterior to F2 subhorizontal; width of pleural field constant from midline anteriorly to maximum width of posterior lobe, increasing along anteroaxis. Smooth, non-scrobiculate. Border convex; maximum width at midline 8% (7–10%) of pygidial length (sag.) exclusive of articulating half-ring; tapering anteriorly. One pair of small, posterolaterally directed posterolateral spines positioned slightly posterior to end of axis on holotype (Pl. 13.11-14). Border furrow moderately impressed, asymmetrical with sharp boundary with pleural field and more gradual transition to border; as wide or wider than border anterior to posterolateral spines, narrowing behind axis to be narrower than border.

Discussion. *Lotagnostus morrisoni* **n. sp.** appears unique among non-scrobiculate species of *Lotagnostus* in the depressed appearance of the axial structures imparted by inflated genal and pleural fields that rise above the axial furrows. The lack of similarly depressed appearance of the axis in specimens of *L. rushtoni* in the same collections confirms that it is a primary character of the species rather than a taphonomic effect. Cephala from the Frederick Valley of Maryland identified as *Lotagnostus* sp. by Rasetti (1959) and reillustrated by Westrop & Landing (2016, fig. 12) display a similar position of the axis relative to the genae and pleural fields, but are easily distinguished by well-developed scrobiculae and strongly depressed lateral lobes of M2. *Lotagnostus morrisoni* also differs from the contemporaneous species *L. rushtoni* **n. sp.** in the presence of the slight nodes in the posterolateral corners of glabellar M3 and the relative proportions of the pygidium.

***Lotagnostus* sp.**
(Plate 16.12, 16.14–16.16)

Material and occurrence. *Hedinaspis-Charchaqia* Fauna: collections 7129-CO (7-4), 7131-CO (0-2), and 7133-CO (4-2) from the Hales Limestone at the Hot Creek section, Nevada.

Discussion. A few specimens in the collections from the Hales represent a non-scrobiculate *Loagnostus* species that is similar to *L. clarki* but differs in having a proportionally shorter (sag.) anteroglabella, and in having the sides of the intranotular axis marked by distinctly impressed notulae or notular furrows.

***Micragnostus* Howell, 1935a**

Type species. *Agnostus calvus* Lake, 1906, by original designation, from Wales.

Discussion. Several specimens in collection 5/22/08B represent one or more genera of a problematic group of similar agnostoids with rather generalized cephala and strongly convex pygidial axes that includes, among others, *Homagnostus, Micragnostus, Oncagnostus* and *Trilobagnostus.* The amount of material from the Windfall is too limited to add anything to recent efforts to identify diagnostic apomorphic traits that will improve the consistency of assignment of species to these closely related genera (e.g., Choi *et al*., 2004; Westrop & Eoff, 2012).

Micragnostus* cf. *M. intermedius
(Plate 7.17–7.18)

Discussion. This single pygidium in collection 5/22/08B from Ninemile Canyon strongly resembles the holotype of *Micragnostus intermedius* (Palmer, 1968) in its transverse F2, parallel trend of the axial furrows from F1 to slightly posterior to F2 posteroaxis, wide and deep border furrow and narrow border. It does, however, display a slightly less inflated, nearly semi-circular posteroaxis. Whether that difference is merely intraspecific variation is undeterminable with the limited material available for comparison.

***Homagnostus* Howell, 1935b**

Type species. *Agnostus pisiformis* var. *obesus* Belt, 1867 by original designation from Wales.

***Homagnostus*? sp.**
(Plate 7.10–7.12, 7.16, 7.21–7.22)

Material and occurrence. *Lotagnostus nolani* Fauna: collection 5/22/08B (2-4) from the Windfall Formation at Ninemile Canyon, Nevada.

Discussion. The features supporting tentative assignment of this rare species in the Windfall to *Homagnostus,* following the generic diagnosis of Shergold & Laurie (1997), include the presence of a median preglabellar furrow, and a strongly convex pygidium with a laterally constricted M2 and inflated posteroaxis.

Family Diplagnostidae Whitehouse, 1936

Subfamily Pseudagnostinae Whitehouse, 1936

***Pseudagnostus* Jaekel, 1909**

Type species. *Agnostus cyclopyge* Tullberg, 1880, by original designation, from Sweden.

***Pseudagnostus*? spp.**
(Plate 16.8, 16.9)

Discussion. The poor state of preservation and largely effaced condition of these two articulated specimens from the *Hedinaspis-Charchaqia* Fauna in the Hot Creek section of the Hales renders assignment even to genus difficult. The posterior placement of the glabellar node on one specimen (Plate 16.9) and suggestion of a broadly expanded posteroaxis on the other (Plate 16.8) is consistent with a spectaculate agnostine, justifying tentative assignment to *Pseudagnostus.* It is possible, however, that the two specimens are not conspecific.

***Rhaptagnostus* Whitehouse, 1936**

Type species. *Agnostus cyclopygeformis* Sun, 1924 from China.

***Rhaptagnostus* cf. *R. convergens* (Palmer, 1955)**
(Plate 7.4–7.6)

Discussion. One largely effaced, subelliptical cephalon in collection 5/22/08B displays the forward placement of the glabellar node between the anterolateral lobes of M3 (the papillionate condition), thereby conforming to the diagnosis of *Rhaptagnostus* (Shergold & Laurie, 1997). In most respects it resembles *R. convergens* (Palmer, 1955), but is more elongate and the median preglabellar furrow is less uniformly impressed, deepest in front of the glabella, shallowing anteriorly and does not reach the border furrow. It also closely resembles *R. papilio* (Shergold, 1971), but that species has much smaller basal glabellar lobes. Given these differences, and lack of an associated pygidium in the collection, the Windfall species is left in open nomenclature.

***Neoagnostus* Kobayashi, 1955**

Type species. *Neoagnostus aspidoides* Kobayashi, 1955, by original designation, from the McKay Group, British Columbia, Canada.

Diagnosis. The diagnosis of Naimark (2016, p. 61–62) that features a "V-shaped" F3 and chevron-shaped F2 glabellar furrows and pygidial axial furrows which fail to surround the posteroaxis, and a pair of inflated nodes located posterior to F2 is accepted.

Other species. *N. bilobus* (Shaw, 1951); *N. longicolis* Kobayashi, 1966; *N. eckardti* Jell, 1985*; N. hangulensis* Lu & Zhou, *in* Lu *et al*., 1981; *N. shiziluensis* Lu and Zhou, 1990; *N. tarjensis* (Gilberto, 2010); *N. parki* **n. sp.**

Discussion. Shergold (1975, 1977) considered *Neoagnostus* a subjective junior synonym of *Pseudorhaptagnostus* Lermontova, 1951, which he treated *sensu lato.* He described a "spectaculate" morphology in which the glabellar node lies posterior to the F2 glabellar furrow which he subdivided into multiple species groups. Among these "spectaculate" forms he included a "*Bilobus group*" that he acknowledged may have represented a genus-level grouping and which included *Neoagnostus aspidoides*, the type species of *Neoagnostus.* Shergold (1980) then provisionally recognized *Neoagnostus* as a valid genus. Shergold *et al.* (1990; Shergold & Laurie, 1997) sought to establish subgenera for *Neoagnostus*, a practice followed by some authors (Nielson, 1997). Naimark (2016) briefly discussed the nomenclatorial history of *Pseudorhaptagnostus* and revived the generic status of *Neoagnostus* without subgenera.

***Neoagnostus parki* n. sp.**
(Plates 14, 15)

Diagnosis. *Neoagnostus* with a relatively long (sag.) preglabellar field. Median preglabellar furrow very weakly impressed to absent, shallowing anteriorly and not reaching the border furrow. F3 indistinct, expressed only as

shallow notches in side of glabella anterior to moderately impressed, chevron-shaped, transglabellar F2. Narrow (tr.), angular glabellar culmination extending as blunt spine to posterior end of large basal glabellar lobes. Pygidium exhibits faintly impressed F1 furrows, moderately impressed F2 furrows and moderately impressed axial furrows that diverge posteriorly from F2, terminating a short distance posterior to pair of slightly inflated bosses.

Etymology. Named in honor of our undergraduate mentor and colleague at Indiana University of Pennsylvania, Frederick R. Park.

Material and occurrence. Holotype CM 41394 is a cephalon from collection 5/22/08B: assigned specimens include 4 cephala CM 41390–41393 and 5 pygidia CM 41352, 41354, 41355 from collection 5/22/08B and 1 cranidium USNM 775752 and 1 pygidium USNM 775753 from USGS collection D3362-CO. *Lotagnostus nolani* Fauna: collections 5/22/08B (62-48) and D3362-CO (4-6) from the Windfall Formation at Ninemile Canyon, Nevada.

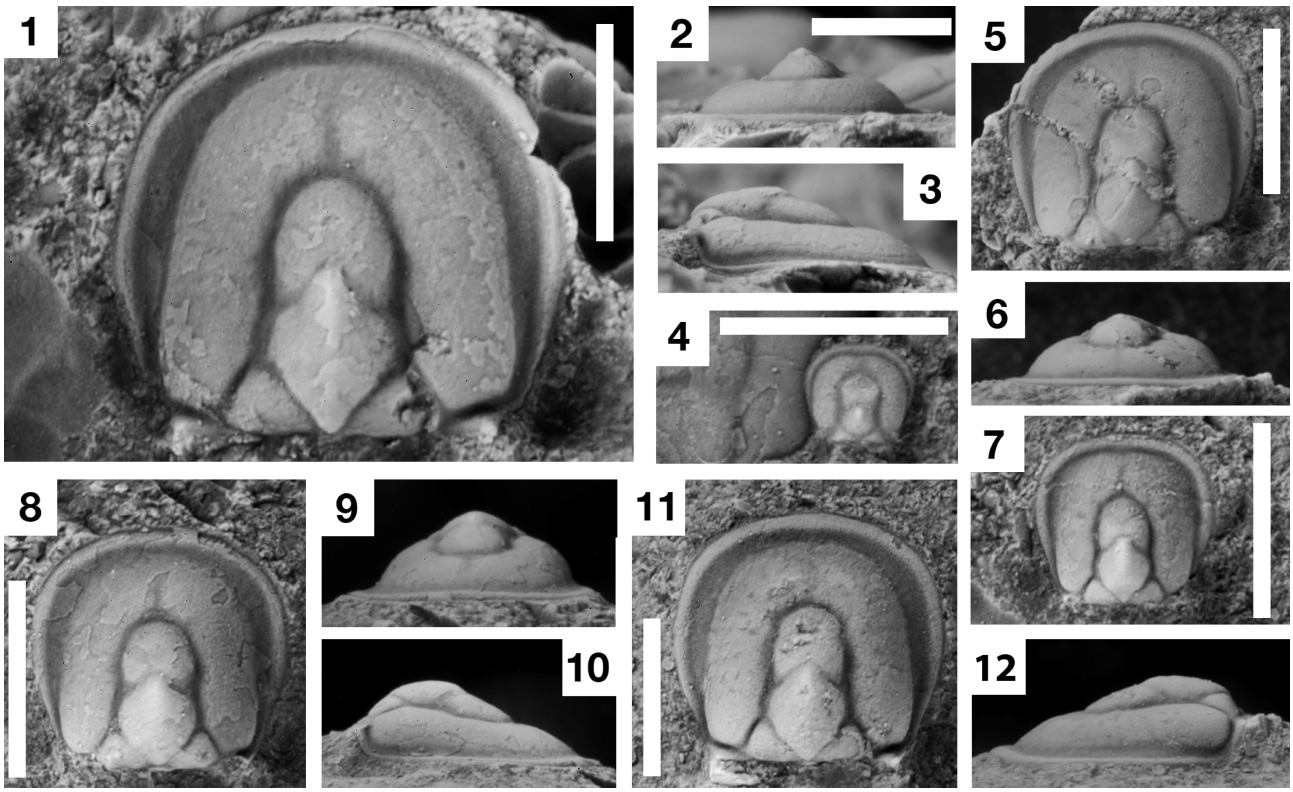

PLATE 14. Cephala of *Neoagnostus parki* **n. sp.** Each white scale bar represents 2mm. 1-3. Holotype, CM 41394, from 5/22/08B, dorsal, anterior, and left lateral views. 4. CM 41391, from 5/22/08B, dorsal view. 5-6. USMN 775752, from D3362-CO, dorsal and anterior views. 7. CM 41392, from 5/22/08B, dorsal view. 8-10. CM 41393, from 5/22/08B, dorsal, anterior, and right lateral views. 11-12. CM 41390, from 5/22/08B, dorsal and left lateral views.

Description. Cephalon subquadrate, cephalic length (sag.) equaling 91% (88–94%) of maximum width (tr.); width at posterior margin 80% (77–91%) of maximum width; moderately (sag.) and strongly (tr.) convex. Glabella long (sag.), 66% length of cephalon, narrow, width (tr.) 31% (27-35%) of cephalic width at cephalon midlength; slightly convex (sag., tr.) standing in low relief above genae. Axial furrows moderately impressed; strongly convergent (30º to midline) along basal lobes; wider (tr.), slightly convergent, and very slightly laterally concave from basal furrow to maximum width of M3; slightly convergent to anterolateral corner, then nearly transverse to midline in specimens with anteriorly truncate glabellas; continue from M3 to midline in even curve on specimens with narrowly rounded front. Confluent M1 and M2 form long composite lobe, 61% (53–69%) of glabellar length (sag.), hexagonal in outline; glabellar culmination angular, extending in most specimens as narrow point that reaches posterior end of basal lobes. Basal furrows moderately impressed, narrow, nearly straight, converging to almost meet, resulting in narrow (tr.) occipital band; basal lobes large but short (exsag.), 20% of glabellar length, triangular in outline. F1 as very shallow indentations in side of glabella at anterior tip of basal lobes or absent; F2 transglabellar, chevon-like, moderately impressed near axial furrow, narrower (sag.) and faintly impressed across middle half to

two thirds of glabella. Weakly inflated glabellar node located at glabellar midlength, just posterior to medial peak of F2. Transglabellar F3 V-shaped, very faintly impressed, usually incomplete, fading medially, isolating most of M3 as long (exsag.), elliptical, slightly inflated lateral lobes. Anteroglabella short (sag.), approximately 16% (14-17%) of cephalic length; front narrowly rounded in some specimens, more truncate in others; descends evenly to axial furrow in lateral view. Acrolobe very slightly constricted in large specimens; quadrate in small specimens, semi-elliptical in larger cephala, widest (tr.) at midlength (sag.) of confluent M1 and M2, narrowing slightly anteriorly to end of glabella, curving inward to midline sharply in small specimens, in even curve in large cephala. Genae slightly convex, gently declined adaxially; moderately convex, steeply declined laterally; gently declined anteriorly from distal end of basal furrow to preglabellar furrow, moderately declined to anterior border furrow. Preglabellar field increases in length (sag.) with size; 20% of cephalic length in smallest specimen, 28% in largest cephalon; gently convex dorsally, moderately declined to border furrow. Border strongly convex, accounts for 7% of cephalic length (sag.) at midline; constant in width anteriorly, tapering rapidly posterior to F2. Border furrow well impressed; broad, widest at anterolateral corners, where it is twice width of border, narrows anteriorly and posteriorly.

Pygidium subquadrate in outline, length (sag.) 83% (74–91%) of maximum width at midlength opposite F2; nearly flat (sag.), very gently convex (tr.). Acrolobe quadrate in small specimens becoming subpentagonal and constricted with increased size. Articulating half ring with gently anteriorly convex margin, posterior margin deeply embayed laterally creating posteriorly projecting medial prong; articulating furrow well impressed, broad (sag.), bowed backward medially, deepest anterolaterally in embayments behind very narrow (exsag.) lateral thirds of half ring. Axial furrows moderately impressed, converge from anterior margin to F2 furrow with slight indentation at position of F1, diverge slightly and shallow, terminating approximately 45% of way to posterior margin. M1 undivided; M2 trisected by faintly impressed longitudinal furrows that outline elongate axial node that widens (tr.) slightly posteriorly, deflecting and slightly overhanging F2; crest of node declines anteriorly from posterior end, terminating at level of F1. F2 transglabellar, straight and directed posteromedially to longitudinal furrows, shallowing as curve around posterior end of axial node. Two slightly inflated lateral bosses and depressed central area at anterior end of posteroaxis; axial furrows posterior to paired bosses very faint to absent; small terminal node on midline at posterior margin of acrolobe confirms that posteroaxis extends to border furrow; very faint notular furrows present on a few exfoliated specimens. Pleural fields broad (tr.), nonscrobiculate, slightly convex, gently declined laterally and posteriorly. Border convex, bears one pair of long (exsag.), slender posterolateral spines directed posteriorly and slightly laterally from margin; border widest anterior to base of posterolateral spines, tapering anteriorly, even in width (sag., exsag.) posteriorly. Border furrow well impressed, broadest anterior to posterolateral spines, narrowing anteriorly, even in width (sag., exsag.) posteriorly.

Discussion. Naimark (2016) retained 6 species within *Neoagnostus* based upon her emended generic diagnosis. All display F3 and median preglabellar furrows that are more continuous and firmly impressed than those of *Neoagnostus parki* **n. sp.** The hexagonal shape of the posterior half of the glabella, between the chevron-shaped F2 and pointed glabellar culmination, also sets *N. parki* apart from all other species of the genus. Although *N. bilobus* (Shaw, 1951) possesses a nearly hexagonal confluent lobe similar to that of *N. parki*, its glabellar culmination is more broadly rounded. Comparison with other species must be done between sclerites of similar size, owing to significant ontogenetic variation arising from allometric growth. The cephalic acrolobe of *N. parki* is subrectangular in small specimens but increases in length (sag.), becoming semielliptical with gently curved and anteriorly convergent margins and a rounded front in larger specimens. Despite the elongation of the acrolobe, and an increase in relative length (sag.) of the frontal area, concomitant broadening of the border furrow and rounding of the anterolateral corners of the cephalon during growth modified the cephalic outline from subrectangular to semiovate. The pygidium of *N. parki* experienced similar elongation of the acrolobe, broadening of the border furrows, and transformation of marginal shape from subrectangular to semiovate during growth (Plate 15).

Neoagnostus parki also differs from the type, *N. aspidoides* Kobayashi, 1955 (p. 473–474, pl. 7, figs 4–5, pl. 9, fig. 5; Shergold, 1977, pl. 16, fig. 16; Shergold *et al.*, 1990, fig. 16, 1a) in having a less tapered glabella, longer preglabellar field, more rounded anterior margin, and narrower anteroglabella. Pygidial comparison is difficult due to the poor quality of the original illustration for the *N. aspidoides* pygidium. Additional features that distinguish *N. bilobus* (Shaw, 1951, p. 112–113, pl. 24, figs 17–22, not pl. 22, fig. 10 = ? *Plicatolina kindlei*; Shergold, 1977, pl. 16, figs 7–8; Shergold, *et al.*, 1990, fig. 16, 1b–1c) from *N. parki* include smaller basal glabellar lobes and a narrower and more strongly inflated pygidial acrolobe. The paired bosses on the front of the posteroaxis that inspired the name of *N. bilobus* are more inflated and surrounded by deep furrows. The pygidial axial node of *N. bilobus* is

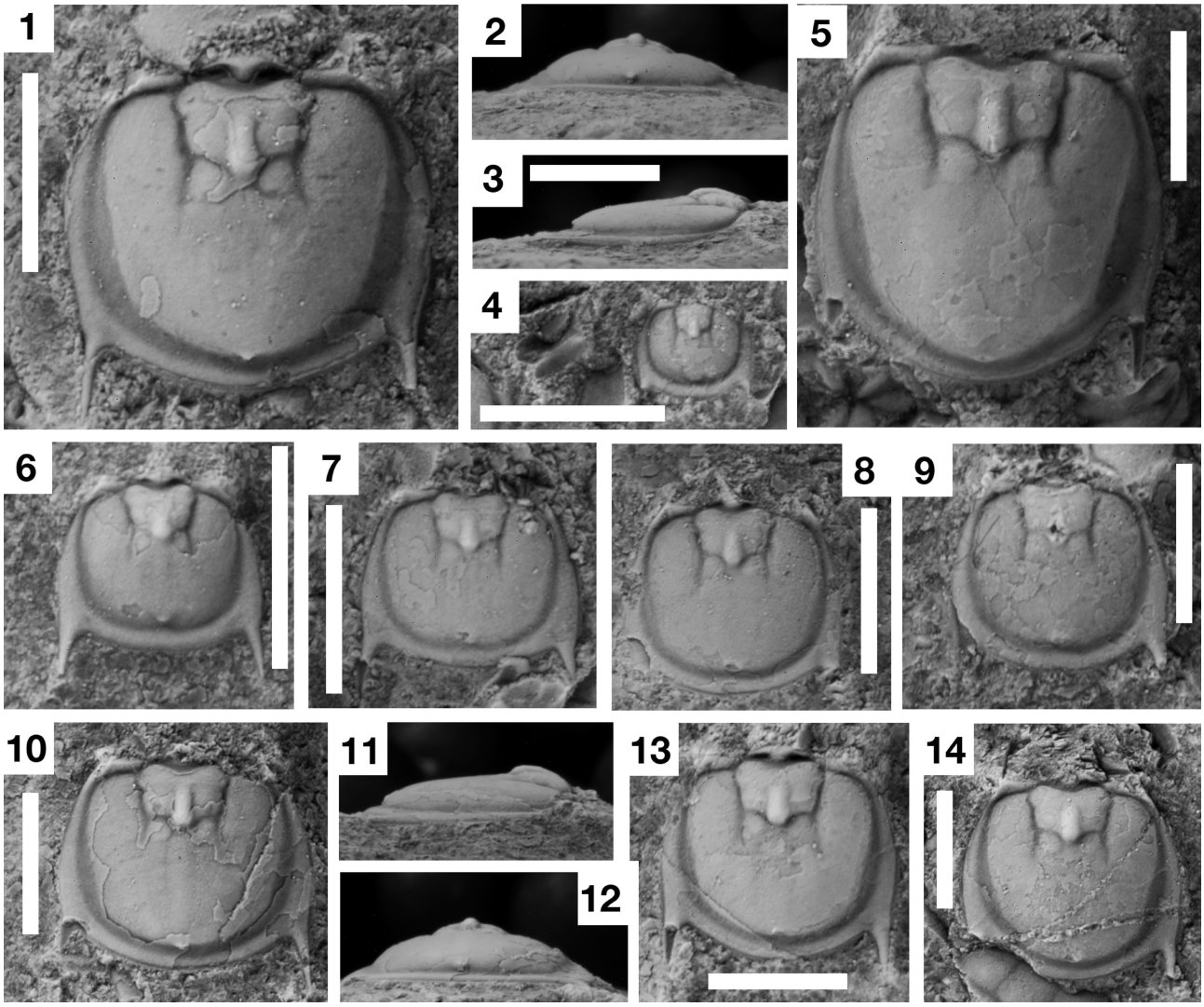

PLATE 15. Pygidia of *Neoagnostus parki* **n. sp.** Each white scale bar represents 2mm. 1-3. CM 41354 from 5/22/08B, dorsal, posterior, and right lateral views. 4. CM 41395, from 5/22/08B, dorsal view. 5. CM 41352, from 5/22/08B, dorsal view. 6. USMN 775753, from D3362-CO, dorsal view. 7. CM 41397, from 5/22/08B, dorsal view. 8. CM 41399, from 5/22/08B, dorsal view. 9. CM 41398, from 5/22/08B, dorsal view. 10-12. CM 41396, from 5/22/08B, dorsal, right lateral, and posterior views. 13. CM 41355, from 5/22/08B, dorsal view. 14. CM 41400, from 5/22/08B, dorsal view.

longer than that of *N. parki*, extending posteriorly past the mid-length of the paired bosses. Deeply incised furrows, a much broader (tr.) glabella, shorter frontal area, a nearly transverse F2, and very small basal lobes distinguish the cephalon of *N. eckardti* Jell, 1985 (p. 58–59, pl. 19, figs 1–5) from that of *N. parki.* While the pygidia of *N. parki* and *N. eckardti* are similar, the post-axial bosses on *N. eckardti* are more prominent and the axial furrows do not diverge posterior to the F2 furrow as they do in *N. parki*. Although comparison with *N. longicollis* Kobayashi, (1966, p. 283, fig. 7) is difficult due to the quality of the original illustrations, the holotype is clearly more quadrate than *N. parki* cephala of similar size and displays a more continuous median preglabellar furrow, a firmly impressed F3, and more transverse F2. The pygidium of *N. longicollis* exhibits a broader border and the axial furrows posterior to F2 are more strongly divergent. Although most of the illustrated sclerites of *N. tarijensis* (Gilberto, 2010, p. 123, fig. 1.1–1.6) are deformed, they confirm that the cephalon has smaller basal glabellar lobes, a more continuous, V-shaped F3, and more transverse F2 than *N. parki*. *Neoagnostus hangulensis* (Lu *et al*., 1981, pl. 2, fig. 1) has a less constricted cephalic acrolobe, narrower border furrows, a continuous median preglabellar furrow that reaches the border furrow, and more inflated bosses at the front of the posteroaxis. The cephalon designated as holotype for *Neoagnostus shiziluensis* by Lu & Zhou, (1990, p. 14, pl. 1, fig.7) more closely resembles that of *N. parki* with respect to shape of the acrolobe, width of border furrow, and cephalic outline. It differs, however, in having a

narrower glabella, smaller basal lobes, and a blunt rather than pointed glabellar culmination. Moreover, none of the three pygidia illustrated for that species compares favorably with that of *N. parki.* The semi-circular and inflated acrolobes of the two small pygidia (figs 9–10) are quite different from the weakly convex, subrectangular acrolobes of *N. parki* pygidia of comparable size. The larger, rectangular pygidium (fig. 11), which is wider than long and has a narrow border furrow of constant width, bears no resemblance to the large pygidia of *N. parki.* It is questionable as to whether that larger pygidium is conspecific with the cephalon and smaller pygidia, one of which came from the same horizon as the holotype. Although Naimark (2016, p. 62) suggested *N. shiziluensis* is a junior synonym of *N. eckardti,* we consider the differences in cephalic outline, glabellar proportions, frontal area length, and depth of furrows sufficient to retain separate species status for the former.

Machairagnostus Harrington & Leanza, 1957

Type species. *Machairagnostus tmetus* Harrington & Leanza, 1957, by original designation, from Argentina.

Diagnosis. The diagnosis and synonymy of Naimark (2016, p. 63) is accepted.

Other species. *M. corrugatus* (Suárez-Soruco, 1975); ? *M. ornatus* Lisogor, 1977; *M. houchengensis* (Zhang, 1981; *M. latus* (Ergaliev, 1983); *M. kentauensis* (Ergaliev, 1983); *Machairagnostus* sp., (Lazarenko *et al.,* 2008).

Discussion. Naimark (2016) discussed the nomenclatorial history of *Pseudorhaptagnostus* and revived the generic status of *Machairagnostus* rather than considering it a subgenus of *Neoagnostus* (Shergold *et al*., 1990: Shergold & Laurie, 1997).

Machairagnostus cf. *M. corrugatus* (Suárez-Soruco, 1975)

(Plate 7.20)

Discussion. A single exfoliated pygidium from collection 5/22/08B conforms to the diagnosis of Naimark (2016) for *Machairagnostus* by exhibiting a clearly defined intranotular axis (=lanceolate field) bounded by well-impressed notular furrows, and a terminal node just inside the border furrow. Although a few exfoliated pygidia of *Neoagnostus parki* from the same collection display very faint notular furrows (e.g. Pl. 15, fig. 10), none compare in depth of incision or are associated with scrobiculae on the pleural fields like those on the specimen here assigned to *Machairagnostus.* Moreover, this specimen is proportionally narrower (tr.) than *N. parki* pygidia of similar size. Given these differences, we consider it unlikely that this unique pygidium is a variant of *N. parki.*

The Windfall specimen differs from all pygidia illustrated for the seven species of *Machairagnostus* listed by Naimark (2016) in displaying a broader, flat border and much longer marginal spines that diverge posteriorly, rather than being subparallel. The pygidia of the type species, *M. tmetus* (Harrington & Leanza, 1957), and the species identified as *M.* sp. by Lazarenko *et al.* (2008, pl. 20, fig. 14, pl. 21, fig. 12) also differ in lacking scrobiculae on the pleural fields and having the sides of the posteroaxis more clearly defined by faintly impressed axial furrows. The pygidium of *M. ornatus* (Lisogor, 1977, pl. 31, fig. 1) is less quadrate, more coarsely scobiculate, and lacks clear definition of the intranotular axis. The poor preservation of the illustrated pygidia of *M. kentauensis* (Ergaliev, 1983, p. 43–44, pl. 3, figs 3–4) makes comparisons difficult. However, the Khazakhstanian specimens clearly display a much broader border furrow and narrower border of less variable width than the Windfall pygidium. *Machairagnostus houchengensis* (Zhang, 1981, pl. 55, fig. 12) has a poorly defined intranotular axis, more strongly constricted acrolobe, and much smaller and more anteriorly positioned posterolateral spines than the Nevada pygidium. The axial features of the Windfall pygidium most closely resemble those displayed by the three pygidia of *M. corrugatus* (Suárez-Soruco, 1975) illustrated by Tortello & Esteban (2003, figs 4.CC–EE). Indeed, the similarity is so strong that the Windfall pygidium might represent that species, with the wider border and longer, more posteriorly positioned spines attributable to intraspecific (ontogenetic) variation. Whether the Windfall pygidium is an ontogenetic variant of *M. corrugatus* or a new, closely related species cannot be determined at present owing to the poor preservation of the border and marginal spines in the smallest pygidium illustrated by Tortello & Esteban (2003, fig. 4.DD), which is similar in size to the Windfall specimen, and the lack of an associated cephalon in the Nevada collection.

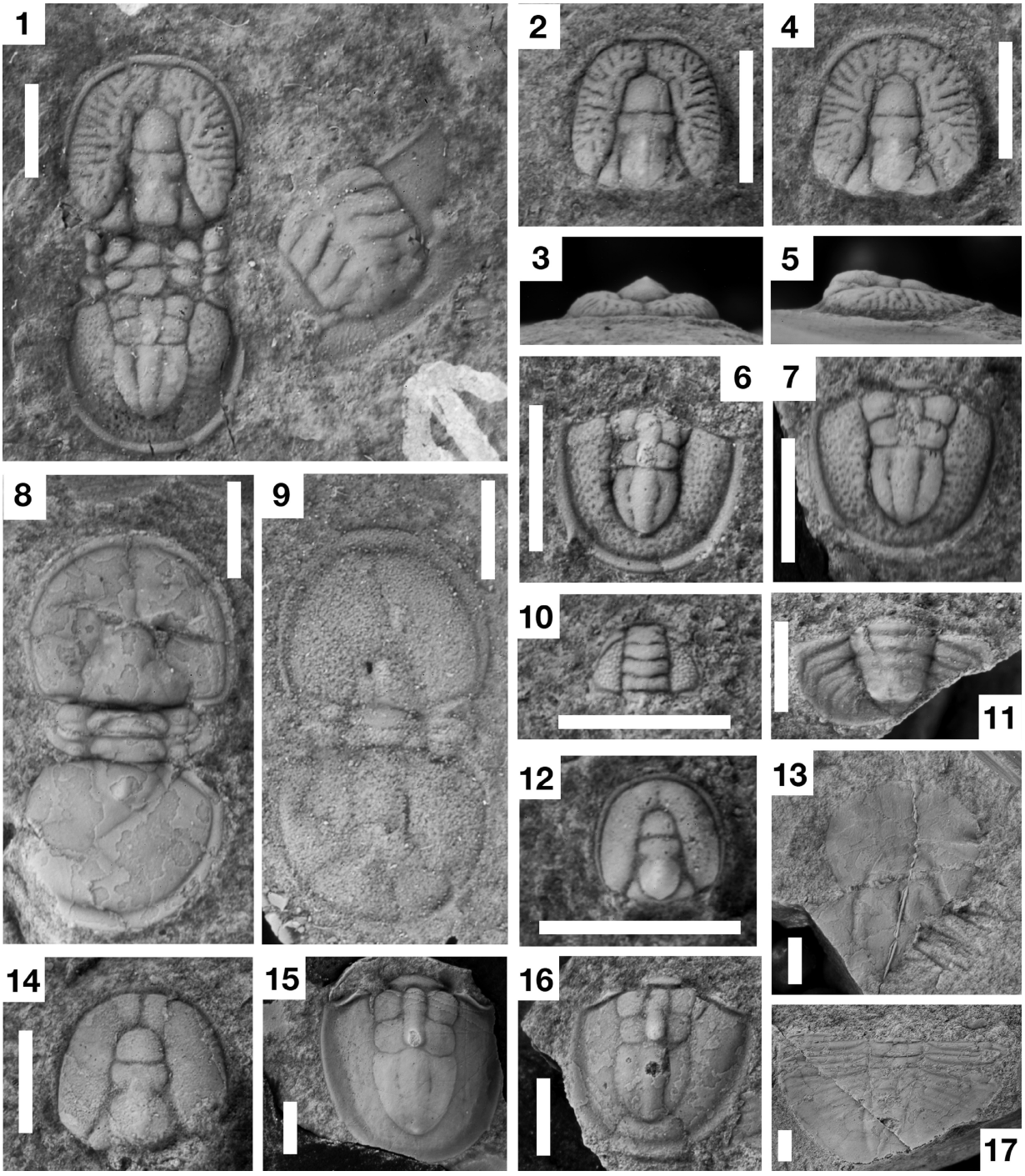

PLATE 16. Taxa from *Hedinaspis-Charchaqia* Fauna in the Hales Formation, Hot Creek section. Each white scale bar represents 2mm. 1. *Lotagnostus nolani* **n. sp.** Carapace (latex peel of external mold), USMN 775754, with *Mendoparabolina nyensis,* cephalon (counterpart of holotype), USMN 218571 (= Taylor, 1976, pl. 3, fig. 16), from D7130-CO, dorsal view, x7.8. 2, 3. *Lotagnostus nolani* **n. sp.** Cephalon, USMN 775755, from D7133-CO, dorsal and anterior views, x11.0. 4-5. *Lotagnostus nolani* **n. sp.** Cephalon, USMN 775756, from D7130-CO, dorsal and lateral views, x9.7. 6. *Lotagnostus nolani* **n. sp.** Pygidium, USMN 775757, from D7130-CO, dorsal view, x12.2. 7. *Lotagnostus nolani* **n. sp.**, pygidium, USMN 775758, from D7130-CO, dorsal view, x10.3. 8. *Pseudagnostus*? sp., carapace, USMN 775759, from D7130-CO, dorsal view, x8.0. 9. *Pseudagnostus*? sp., carapace, USMN 775760, from D7133-CO, dorsal view, x8.3. 10. *Mendoparabolina nyensis* (Taylor, 1976), small cranidium, USMN 775761, from D7133-CO, dorsal, x14.3. 11. *Mendoparabolina nyensis* (Taylor, 1976), pygidium, USMN 775762, from D7130-CO, dorsal view, x7.5. 12. *Lotagnostus* sp., cephalon, USMN 775763, from D7130-CO, dorsal view, x16.8. 13. Ceratopygid undet., cranidium, USMN 775764, from D7129-CO, dorsal view, x3.9. 14. *Lotagnostus* sp., cephalon, USMN 775765, from D7130-CO, dorsal view, x8.6. 15. *Lotagnostus* sp., pygidium, USMN 775766, from D7131-CO, dorsal view, x4.4. 16. *Lotagnostus* sp., pygidium, USMN 775767, from D7130-CO, dorsal view, x6.5. 17. Ceratopygid undet., pygidium, USMN 775768, from D7129-CO, dorsal view, x2.6.

Acknowledgements

K.C. McKinney (U.S. Geological Survey), Mark Florence and Jessica Nakano (Smithsonian National Museum of Natural History), and Michele Coyne (Natural Resources Canada) are thanked for facilitating loan of archived fossil collections and field notes. Indiana University of Pennsylvania (IUP) students T.J. Allen, A.J. Voegtle, and W.T. Kamerer assisted in field work and/or sample preparation. JFT acknowledges financial support in the form of grants from the IUP University Senate Research Committee for field work in Nevada, and from the National Science Foundation (Award 1325333) for Alaskan field work. Harvey Belkin (U.S.G.S.) is thanks for assistance with SEM photography of the conodonts, and Randall C. Orndorrf provided a helpful check on usage of geologic names. Jonathan M. Adrain and M. Franco Tortello provided valuable comments on an early draft of the manuscript. John R. Laurie and Stephen R. Westrop provided thorough reviews that greatly improved the paper.

References

Adrain, J.M. (2011) Class Trilobita Walch, 1771. *In*: Zhang, Z.-Q. (Ed.), Animal biodiversity: An outline of higher-level classification and survey of taxonomic richness. *Zootaxa*, 3148 (1), 104–109. https://doi.org/10.11646/zootaxa.3148.1.15

Adrain, J.M. & Westrop, S.R. (2004) A Late Cambrian (Sunwaptan) silicified trilobite fauna from Nevada. *Bulletins of American Paleontology*, 365, 1–56.

Ahlberg, P. & Terfelt, F. (2012) Furongian (Cambrian) agnostoids of Scandinavia and their implications for intercontinental correlation. *Geological Magazine*, 149, 1001–1012. https://doi.org/10.1017/S0016756812000167

Apollonov, M.K., Chugaeva, M.N., Dubinina, S.V. & Zhemchuzhnikov, V.G. (1988) Batyrbay section, southern Kazakhstan, U.S.S.R.—Potential stratotype for the Cambrian – Ordovician boundary. *Geological Magazine*, 25, 445–449. https://doi.org/10.1017/S0016756800013066

Bagnoli, G., Peng, S.-C., Qi, Y.-P. & Wang, C. (2017) Conodonts from the Wa'ergang section, China, a potential GSSP for the uppermost stage of the Cambrian. *Revista Italiana di Paleontolgia e Stratigrafia*, 123, 1–10. https://doi.org/10.13130/2039-4942/8003

Bao, J.-S. & Jago, J.B. (2000) Late Late Cambrian trilobites from near Birch Inlet, south-western Tasmania. *Palaeontology*, 43, 881–917. https://doi.org/10.1111/1475-4983.00154

Belt, T. (1867) On some new trilobites from the Upper Cambrian rocks of north Wales. *Geological Magazine*, 4, 294–295. https://doi.org/10.1017/S0016756800205748

Billings, E. (1860) On some new species of fossils from the limestone at Point Lévi, opposite Quebec. *Canadian Naturalist and Geologist*, 5, 301–24.

Billings, E. (1865) *Paleozoic Fossils*, 4, 169–344. https://doi.org/10.5962/bhl.title.69671

Benedetto, J.L. (1977) Una nueva fauna de trilobites Tremadocianos de la Provincia de Jujuy (Sierra de Cajas), Argentina. *Ameghiniana*, 14, 186–214.

Brady, M.J. & Rowell, A.J. (1976) Upper Cambrian subtidal blanket carbonate of the miogeocline, eastern Great Basin. *Brigham Young University*, Geology Series, 23, 153–163.

Brezinski, D.K., Taylor, J.F. & Repetski, J.E. (2012) Sequential development of platform to off-platform facies of the great American carbonate bank in the central Appalachians. *In:* Derby, J.R., Fritz, R.D, Longacre, S. A., Morgan, W.A. & Sternbach, C.A. (Eds.), *The Great American Carbonate Bank: The Geology and Petroleum Potential of the Cambro-Ordovician Sauk Sequence of Laurentia. Memoir 98*. The American Association of Petroleum Geologists, pp. 383–420. https://doi.org/10.1306/13331500M983500

Bridge, J. (1930) Geology of the Eminence and Cardareva Quadrangles. *Missouri Bureau of Geology and Mines*, Series 2, 24, 1–228.

Burmeister, H. (1843) *Die Organisation der Trilobiten aus ihren lebenden Verwandten entwickelt; nebst einer systematischen Uebersicht aller zeither beschriebenen Arten*. Reimer, Berlin, 147 pp. https://doi.org/10.5962/bhl.title.9086

Choi, D.K., Lee, L.G. & Sheen, B.C. (2004) Stop 12. Machari Formation at the Gonggiri section. *In*: Choi, D.K., Chough, S.K., Fithes, W.R., Kwon, Y.K., Lee, S.-B., Kang, I., Woo, J. & Sohn, J.W. (Eds.), *Field Trip Guide for IX International Conference of the Cambrian Stage Subdivision Working Group, Cambrian in the Land of Morning Calm. Paleontological Society of Korea, Special Publication 8*. Paleontological Society of Korea, Seoul, pp. 51–56.

Clark, T.H. (1924) The paleontology of the Beekmantown series at Lèvis, Quebec. *Bulletins of American Paleontology*, 10, 1–134.

Cook, H.E. & Taylor, M.E. (1975) Early Paleozoic continental margin sedimentation, trilobite biofacies, and the thermocline,

western United States. *Geology*, 3, 559–562.
https://doi.org/10.1130/0091-7613(1975)3%3C559:EPCMST%3E2.0.CO;2
Cook, H.E. & Taylor, M.E. (1977) Comparison of continental slope and shelf environments in the Upper Cambrian and lowest Ordovician of Nevada. *In*: Cook, H.E. & Enos, P. (Eds.), *Deep-water carbonate environments. SEPM (Society for Sedimentary Geology) Special Publication 25*. SEPM, Tulsa, Oklahoma, pp. 51–81.
https://doi.org/10.2110/pec.77.25.0051
Cooper, R.A., Nowlan, G.S. & Williams, S.H. (2001) Global stratotype section and point for base of the Ordovician System. *Episodes*, 24, 19–28.
https://doi.org/10.18814/epiiugs/2001/v24i1/005
Dong, X.-P. & Zhang, H.-Q. (2017) Middle Cambrian through lowermost Ordovician conodonts from Hunan, South China. *Paleontological Society Memoir*, 73, 1–89.
https://doi.org/10.1017/jpa.2015.43
Ergaliev, G.K. (1983) Some trilobites from the Upper Cambrian and Lower Ordovician of the Bol'shoi Karatau Range and Ulutai. *In*: Apollonov, M.K., Bandelotov, S.M. & Ivshin, N.K., (Eds.), *Stratigrafiya i paleontologiya nizhnego paleozoya Kazakhstana (Stratigraphy and paleontology of the Lower Paleozoic of Kazakhstan).* Nauka, Alma-Ata, pp. 35–66. [in Russian]
Esteban, S.B. & Tortello, M.F. (2007) Latest Cambrian sedimentary settings and trilobite faunas from the western Cordillera Oriental, Argentina. *Memoirs of the Association of Australasian Paleontologists*, 34, 431–460.
Ethington, R.L. (1981) Conodonts and other microfossils and age of the *Caryocaris* Shale, central Nevada. *Journal of Paleontology*, 55, 780–787.
Fortey, R.A. (1974) The Ordovician trilobites of Spitzbergen, I. Olenidae. *Norsk Polarinstitutt Skrifter*, 160, 1–129.
Fortey, R.A. (1983) Cambrian-Ordovician boundary beds in western Newfoundland and their phylogenetic significance. *Special Papers in Palaeontology*, 30, 179–211.
Gilberto, J.H. (2010) Nuevos trilobites de la Formacion Iscayach (Tarija-Bolivia). *Memorias del XIX Congreso Geologico Boliviano*, 2000 (1), 123–126.
Harrington, H.J. (1938) Sombre las faunas del Ordoviciano Inferior del Norte Argentino. *Revista del Museo de La Plata, Sección Paleontologica*, New Series, 1, 109–289.
Harrington, H.J. & Leanza, A.F. (1957) *Ordovician Trilobites of Argentina*. University of Kansas Press, Lawrence, 276 pp.
Harrington, H.J., Henningsmoen, G., Howell, B.F., Jaanusson, V., Lochman-Balk, C., Moore, R.C., Poulsen, C., Rasetti, F., Richter, E., Richter, R., Schmidt, H., Sdzuy, K., Struve, W., Tripp, R., Weller, J.M. & Whittington, H.B. (1959) Systematic descriptions. *In*: Moore, R.C. (Ed.), *Treatise on Invertebrate Paleontology. Part O.* Geological Society of America and University of Kansas Press, Lawrence and Boulder, pp. 170–526.
Henningsmoen, G. (1957) The trilobite family Olenidae with descriptions of Norwegian material and remarks on the Olenid and Tremadocian Series*. Skrifter utgitt ave Det Norske Videnskaps—Academi i Oslo*, 1 (Matematisk-naturvidenskapelig klasse 1), 1–303.
Howell, B.F. (1935a) Cambrian and Ordovician trilobites from Herault, southern France. *Journal of Paleontology*, 9, 222–238.
Howell, B.F. (1935b) Some New Brunswick Cambrian agnostians. *Bulletin of the Wagner Free Institute of Science*, 10, 13–16.
Jaekel, O. (1909) Über die Agnostiden. *Zeitschrift deutsche geologische Gesellschaft*, 61, 380–401.
Jahangir, H., Ghobadi Pour, M., Ashuri, A. & Aminia, A. (2016) Terminal Cambrian and Early Ordovician (Tremadocian) conodonts from eastern Alborz, north-central Iran. *Alcheringa*, 40, 219–243.
https://doi.org/10.1080/03115518.2016.1118298
James, N.P., Stevens, R.K., Barnes, C.R. & Knight, I. (1989) Evolution of a lower Paleozoic continental-margin carbonate platform, northern Canadian Appalachians. *In:* Crevello, P.D., Wilson, J.L., Sarg, J.F. & Read, J.F. (Eds.), *Controls on carbonate platform and basin development. SEPM Special Publication 44.* Society of Economic Paleontologists and Mineralogists, Tulsa, Oklahoma, pp. 123–146.
https://doi.org/10.2110/pec.89.44.0123
Jell, P.A. (1985) Tremadoc trilobites of the Digger Island Formation, Waratah Bay, Victoria. *Memoirs of the Museum of Victoria*, 46, 53–88.
https://doi.org/10.24199/j.mmv.1985.46.03
Jell, P.A. & Adrain, J.M. (2003) Available generic names for trilobites. *Memoirs of the Queensland Museum*, 48, 331–553.
Keller, M. (1999) Argentine Precordillera. Sedimentary and plate tectonic history of a Laurentian crustal fragment in South America. *Geological Society of America Special Paper*, 341, 131.
https://doi.org/10.1130/0-8137-2341-8.1
Kobayashi, T. (1955) The Ordovician fossils of the McKay Group in British Columbia, western Canada, with a note on the early Ordovician paleogeography. *Journal of the Faculty of Science University of Tokyo*, Section 2, 9, 355–493.
Kobayashi, T. (1966) The Cambro-Ordovician formations and faunas of South Korea, Part X. Stratigraphy of the Chosen Group in Korea and South Manchuria and its relation to the Cambro-Ordovician formations of other areas, Section B. The Chosen Group of North Korea and northeast China. *Journal of Faculty of Science, University of Tokyo*, Section II, 16 (2), 209–311.
Lake, P. (1906) A Monograph of British Cambrian trilobites. *Monographs of the Palaeontological Society*, 1906 (Part 1), 1–28.
https://doi.org/10.1080/02693445.1906.12035525

Lake, P. (1913) A Monograph of British Cambrian trilobites. *Monographs of the Palaeontological Society*, 1913 (Part 4), 65–88.
https://doi.org/10.1080/02693445.1913.12035562
Landing, E., Westrop, S.R. & Adrain, J.M (2011) The Lawsonian Stage – the *Eoconodontus notchpeakensis* (Miller, 1969) FAD and HERB carbon isotope excursion define a globally correlatable terminal Cambrian stage. *Czech Geological Survey Bulletin of Geosciences*, 86, 621–640.
https://doi.org/10.3140/bull.geosci.1251
Landing, E., Westrop, S.R. & Miller, J.F. (2010) Globally practical base for the uppermost Cambrian (Stage 10)—the *Eoconodontus notchpeakensis* and the Lawsonian Stage. *In*: Fatka, O. & Budil, P. (Eds.), *The 15th Field Conference of the Cambrian Stage Subdivision Working Group, International Subcommission on Cambrian Stratigraphy. Abstracts and Excursion Guide, Prague, Czech Republic and south-eastern Germany.* Czech Geological Survey, Prague, pp. 18.
Lazarenko, N. P., Gogin, I.Y., Pegel, T.V., Sukhov, S.S., Abaimova, G.P., Egorova, L.I., Federov, A.B., Raevskaya, E.G. & Ushatinskaya, G.T. (2008) Excursion 1b. Cambrian stratigraphy of the northeastern Siberian Platform and potential stratotypes of lower boundaries of proposed Upper Cambrian Chekurovkian and Nelegerian stages in the Ogon'or Formation section at Khos-Nelege River: the boundaries are defined by the FAD of *Agnostotes orientalis* and *Lotagnostus americanus*. *In*: Rozanov, A.Y. &Varlamov, A.I. (Eds.), *The Cambrian System of the Siberian Platform. Part 2. North-east of the Siberian Platform.* PIN RAS, Moscow and Novosibirsk, pp. 61–139.
Leopold, L.B. & Baker, A.A. (1996) Memorial to Thomas Brennan Nolan. *Geological Society of America Memorials*, 27, 33–34.
Lermontova, E.V. (1951) Verkhnekembriyskie trilobity i brakhiopody Boshche-Kulya (severo-vostochnyy Kazakhstan) (Upper Cambrian trilobites and brachiopods of Boshche-Kul, northeastern Kazakhstan). Vsegei, Moscow, 49 pp. [in Russian]
Linnarsson, J.G.O. (1869) Om Vestergötslands Cambriska och Siluriska aflagringar. *Kongliga Svenska Vetenskapsakakademiens. Handlingar*, 8, 1–89.
Lisogor, K.A. (1977) Biostratigraphy and trilobites of the Upper Cambrian and Tremadocian of the Maly Karatau (southern Kazakhstan) *In*: Zhuravleva, I.T. & Rozova, A.V. (Eds.), Biostratigraphy and fauna of the Upper Cambrian and boundary strata: New data on the Asian USSR. *Akademiya Nauk SSSR, Sibiriskoe Otdelenie, Instituta Geologii i Geofiziki Trudy*, 313, 197–265. [in Russian]
Longacre, S.A. (1970) Trilobites of the Upper Cambrian Ptychaspid Biomere Wilberns Formation, Central Texas. *Paleontological Society Memoir*, 4, 1–70.
https://doi.org/10.23867/RI0066D
Lu, Y.-H. (1964) Trilobites. *In:* Wang, Y. (Ed.), *Index Fossils of South China*. Science Press, Beijing, pp. 31–41. [in Chinese]
Lu, Y.-H. & Lin, H.-L. (1980) Cambro-Ordovician boundary in western Zhejiang and the trilobites contained therein. *Acta Geologica Sinica*, 19, 118–134. [in Chinese with English summary]
Lu, Y.-H. & Lin, H.-L. (1984) Late Late Cambrian and earliest Ordovician trilobites of Jingshan-Changshan area, Zhejiang. *In*: Nanjing Institute of Geology and Palaeontology (Ed.), *Stratigraphy and Palaeontology of Systemic boundaries in China, Cambrian-Ordovician Boundary. Vol. 1*. Anhui Science and Technology Publishing House, Hefei, pp. 45–143.
Lu, Y.-H. & Lin, H.-L. (1989) The Cambrian trilobites of western Zhejiang. *Palaeontologia Sinica,* 178, 1–287. [in Chinese with English summary]
https://doi.org/10.1007/978-3-662-12662-2_1
Lu, Y.-H. & Zhou, T.-R. (1990) Trilobites across the Cambrian-Ordovician boundary of the transitional region of Sandu, southeastern Guizhou. *Palaeontologia Cathayana*, 5, 1–84.
https://doi.org/10.1007/978-3-662-12662-2_1
Lu, Y.-H., Lin, H.-L., Han, N.-R., Li, L.-Z. & Ju, T.-Y (1984) On the Cambrian-Ordovician boundary of the Jiangshan-Changshan area, W. Zhejiang. *In*: Nanjing Institute of Geology and Palaeontology (Ed.), *Stratigraphy and Palaeontology of Systemic boundaries in China, Cambrian-Ordovician Boundary. Vol. 1.* Anhui Science and Technology Publishing House, Hefei, pp. 9–44.
Ludvigsen, R. (1982) Upper Cambrian and Lower Ordovician trilobite biostratigraphy of the Rabbitkettle Formation, western District of Mackenzie. *Royal Ontario Museum Life Sciences Contributions*, 134, 1–188.
https://doi.org/10.5962/bhl.title.52077
Ludvigsen, R. & Tuffnell, P.A. (1983) A revision of the Ordovician trilobite *Triarthrus* Green. *Geological Magazine*, 120, 567–577.
https://doi.org/10.1017/S0016756800027722
Ludvigsen, R. & Westrop, S.R. (1986) Classification of the Late Cambrian trilobite *Idiomesus* Raymond. *Canadian Journal of Earth Sciences*, 23, 300–307.
https://doi.org/10.1139/e86-033
Ludvigsen, R., Westrop, S.R. & Kindle, C.H. (1989) Sunwaptan (Upper Cambrian) trilobites of the Cow Head Group, western Newfoundland, Canada. *Palaeontographica Canadiana*, No. 6, 1–175.
Matthew, G.F. (1901) New species of Cambrian fossils from Cape Breton. *Bulletin of the Natural History Society of New Brunswick*, 4, 269–86.
M'Coy, F. (1849) On the classification of some British fossil Crustacea with notices of some forms in the University collection at Cambridge. *Annals and Magazine of Natural History*, 4, 161–179 + 330–335 + 392.

https://doi.org/10.1080/03745486009494810
Merriam, C.W. (1963) Paleozoic rocks of Antelope Valley, Eureka and Nye Counties, Nevada. *United States Geological Survey Professional Paper*, 423, 1–63.
https://doi.org/10.3133/pp423
Miller J.F., Evans, K.R., Freeman, R.L., Ripperdan, R.L. & Taylor, J.F. (2011) Proposed stratotype for the base of the Lawsonian Stage (Cambrian Stage 10) at the First appearance datum of *Eoconodontus notchpeakensis* (Miller) in the House Range, Utah, USA. *Bulletin of Geoscience*, 86, 595–620.
https://doi.org/10.3140/bull.geosci.1255
Miller, J.F., Evans, K.R., Freeman, R.L., Loch, J.D., Ripperdan, R.L. & Taylor, J.F. (2018) Combining biostratigraphy, carbon isotope stratigraphy and sequence stratigraphy to define the base of Cambrian Stage 10. *Australasian Palaeontological Memoirs*, 51, 19–64.
Miller, J.F., Ripperdan, R.L., Loch, J.D., Freeman, R.L., Evans, K.R., Taylor, J.F. & Tolbart, Z.C. (2015) Proposed GSSP for the base of Cambrian Stage 10 at the lowest occurrence of *Eoconodontus notchpeakensis* in the House Range, Utah, USA. *Annales de Paléontologie*, 101, 199–211.
https://doi.org/10.1016/j.annpal.2015.04.008
Miller, J.F., Evans, K.R., Loch, J.D., Ethington, R.L., Stitt, J.H., Holmer, L. & Popov, L.E. (2003) Stratigraphy of the Sauk III interval (Cambrian-Ordovician) in the Ibex area, western Millard County, Utah and central Texas: *Brigham Young University, Geology Studies*, 47, 23–118.
Naimark, E.B. (2016) Revision of *Pseudorhaptagnostus* Lermontova (? Trilobita, Agnostida). *Paleontological Journal*, 50, 54–68.
https://doi.org/10.1134/S0031030116010081
Nicoll, R.S., Miller, J.F., Nolan, G.S., Repetski, J.E. & Ethington, R.L. (1999) *Iapetonudus* (N. gen.) and *Iapetognathus* Landing, unusual earliest Ordovician multielement conodont taxa and their utility for biostratigraphy. *Brigham Young University, Geology Studies*, 44, 27–101.
Nielsen, A.T. (1997) A review of Ordovician agnostoid genera (Trilobita). *Transactions of the Royal Society of Edinburgh: Earth Science*, 87, 463–501.
https://doi.org/10.1017/S0263593300018150
Nolan, T.B., Merriam, C.W. & Williams, J.S. (1956) The stratigraphic section in the vicinity of Eureka, Nevada. *United States Geological Survey Professional Paper*, 276, 1–77.
https://doi.org/10.3133/pp276
Öpik, A.A. (1967) The Mindyallan fauna of north-western Queensland. *Bureau of Mineral Resources, Geology and Geophysics Bulletin,* 74, 1–404, 1–167. [in 2 volumes]
Osleger, D. & Read, J.F. (1993) Comparative analysis methods used to define eustatic variations in outcrop; Late Cambrian interbasinal sequence development. *American Journal of Science*, 293, 157–216.
https://doi.org/10.2475/ajs.293.3.157
Palmer, A.R. (1955) Upper Cambrian Agnostidae of the Eureka district, Nevada. *Journal of Paleontology*, 29, 86–101.
Palmer, A.R. (1965) Trilobites of the Late Cambrian Pterocephalid Biomere in the Great Basin, United States. *United States Geological Survey Professional Paper*, 493, 1–105.
https://doi.org/10.3133/pp493
Palmer, A.R. (1968) Cambrian trilobites of east-central Alaska. *United States Geological Survey Professional Paper*, 559-B, 1–115.
https://doi.org/10.3133/pp559B
Palmer, A.R. (1971) The Cambrian of the Great Basin and adjacent areas, western United States. *Lower Palaeozoic rocks of the world*, 1 (Cambrian of the New World), 1–78.
Pegel, T.V. (2000) Evolution of trilobite biofacies in Cambrian basins on the Siberian platform. *Journal of Paleontology*, 74, 1000–1019.
https://doi.org/10.1666/0022-3360(2000)074<1000:EOTBIC>2.0.CO;2
Peng, S.-C. (1984) Cambrian-Ordovician boundary in the Cili-Taoyuan border area, northwestern Hunan. *In*: Nanjing Institute of Geology and Palaeontology, Academia Sinica (Ed.), *Stratigraphy and paleontology of systemic boundaries in China, Cambrian and Ordovician boundary. Vol. 1.* Anhui Science and Technology Publishing House, Hefei, pp. 285–405.
Peng, S.-C. (1992) Upper Cambrian biostratigraphy and trilobite faunas of the Cili-Taoyuan area, north-western Hunan, China. *Association of Australasian Paleontologists Memoir*, 13, 1–119.
Peng, S.-C. & Babcock, L.E. (2005) Two Cambrian agnostoid trilobites, *Agnostotes orientalis* (Kobayashi, 1935) and *Lotagnostus americanus* (Billings, 1860): Key species for defining global stages of the Cambrian System. *Geosciences Journal*, 9, 107–15.
https://doi.org/10.1007/BF02910573
Peng, S.-C., Babcock, L.E., Zuo, J.-X. & Zhu, X.-J. (2014) A potential GSSP for the base of the uppermost Cambrian stage, coinciding with the first appearance of *Lotagnostus americanus* at Wa'ergang, Hunan, China. *GFF*, 136, 208–213.
https://doi.org/10.1080/11035897.2013.865666
Peng, S.-C., Babcock, L.E., Zhu, X.-J., Terfelt, F. & Dai, T. (2015) Intraspecific variation and taphonomic alteration in the Cambrian (Furongian) agnostoid *Lotagnostus americanus*: new information from China. *Bulletin of Geosciences*, 90, 281–306.

https://doi.org/10.3140/bull.geosci.1500
Peng S.-C., Babcock, L.E., Zuo, J.-X., Zhu, X.-J., Lin H.-L., Yang, X.-C., Qi, Y.-P., Bagnoli, G. & Wang, L. (2012) Global standard Stratoptype Section and Point (GSSP) for the base of the Jiangshanian Stage (Cambrian, Furongian) at Duibian, Jiangshan, Zhejiang, southeast China. *Episodes*, 35, 462–277.
https://doi.org/10.18814/epiiugs/2012/v35i4/002
Rasetti, F. (1944) Upper Cambrian trilobites from the Lévis Conglomerate. *Journal of Paleontology*, 18, 229–258.
Rasetti, F. (1954) Early Ordovician trilobites faunules from Quebec and Newfoundland. *Journal of Paleontology*, 28, 581–587.
Rasetti, F. (1959) Trempealeauian trilobites from the Conococheague, Frederick, and Grove Limestones of the central Appalachians. *Journal of Paleontology*, 33, 375–398.
Robison, R.A. (1982) Some Middle Cambrian agnostoid trilobites from western North America. *Journal of Paleontology*, 56, 132–160.
Robison, R.A. & Pantoja-Alor, J. (1968) Tremadocian trilobites from the Nochixtlán region, Oaxaca, Mexico. *Journal of Paleontology*, 42, 767–800.
Rusconi, C. (1951a) Trilobitas cambricos del Cerro Pelado (Mendoza). *Boletin Paleontologico de Buenos Aires*, 24, 1–4.
Rusconi, C. (1951b) Mas trilobitas cambricos de San Isidro Cerro Pelado y Canota. *Revista del Museo de Historia Natural de Mendoz*, 5, 3–30.
Rusconi, C. (1955a) Mas fosiles cambricos y ordovicios de San Isidro, Mendoza. *Boletin Paleontologico de Buenos Aires*, 31, 1–4.
Rusconi, C. (1955b) Fosiles cambricos y ordovicios al Oeste de San Isidro, Mendoza. *Revista del Museo de Historia Natural de Mendoza*, 8, 3–64.
Rushton, A.W.A. (2009) Revision of the Furongian agnostoid *Lotagnostus trisectus* (Salter). *Memoirs of the Association of Australasian Paleontologists*, 37, 273–279.
Salter, J.W. (1864a) A monograph of the British trilobites from the Cambrian, Silurian, and Devonian formations. *Monographs of the Palaeontographical Society of London*, 1864, 1–80.
https://doi.org/10.1080/02693445.1864.12113212
Salter, J.W. (1864b) Figures and descriptions illustrative of British organic remains. Decade XI, Trilobites. *Memoirs of the Geological Survey of the United Kingdom*, 1864, 1–64.
Shaw, A.B. (1951) The paleontology of northwestern Vermont. I. New Late Cambrian trilobites. *Journal of Paleontology*, 25, 97–114.
Shergold, J.H. (1971) Late Upper Cambrian trilobites from the Gola beds, western Queensland. *Australian Bureau of Mineral Resources, Geology and Geophysics Bulletin*, 112, 1–127.
Shergold, J.H. (1975) Late Cambrian and Early Ordovician trilobites from the Burke River Structural Belt, western Queensland, Australia. *Australian Bureau of Mineral Resources, Geology and Geophysics Bulletin*, 153, 1–251.
Shergold, J.H. (1977) Classification of the trilobite *Pseudagnostus*. *Palaeontology*, 20, 69–100.
Shergold, J.H. (1980) Late Cambrian Trilobites from the Chatsworth Limestone, western Queensland. *Australian Bureau of Mineral Resources, Geology and Geophysics Bulletin*, 186, 1–111.
Shergold, J.H. & Laurie, J.R. (1997) Introduction to the Suborder Agnostina. *In*: *Treatise on Invertebrate Paleontology. Pt. O. Arthropoda 1. Trilobita. Revised. Vol. 1*. Geological Society of America and University of Kansas Press, Lawrence, pp. 331–338.
Shergold, J.H., Bordonaro, O. & Liñán, E. (1995) Late Cambrian agnostoid trilobites from Argentina. *Palaeontology*, 38, 241–257.
Shergold, J.H., Laurie, J.R. & Sun, X.-W. (1990) Classification and review of the trilobite of the trilobite order Agnostida Salter, 1864: An Australian perspective. *Australian Bureau of Mineral Resources, Geology, and Geophysics Report*, 296, 1–92.
Siebold, C.T.E. Von & Stannius, H. (1845) *Lehrbuch der verleichenden Anatomie der Virbellosen Thiere*. Veit, Berlin, 482 pp.
https://doi.org/10.5962/bhl.title.10707
Stitt, J.H. (1971) Late Cambrian and earliest Ordovician trilobites, Timbered Hills and lower Arbuckle groups, western Arbuckle Mountains, Murray County, Oklahoma. *Oklahoma Geological Survey Bulletin*, 110, 1–83.
Suárez-Soruco, R. (1975) Nuevos trilobites del Tremadociano inferior del sur de Bolivia. *Revista Técnica de Yacimientos Petrolíferos Fiscales Bolivianos*, 4, 129–146.
Sun, Y.-C. (1924) Contribution to the Cambrian trilobite faunas of China. *Palaeontologia Sinica*, Series B, 1, 1–109.
Taylor, J.F., Repetski, J.E. & Roebuck, C.A. (1996) Stratigraphic significance of trilobite and conodont faunas from the Cambrian-Ordovician shelfbreak facies in the Frederick Valley, Maryland. *Studies in Maryland geology, Maryland Geological Survey Special Publication*, 3, 141–163.
Taylor, J.F., Brezinski, D.K., Repetski, J.E. & Walsh, N.M. (2009) The Adamstown Submergence Event: faunal and sedimentological record of a late Cambrian (Furongian) transgression in the Appalachian Region. *Memoirs of the Association of Australasian Palaeontologists*, 37, 641–667.
Taylor, J.F., Kennedy, D.J., Miller, J.F. & Repetski, J.E. (1991) Uppermost Cambrian slope deposits at Highgate Gorge, Vermont; a minor miscorrelation with major consequence for conodont- and trilobite-based chronocorrelation. *Journal of Paleontology*, 65, 855–862.
https://doi.org/10.1017/S0022336000037823
Taylor, J.F., Repetski, J.E., Loch, J.D. & Leslie, S.A. (2012) Biostratigraphy and chronostratigraphy of the Cambrian—Ordovician

great American carbonate bank. *In*: Derby, J.R., Fritz, R.D., Longacre, S.A., Morgan, W.A. & Sternbach, C.A. (Eds.), *The great American carbonate bank: The geology and economic resources of the Cambrian—Ordovician Sauk megasequence of Laurentia. Vol 98*. The American Association of Petroleum Geologists, pp. 15–35. https://doi.org/10.1306/13331488M983497

Taylor, M.E. (1976) Indigenous and redeposited trilobites from Late Cambrian basinal environments of central Nevada. *Journal of Paleontology*, 25, 97–114.

Taylor, M.E. (1977) Late Cambrian of western North America; trilobite biofacies, environmental significance, and biostratigraphic implications. *In: Concepts and Methods in Biostratigraphy*. Dowden, Hutchinson & Ross, Stroudsburg, Pennsylvania, pp. 397–425.

Taylor, M.E. & Cook, H.E. (1976) Continental shelf and slope facies in the Upper Cambrian and lowest Ordovician of Nevada. *Brigham Young University Geology Studies*, 23, 181–214.

Taylor, M.E. & Repetski, J.E. (1985) Early Ordovician eustatic sea-level changes in northern Utah and southeastern Idaho. *Utah Geological Association Publication*, 14, 237–247.

Tortello, M.F. (2014) A systematic revision of the late Furongian trilobites from Cerro Pelado, Mendoza, Argentina. *Ameghiniana*, 51, 295–310. https://doi.org/10.5710/AMGH.28.05.2014.2714

Tortello, M.F. (2018) Redescription of a *Lotagnostus – Mendoparabolina* faunule (Trilobita; late Furongian from Quebrada San Isidro, Precordillera of Mendoza, Argentina. *PalZ*, 92, 373–386. https://doi.org/10.1007/s12542-018-0403-y

Tortello, M.F. & Bordonaro, O.L. (1997) Cambrian agnostoid trilobites from Mendoza, Argentina: A systematic revision and biostratigraphic implications. *Journal of Paleontology*, 71, 74–86. https://doi.org/10.1017/S002233600003897X

Tortello, M.F. & Esteban, S.B. (2003) Trilobites del Cámbrico Tardío de la Formación Lampazar (Sierra de Cajas, Jujuy, Argentina). Implicancias bioestratigráficas y paleoambientales. *Ameghiniana*, 40, 232–344.

Tortello, M.F., Zeballo, F.J. & Monti, D.S. (2018) A late Furongian trilobite assemblage from the eastern Cordillera Oriental (Santa Rosita Formation; Jujuy, Argentina) and its biostratigraphical significance. *Revista Museo Argentino de Ciencias Naturales*, New Series, 20, 271–282. https://doi.org/10.22179/REVMACN.20.601

Troedsson, G.T. (1937) On the Cambro-Ordovician faunas of western Quruq Tagh, eastern Tien-Shan. *Palaeontologia Sinica*, 2, 1–74.

Troedsson, G.T. (1951) *Hedinaspis*, a new name for *Hedinia* Troedsson, non Navás. *Geologiska Föreningens i Stockholm Förhandlingar,* 73, 695. https://doi.org/10.1080/11035895109452864

Tullberg, S.A. (1880) *Agnostus*-arterna i de Kambriska afflagringarne vid Andrarum. *Sveriges Geologiska Undersökning*, 42, 1-37.

Walch, J.E.I. (1771) *Die naturgeschichte der verteinerungen, Dritter Theil. Zur erläuterung der Knorrischen Sammlung von Merkwürdigkeiten der Natur*. P.J. Felstecker, Nurnberg, 235 pp.

Wang, X-F., Stouge, S., Maletz, J., Bagnoli, G., Qi, Y.-P., Raevskaya, E.G., Wang, C-S. & Yan, C.-B. (2021) The Xiaoyangqiao section, Dayangcha, North China: the new global Auxiliary Boundary Stratotype Section and Point (ASSP) for the base of the Ordovician System. *Episodes*, 44, 359–383. https://doi.org/10.18814/epiiugs/2020/020091

Westergård, A.H. (1922) Sveriges olenidskiffer. *Sveriges Geologiska Undersökning. Afhandlingar och Uppsatser*, Series C, 18, 1–205.

Westrop, S.R. (1986) Trilobites of the Upper Cambrian Sunwaptan Stage, southern Canadian Rocky Mountains, Alberta. *Palaeontographica Canadiana*, 3, 1–179.

Westrop, S.R. (1995) Sunwaptan and Ibexian (Upper Cambrian-Lower Ordovician) trilobites of the Rabbitkettle Formation, northern Mackenzie Mountains, northwest Canada. *Palaeontographica Canadiana*, 12, 1–75.

Westrop, S.R. & Adrain, J.M. (2004) A Late Cambrian (Sunwaptan) silicified trilobite fauna from Nevada. *Bulletins of American Paleontology*, 365, 1–56.

Westrop, S.R. & Adrain, J.M. (2007) *Bartonaspis* new genus, a trilobite species complex from the base of the Upper Cambrian Sunwaptan Stage in North America. *Canadian Journal of Earth Sciences*, 44, 987–1003. https://doi.org/10.1139/e07-009

Westrop, S.R. & Adrain, J.M. (2016) Revision of *Irvingella tropica* Öpik, 1963 from Australia and related species from North America: implications for correlation of the base of the Jiangshanian Stage (Cambrian, Furongian). *Memoirs of the Association of Australasian Palaeontologists*, 49, 395–432.

Westrop, S.R. & Eoff, J.D. (2012) Late Cambrian (Furongian, Paibian, Steptoean) agnostoid arthropods from the Cow Head Group, western Newfoundland. *Journal of Paleontology*, 86, 201–237. https://doi.org/10.1666/11-034.1

Westrop, S.R. & Landing, E. (2016) The agnostoid arthropod *Lotagnostus* Whitehouse, 1936 (late Cambrian: Furongian) from Avalonian Cape Breton Island (Nova Scotia, Canada) and its significance for international correlation. *Geological Magazine*, 86, 569–594. https://doi.org/10.1017/S0016756816000571

Westrop, S.R., Adrain, J.M. & Landing, E. (2011) The Cambrian (Sunwaptan, Furongian) agnostoid arthropod *Lotagnostus* Whitehouse, 1936, in Laurentian and Avalonian North America: Systematics and biostratigraphic significance. *Bulletin of Geosciences*, 86, 569–594.
https://doi.org/10.3140/bull.geosci.1256

Whitehouse, F.W. (1936) The Cambrian faunas of northeastern Australia, Parts 1 and 2. *Memoirs of the Queensland Museum*, 11, 59–112.

Whittington, H.B. (1997) Morphology of the exoskeleton. *In*: *Treatise on Invertebrate Paleontology, Pt. O, Trilobita, revised.* Geological Society of America and University of Kansas Press, Lawrence, pp. 1–85.

Xiang, L.-W. & Zhang, T.-R. (1985) Systematic descriptions of trilobite fossils. *In*: Wang, Z.-H. (Ed.), Stratigraphy and trilobite faunas of the Cambrian in the western part of northern Tianshan, Xinjiang. *Peoples' Republic of China Ministry of Geology and Mineral Resources Geological Memoirs*, Series 2, 4, 64–136.

Young, J.C. (1960) Structure and stratigraphy in north Schell Creek Range. *Intermountain Association of Petroleum Geologists, 11th annual Field Conference Guidebook*, 1960, 158–172.

Zhang, T.-R. (1981) Trilobita. *In*: *Paleontological Atlas of North-west China, Xinjiang Province, Vol. 1.* Geological Publishing House, Beijing, pp. 134–213. [in Chinese]